The genomes of polyextremophilic Cyanidiales contain 1% horizontally transferred genes with diverse adaptive functions

Alessandro W. Rossoni[1#], Dana C. Price[2], Mark Seger[3], Dagmar Lyska[1], Peter Lammers[3], Debashish Bhattacharya[4] & Andreas P.M. Weber[1*]

[1]Institute of Plant Biochemistry, Cluster of Excellence on Plant Sciences (CEPLAS), Heinrich Heine University, Universitätsstraße 1, 40225 Düsseldorf, Germany
[2]Department of Plant Biology, Rutgers University, New Brunswick, NJ 08901, USA
[3]Arizona Center for Algae Technology and Innovation, Arizona State University, Mesa, AZ 85212, USA
[4]Department of Biochemistry and Microbiology, Rutgers University, New Brunswick, NJ 08901, USA

***Corresponding author**: Prof. Dr. Andreas P.M. Weber,
e-mail: andreas.weber@uni-duesseldorf.de

Abstract

The role and extent of horizontal gene transfer (HGT) in eukaryotes are hotly disputed topics that impact our understanding regarding the origin of metabolic processes and the role of organelles in cellular evolution. We addressed this issue by analyzing 10 novel Cyanidiales genomes and determined that 1% of their gene inventory is HGT-derived. Numerous HGT candidates originated from polyextremophilic prokaryotes that live in similar habitats as the Cyanidiales and encodes functions related to polyextremophily. HGT candidates differ from native genes in GC-content, number of splice sites, and gene expression. HGT candidates are more prone to loss, which may explain the nonexistence of a eukaryotic pan-genome. Therefore, absence of a pan-genome and cumulative effects fail to provide substantive arguments against our hypothesis of recurring HGT followed by differential loss in eukaryotes. The maintenance of 1% HGTs, even under selection for genome reduction underlines the importance of non-endosymbiosis related foreign gene acquisition.

Introduction

Eukaryotes transmit their nuclear and organellar genomes from one generation to the next in a vertical manner. As such, eukaryotic evolution is primarily driven by the accumulation, divergence (e.g., due to mutation, insertion, duplication), fixation, and loss of gene variants over time. In contrast, horizontal gene transfer (HGT) is the is the inter- and intraspecific transmission of genes from parents to their offspring. HGT in Bacteria [1-3] and Archaea [4] is widely accepted and recognized as an important driver of evolution leading to the formation of pan-genomes [5, 6]. A pan-genome comprises all genes shared by any defined phylogenetic clade and includes the so-called core (shared) genes associated with central metabolic processes, dispensable genes present in a subset of lineages often associated with the origin of adaptive traits, and lineage-specific genes [6]. This phenomenon is so pervasive that it has been questioned whether prokaryotic genealogies can be reconstructed with any confidence using standard phylogenetic methods [7, 8]. In contrast, as eukaryote genome sequencing has advanced, an increasing body of data has pointed towards the existence of HGT in these taxa, but at much lower rates than in prokaryotes [9]. The frequency and impact of eukaryotic HGT outside the context of endosymbiosis and pathogenicity however, remain hotly debated topics in evolutionary biology. Opinions range from the existence of ubiquitous and regular occurrence of eukaryotic HGT [10] to the almost complete dismissal of any eukaryotic HGT outside the context of endosymbiosis as being Lamarckian, thus false, and resulting from analysis artefacts [11, 12]. HGT sceptics favor the alternative hypothesis of differential loss (DL) to explain the current data. DL imposes strict vertical inheritance (eukaryotic origin) on all genes outside the context of pathogenicity and endosymbiosis, including putative HGTs. Therefore, all extant genes have their root in LECA, the last eukaryotic common ancestor. Patchy gene distributions are the result of multiple ancient paralogs in LECA that have been lost over time in some eukaryotic lineages but retained in others. Under this view, there is no eukaryotic pan-genome, there are no cumulative effects (e.g., the evolution of eukaryotic gene structures and accrual of divergence over time), and therefore, mechanisms for the uptake and integration of foreign DNA in eukaryotes are unnecessary.

A comprehensive analysis of the frequency of eukaryotic HGT was recently done by Ku et al. [13]. These authors reported the absence of eukaryotic HGT candidates sharing over 70% protein identity with their putative non-eukaryotic donors (for very recent HGTs, this figure could be as high as 100%). Furthermore, no continuous sequence identity distribution was detected for HGT candidates across eukaryotes and the “the 70% rule” was proposed

(“*Coding sequences in eukaryotic genomes that share more than 70% amino acid sequence identity to prokaryotic homologs are most likely assembly or annotation artifacts.*”) [13]. However, as noted by others [14, 15], this result was obtained by categorically dismissing all eukaryotic HGT singletons located within non-eukaryotic branches as assembly/annotation artefacts, as well as those remaining that exceeded the 70% threshold. In addition, all genes that were presumed to be of organellar origin were excluded from the analysis, leaving a small dataset extracted from already under-sampled eukaryotic genomes.

Given these uncertainties, the aim of our work was to systematically analyze eukaryotic HGT using the Cyanidiales as model organisms. The Cyanidiales comprise a monophyletic clade of polyextremopilic, unicellular red algae (Rhodophyta) that thrive in acidic and thermal habitats worldwide (e.g., volcanoes, geysers, acid mining sites, acid rivers, urban wastewaters, geothermal plants) [16]. With a divergence age estimated to be around 1.92 - 1.37 billion years [17], the Cyanidiales are the earliest split within Rhodophyta and define one of oldest surviving eukaryotic lineages. They are located near the root of the supergroup Archaeplastida, whose ancestor underwent the primary plastid endosymbiosis with a cyanobacterium that established photosynthesis in eukaryotes [18, 19]. In the context of HGT, the Cyanidiales became more broadly known after publication of the genome sequences of *Cyanidioschyzon merolae* 10D [20, 21], *Galdieria sulphuraria* 074W [22], and *Galdieria phlegrea* DBV009 [23]. The majority of putative HGTs in these taxa was hypothesized to have provided selective advantages during the evolution of polyextremophily, contributing to the ability of *Galdieria*, *Cyanidioschyzon*, and *Cyanidium* to cope with extremely low pH values, temperatures above 70°C, as well as high salt and toxic heavy metal ion concentrations [16, 24-26]. In such environments, they can represent up to 90% of the total biomass, competing with specialized Bacteria and Archaea [27], although some Cyanidiales strains also occur in more temperate environments [23, 28-31]. The integration and maintenance of HGT-derived genes, in spite of strong selection for genome reduction in these taxa [32] underlines the potential ecological importance of this process to niche specialization [22, 23, 33-36]. For this reason, we chose the Cyanidiales as a model lineage for studying eukaryotic HGT.

It should be appreciated that the correct identification of HGT based on sequence similarity and phylogeny is rarely trivial and unambiguous, leaving much space for interpretation and erroneous assignments. In this context, previous findings regarding HGT in Cyanidiales were based on single genome analyses and have therefore been questioned [13].

Many potential error sources need to be excluded during HGT analysis, such as possible bacterial contamination in the samples, algorithmic errors during genome assembly and annotation, phylogenetic model misspecification, and unaccounted for gene paralogy [14]. In addition, eukaryotic HGT reports based on single gene tree analysis are prone to misinterpretation and may be a product of deep branching artefacts and low genome sampling. Indeed, false claims of prokaryote-to-eukaryote HGT have been published [37, 38] which were later corrected [39, 40].

Here, we used multi-genomic analysis with 13 Cyanidiales lineages (including 10 novel long-read genome sequences) from 9 geographically isolated habitats. This approach increased phylogenetic resolution within Cyanidiales to allow more accurate assessment of HGT while avoiding many of the above-mentioned sources of error. The following questions were addressed by our research: (i) did HGT have a significant impact on Cyanidiales evolution? (ii) Are previous HGT findings in the sequenced Cyanidiales genomes an artefact of short read assemblies, limited genome databases, and uncertainties associated with single gene trees, or do they hold up with added sampling? (iii) And, assuming that evidence of eukaryotic HGT is found across multiple Cyanidiales species, are cumulative effects observable, or is DL the better explanation for these results?

Materials and Methods

Cyanidiales strains used for draft genomic sequencing

Ten Cyanidiales strains (**Figure 1**) were sequenced in 2016/2017 using the PacBio RS2 (Pacific Biosciences Inc., Menlo Park, CA) technology [41] and P6-C4 chemistry (the only exception being *C. merolae* Soos, which was sequenced as a pilot study using P4-C2 chemistry in 2014). Seven strains, namely *G. sulphuraria* 5572, *G. sulphuraria* 002, *G. sulphuraria* SAG21.92, *G. sulphuraria* Azora, *G. sulphuraria* MtSh, *G. sulphuraria* RT22 and *G. sulphuraria* MS1 were sequenced at the University of Maryland Institute for Genome Sciences (Baltimore, MD). The remaining three strains, *G. sulphuraria* YNP5578.1, *G. phlegrea* Soos, and *C. merolae* Soos were sequenced at the Max-Planck-Institut für Pflanzenzüchtungsforschung (Cologne, Germany). To obtain axenic and monoclonal genetic material for sequencing, single colonies of each strain were grown at a temperature of 37°C in the dark on plates containing glucose as the sole carbon source (1% Gelrite mixed 1:1 with 2x Allen medium [42], 50 µM Glucose). The purity of single colonies was assessed using microscopy (Zeiss Axio Imager 2, 1000x) and molecular markers (18S, *rbcL*). Long read DNA was extracted using a genomic-tip 20/G column following the steps of the "YEAST"

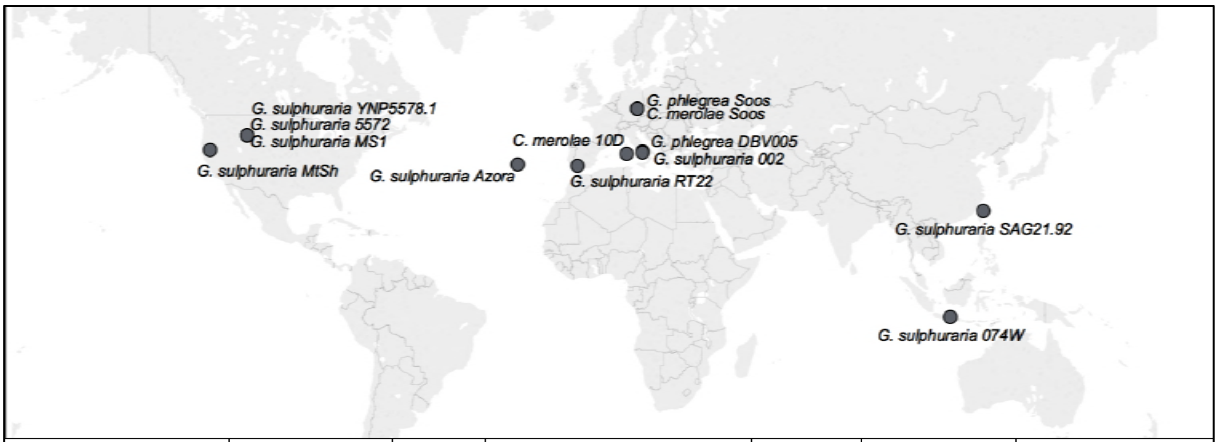

Species	Origin	Country	Habitat	Habitat pH	Habitat Temp (°C)	Source
C. merolae 10D*	Sardinia	Italy	Acidic Hot Spring	1.5	Up to 45°C	ATCC®, T. Kuroiwa
C. merolae Soos	Soos National Park	CZ	Diatom field	0.8 - 2	< 0° - 30°C	W. Gross, M. Seger
G. phlegrea DBV009*	Nepi	Italy	Sulphuar Spring	0.8	12°C	G. Pinto, ACUF
G. phlegrea Soos	Soos National Park	CZ	Diatom field	0.8 - 2	< 0° - 30°C	W. Gross, M. Seger
G. sulphuraria 002 (S)	La Solfatara	Italy	na	1	36°C	G. Pinto
G. sulphuraria 074W*	Mount Lawu	Indonesia	Fumaroles	na	35°C	W. Gross, P. De Luca
G. sulphuraria 5572	Norris Basin, YNP	USA	Acidic soil	1	55°C	M. Seger, R. W. Castenholz
G. sulphuraria Azora	Azores	Portugal	Porous sandstone, endolithic	2.1	na	W. Gross, A. Flechner
G. sulphuraria MS1	Nymph Creek, YNP	USA	Acid stream	3	42°C	M. Seger, R. W. Castenholz
G. sulphuraria MtSh	Mount Shasta	USA	Soil, close to mountain peak (4300m)	2.2	na	W. Gross, R. R. Pausewein
G. sulphuraria RT22	Rio Tinto, Berrocal	Spain	Riverbank, endolithic	2.5	na	W. Gross, R. R. Pausewein
G. sulphuraria SAG21.92	Yangmingshan	Taiwan	Hot spring	na	na	J. T.
G. sulphuraria YNP5578.1	Nymph Creek, YNP	USA	Acid stream	3	42°C	M. Seger, R. W. Castenholz

Figure 1 – Geographic origin and habitat description of the analyzed Cyanidiales strains. Available reference genomes are marked with an asterisk (*), whereas "na" indicates missing information.

DNA extraction protocol (QIAGEN N.V., Hilden, Germany). The size and quality of DNA were assessed via gel electrophoresis and the Nanodrop instrument (Thermo Fisher Scientific Inc, Waltham, MA).

Assembly

All genomes (excluding the already published *G. sulphuraria* 074W*, G. phlegrea* DBV009 and *C. merolae* 10D) were assembled using canu version 1.5 [43]. The genomic sequences were polished three times using the Quiver algorithm [44]. Different versions of each genome were assessed using BUSCO v.3 [45] and the best performing genome was chosen as reference for gene model prediction. Each genome was queried against the National Center for Biotechnology Information (NCBI) nr database [46] in order to detect contigs consisting exclusively of bacterial best blast hits (i.e., possible contamination). None were found.

Gene prediction

Gene and protein models for the 10 sequenced Cyanidiales were predicted using MAKER v3 beta [47]. MAKER was trained using existing protein sequences from *Cyanidioschyzon merolae* 10D and *Galdieria sulphuraria* 074W, for which we used existing RNA-Seq (*A. W. Rossoni & G. Schoenknecht, under review*) data with expression values >10 FPKM [48] combined with protein sequences from the UniProtKB/Swiss-Prot protein database [49].

Augustus [50], GeneMark ES [51], and EVM [52] were used for gene prediction. MAKER was run iteratively and using various options for each genome. The resulting gene models were again assessed using BUSCO v.3 [45] and PFAM 31.0 [53]. The best performing set of gene models was chosen for each species.

Sequence annotation

The transcriptomes of all sequenced species and those of *Cyanidioschyzon merolae* 10D, *Galdieria sulphuraria* 074W and *Galdieria phlegrea* DB10 were annotated (re-annotated) using BLAST2GO PRO v.5 [54] combined with INTERPROSCAN [55] in order to obtain the annotations, Gene Ontology (GO)-Terms [56], and Enzyme Commission (EC)-Numbers [57]. KEGG orthology identifiers (KO-Terms) were obtained using KAAS [58, 59] and PFAM annotations using PFAM 31.0 [53].

Orthogroups and phylogenetic analysis

The 81,682 predicted protein sequences derived from the 13 genomes listed in Table 1 were clustered into orthogroups (OGs) using OrthoFinder v. 2.2 [60]. We queried each OG member using DIAMOND v. 0.9.22 [61] to an in-house database comprising NCBI RefSeq sequences with the addition of predicted algal proteomes available from the JGI Genome Portal [62], TBestDB [63], dbEST [64], and the MMETSP (Moore Microbial Eukaryote Transcriptome Sequencing Project) [65]. The database was partitioned into four volumes: Bacteria, Metazoa, remaining taxa, and the MMETSP data. To avoid taxonomic sampling biases due to under/overabundance of particular lineages in the database, each volume was queried independently with an expect (*e*-value) of 1 x $10^{-5,}$ and the top 2,000 hits were saved and combined into a single list that was then sorted by descending DIAMOND bitscore. Proteins containing one or more bacterial hits (and thus possible HGT candidates) were retained for further analysis, whereas those lacking bacterial hits were removed. A taxonomically broad list of hits was selected for each query (the maximum number of genera selected for each taxonomic phylum present in the DIAMOND output was equivalent to 180 divided by the number of unique phyla), and the corresponding sequences were extracted from the database and aligned using MAFFT v7.3 [66] together with queries and hits selected in the same manner for remaining proteins assigned to the same OG (duplicate hits were removed). A maximum-likelihood phylogeny was then constructed for each alignment using IQTREE v7.3 [67] under automated model selection, with node support calculated using 2,000 ultrafast bootstraps. Single-gene trees for the referenced HGT candidates from previous research regarding *G. sulphuraria* 074W [22] and *G. phlegrea* DBV009 [23] were constructed in the same manner, without assignment to OG. To create the algal species tree, the OG assignment was re-run with the addition of proteomes from outgroup taxa *Porphyra umbilicalis* [68], *Porphyridium purpureum* [34], *Ostreococcus tauri* RCC4221 [69], and *Chlamydomonas reinhardtii* [70]. Orthogroups were parsed and 2,090 were selected that contained single-copy representative proteins from at least 12/17 taxa; those taxa with multi-copy representatives were removed entirely from the OG. The proteins for each OG were extracted and aligned with MAFFT, and IQTREE was used to construct a single maximum-likelihood phylogeny via a partitioned analysis in which each OG alignment represented one partition with unlinked models of protein evolution chosen by IQTREE. Consensus tree branch support was determined by 2,000 UF bootstraps.

Detection of HGTs

All phylogenies containing bacterial sequences were inspected manually. Only trees in which there were at least two different Cyanidiales sequences and at least three different non-eukaryotic donors were retained. Phylogenies with cyanobacteria and Chlamydiae as sisters were considered as EGT and excluded from the analysis. Genes that were potentially transferred from cyanobacteria were only accepted as HGT candidates when homologs were absent in other photosynthetic eukaryotes; i.e., the cyanobacterium was not the closest neighbor, and when the annotation did not include a photosynthetic function, to discriminate from EGT. Furthermore, phylogenies containing inconsistencies within the distribution patterns of species, especially at the root, or UF values below 70% spanning over multiple nodes, were excluded. Each orthogroup was queried against NCBI nr to detect eukaryotic homologs not present in our databases. The conservative approach to HGT assignment used here allowed identification of robust candidates for in-depth analysis. This may however have come at the cost of underestimating HGT at the single species level. Furthermore, some of the phylogenies that were rejected because < 3 non-eukaryotic donors were found may have resulted from current incomplete sampling of prokaryotes. For example, OG0001817 is present in the sister species *G. sulphuraria* 074W and *G. sulphuraria* MS1 but has a single bacterial hit (*Acidobacteriaceae bacterium* URHE0068, CBS domain-containing protein, GI:651323331).

Results

Features of the newly sequenced Cyanidiales genomes

Genome sizes of the 10 targeted Cyanidiales range from 12.33 Mbp - 15.62 Mbp, similar to other members of this red algal lineage [20, 22, 23] (**Table 1**). PacBio sequencing yielded 0.56 Gbp – 1.42 Gbp of raw sequence reads with raw read N50 ranging from 7.9 kbp – 14.4 kbp, which translated to a coverage of 28.91x – 70.99x at the unitigging stage (39.46x – 91.20x raw read coverage) (**Supplementary Material, Figure 1S and Table 1S**). We predicted a total of 61,869 novel protein coding sequences which, together with the protein data sets of the already published Cyanidiales species (total of 81,682 predicted protein sequences), capture 295/303 (97.4%) of the highly conserved eukaryotic BUSCO dataset. Each species, taken individually, scored an average of 92.7%. In spite of massive gene losses observed in the Cyanidiales [32], these results corroborate previous observations that genome reduction has only had a minor influence on the core eukaryotic gene inventory in free-living organisms [71]. Even *C. merolae* Soos, the species with the most limited coding capacity (4,406 protein sequences), includes 89.5% of the eukaryotic BUSCO dataset. The number of contigs obtained from the *Galdieria* genomes ranged between 101 – 135. *G. sulphuraria* 17.91 (a strain different from the ones sequenced) was reported to have 40 chromosomes, and strains isolated from Rio Tinto (Spain), 47 or 57 chromosomes [72]. Pulsed-field gel electrophoresis indicates that *G. sulphuraria* 074W has approximately 42 chromosomes that are between 100 kbp and 1 Mbp in size [73]. The genome assembly of *C. merolae* Soos

Strain	Genome Stats				Gene Stats		HGT Stats		HGT vs Native Gene Subsets						Annotations			
	Genome Size (Mb)	Contigs	Contig N50 (kb)	%GC Content	Genes	Orthogroups	HGT Orthogroups	HGT Genes	%GC Native	%GC HGT	(%) Multiexon Native	(%) Multiexon HGT	Exon/ Gene Native	Exon/ Gene HGT	EC	PFAM	KEGG	GO
G. sulphuraria 074W#	13.78	433	172.3	36.89	7174	5265	51	55	38.99	39.62*	73.6	47.3*	2.25	3.2*	938	3073	3241	6572
G. sulphuraria MS1	14.89	129	172.1	37.62	7441	5389	54	58	39.59	40.79*	83.4	62.1*	2.5	3.88*	930	3077	3178	6564
G. sulphuraria RT22	15.62	118	172.9	37.43	6982	5186	51	54	39.54	40.85*	74.7	51.9*	2.63	3.95*	941	3118	3223	6504
G. sulphuraria SAG21	14.31	135	158.2	37.92	5956	4732	44	47	40.04	41.47*	84.8	83.0	4.02	5.03*	931	3047	3143	6422
G. sulphuraria MtSh	14.95	101	186.6	40.04	6160	4746	46	47	41.33	42.48*	79.7	63.8*	3.15	4.32*	939	3114	3244	6450
G. sulphuraria Azora	14.06	127	162.3	40.10	6305	4905	49	58	41.34	42.57*	84.5	75.9*	2.68	4.03*	934	3072	3181	6474
G. sulphuraria YNP5587.1	14.42	115	170.8	40.05	6118	4846	46	46	41.33	42.14*	74.5	54.3*	2.61	3.65*	938	3084	3206	6516
G. sulphuraria 5572	14.28	108	229.7	37.99	6472	5009	46	53	39.68	40.5*	78.4	45.3*	2.15	3.53*	936	3108	3252	6540
G. sulphuraria 002	14.11	107	189.3	39.16	5912	4701	46	52	40.76	41.35*	97.1	50.0*	2.37	3.73*	927	3060	3184	6505
G. phlegrea DBV009#	11.41	9311	2.0	37.86	7836	5562	54	62	39.97	40.58*	na	na	na	na	935	3018	3125	6512
G. phlegrea Soos	14.87	108	201.1	37.52	6125	4624	44	47	39.57	40.73*	77.5	43.2*	2.19	3.33*	929	3034	3197	6493
C. merolae 10D#	16.73	22	859.1	54.81	4803	3980	33	33	56.57	56.57	0.5	0.0	1	1.01	883	2811	2832	6213
C. merolae Soos	12.33	35	567.5	54.33	4406	3574	34	34	54.84	54.26	9.4	2.9	1.06	1.1	886	2787	2823	6188

Table 1 – Summary of the 13 analyzed Cyanidiales genomes. The existing genomes of *Galdieria sulphuraria* 074W, *Cyanidioschyzon merolae* 10D, and *Galdieria phlegrea* are marked with "#". The remaining 10 genomes are novel. **Genome Size (Mb)**: size of the genome assembly in Megabases. **Contigs**: number of contigs produced by the genome assembly. The contigs were polished with quiver **Contig N50 (kb)**: Contig N50. **%GC Content**: GC content of the genome given in percent. **Genes**: transcriptome size of species. **Orthogroups:** All Cyanidiales genes were clustered into a total of 9075 OGs. Here we show how many OGs there are per species. **HGT Orthogroups**: Number of OGs derived from HGT. **HGT Genes:** Number of HGT gene candidates found in species. **%GC Native:** GC content of the native transcriptome given in percent. **%GC HGT:** GC content of the HGT gene candidates given in percent **% Multiexon Native:** % of multiallelic genes in the native transcriptome. **% Multiexon HGT:** percent of multiallelic genes in the HGT gene candidates. **S/M Native:** Ratio of Multiexonic vs Singleexonic genes in native transcriptome. **S/M HGT:** Ratio of Multiexonic vs Singleexonic genes in HGT candidates. Asterisks (*) denote a significant difference ($p <= 0.05$) between native and HGT gene subsets. **EC**, **PFAM**, **GO**, **KEGG**: Number of species-specific annotations in EC, PFAM, GO, KEGG.

produced 35 contigs, which approximates the 22 chromosomes (including plastid and mitochondrion) of the *C. merolae* 10D telomere-to-telomere assembly. Whole genome alignments indicate that a portion of the assembled contigs represent complete chromosomes.

Orthogroups and phylogeny

The 81,682 predicted protein sequences from all 13 genomes clustered into a total of 9,075 orthogroups and phylogenetic trees were built for each orthogroup. The reference species tree was constructed using 2,090 OGs that contained a single-copy gene in at least 12 of the 17 taxa (*Porphyra umbilicalis* [68], *Porphyridium purpureum* [34], *Ostreococcus tauri* RCC4221 [69], and *Chlamydomonas reinhardtii* [70] were added to the dataset as outgroups). As a result, the species previously named *G. sulphuraria* Soos and *C. merolae* MS1 were reannotated as *G. phlegrea* Soos and *G. sulphuraria* MS1. Given these results, we sequenced a second genome of *C. merolae* and a representative of the *G. phlegrea* lineage. The species tree reflects previous findings that suggest more biodiversity exists within the Cyanidiales [29]. Than is represented by the taxa in the phylogeny (**Figure 2**).

Figure 2 (below) – Species tree of the 13 analyzed Cyanidiales genomes using other unicellular and aquatic red (*Porphyra umbilicalis, Porphyridium purpureum*) and green algae (*Ostreococcus tauri*, *Chlamydomonas reinhardtii*) as outgroups. IQTREE was used to construct a single maximum-likelihood phylogeny based on orthogroups containing single-copy representative proteins from at least 12 of the 17 taxa (13 Cyanidiales + 4 Other). Each orthogroup alignment represented one partition with unlinked models of protein evolution chosen by IQTREE. Consensus tree branch support was determined by 2,000 rapid bootstraps. All nodes in this tree had 100% bootstrap support, and are therefore not shown. Divergence time estimates are taken from Yang et al., 2016 [74]. Similarity is derived from the average one-way best blast hit protein identity (minimum protein identity threshold = 30%). The minimal protein identity between two *G. sulphuraria* strains was 65.4%, measured between *G. sulphuraria* SAG21.92, which represent the second most distant sampling locations (12,350 km). Similar lineage boundaries were obtained for the *C. merolae* samples (66.4% protein identity), which are separated by only 1150 km.

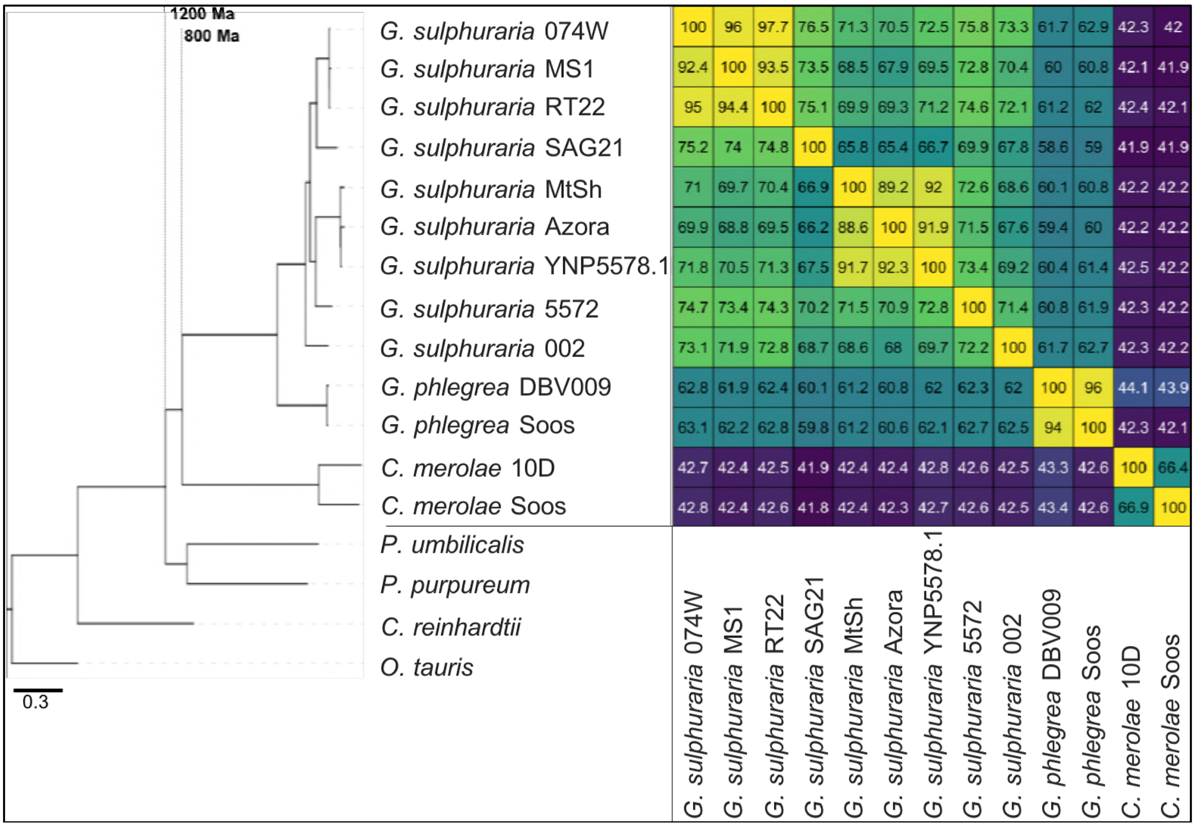

	G. sulphuraria 074W	*G. sulphuraria* MS1	*G. sulphuraria* RT22	*G. sulphuraria* SAG21	*G. sulphuraria* MtSh	*G. sulphuraria* Azora	*G. sulphuraria* YNP5578.1	*G. sulphuraria* 5572	*G. sulphuraria* 002	*G. phlegrea* DBV009	*G. phlegrea* Soos	*C. merolae* 10D	*C. merolae* Soos
G. sulphuraria 074W	100	96	97.7	76.5	71.3	70.5	72.5	75.8	73.3	61.7	62.9	42.3	42
G. sulphuraria MS1	92.4	100	93.5	73.5	68.5	67.9	69.5	72.8	70.4	60	60.8	42.1	41.9
G. sulphuraria RT22	95	94.4	100	75.1	69.9	69.3	71.2	74.6	72.1	61.2	62	42.4	42.1
G. sulphuraria SAG21	75.2	74	74.8	100	65.8	65.4	66.7	69.9	67.8	58.6	59	41.9	41.9
G. sulphuraria MtSh	71	69.7	70.4	66.9	100	89.2	92	72.6	68.6	60.1	60.8	42.2	42.2
G. sulphuraria Azora	69.9	68.8	69.5	66.2	88.6	100	91.9	71.5	67.6	59.4	60	42.2	42.2
G. sulphuraria YNP5578.1	71.8	70.5	71.3	67.5	91.7	92.3	100	73.4	69.2	60.4	61.4	42.5	42.2
G. sulphuraria 5572	74.7	73.4	74.3	70.2	71.5	70.9	72.8	100	71.4	60.8	61.9	42.3	42.2
G. sulphuraria 002	73.1	71.9	72.8	68.7	68.6	68	69.7	72.2	100	61.7	62.7	42.3	42.2
G. phlegrea DBV009	62.8	61.9	62.4	60.1	61.2	60.8	62	62.3	62	100	96	44.1	43.9
G. phlegrea Soos	63.1	62.2	62.8	59.8	61.2	60.6	62.1	62.7	62.5	94	100	42.3	42.1
C. merolae 10D	42.7	42.4	42.5	41.9	42.4	42.4	42.8	42.6	42.5	43.3	42.6	100	66.4
C. merolae Soos	42.8	42.4	42.6	41.8	42.4	42.3	42.7	42.6	42.5	43.4	42.6	66.9	100

Analysis of HGTs

The most commonly used approach to identify HGT candidates is to determine the position of eukaryotic and non-eukaryotic sequences in a maximum likelihood tree. Using this approach, 96 OGs were identified in which Cyanidiales genes shared a monophyletic descent with prokaryotes, representing 1.06% of all OGs. A total of 641 single Cyanidiales sequences are considered as HGT candidates (**Table 1**). The amount of HGT per species varied considerably between members of the *Cyanidioschyzon* (33 - 34 HGT events, all single copy genes) and *Galdieria* lineages with 44 – 54 HGT events (52.6 HGT origins on average, 47 – 62 HGT gene candidates). In comparison to previous studies [22, 23], no evidence of massive gene family expansion regarding HGT genes was found because the maximum number of gene copies in HGT orthogroups was three. We note, however, that one large gene family of STAND-type ATPases that was previously reported to originate from an archaeal HGT [22] did not meet the criteria used in our restrictive Blast searches; i.e., the 10^{-5} *e*-value cut-off for consideration and a minimum of three different non-eukaryotic donors. This highly diverged family requires more sophisticated comparative analyses that were not done here (**Supplementary Material, Chapter 1S**).

Gene co-localization on raw sequence reads

One major issue associated with previous HGT studies is the incorporation of contaminant DNA into the genome assembly, leading to incorrect results [37-40]. Here, we screened for potential bacterial contamination in our tissue samples using PCR analysis of extracted DNA with the *rbcL* and 18S rRNA gene markers prior to sequencing. No instances of contamination were found. Furthermore, our work relied on PacBio RSII long-read sequencing technology, whereby single reads frequently exceed 10 kbp of DNA. Given these robust data, we also tested for co-occurrence of HGT gene candidates and “native” genes in the same read. The protein sequences of each species were queried with tblastn (10^{-5} *e*-value, 75 bitscore) against a database consisting of the uncorrected PacBio RSII long reads. This analysis showed that 629/641 (98.12%) of the HGT candidates co-localize with native red algal genes on the same read (38,297 reads in total where co-localization of native genes and HGT candidates was observed). It should be noted that the 10 novel genomes we determined share HGT candidates with *C. merolae* 10D, *G. sulphuraria* 074W, and *G. phlegrea* DBV009, which were sequenced in different laboratories, at different points in time, using different technologies, and assembly pipelines. Hence, we consider it highly unlikely that these HGT candidates result from bacterial contamination. As the accuracy of long read sequencing technologies further increases, we believe this criterion for excluding bacterial contamination provides an additional piece of evidence that should be added to the guidelines for HGT discovery [14].

Differences in molecular features between native and HGT-derived genes

A core prerequisite of the HGT theory (and cumulative effects) is that horizontally acquired genes have different structural characteristics when compared to native genes. The passage of time is required (and expected) to erase these differences. Therefore, we searched for differences in genomic features between HGT candidates and native Cyanidiales genes with regard to: (1) GC-content, (2) the number of spliceosomal introns and the exon/gene ratio, (3) differential transcription, (4) percent protein identity between HGT genes and their non-eukaryotic donors, and (5) cumulative effects as indicators of their non-eukaryotic origin [9, 13, 22].

GC-content: All 11 *Galdieria* species showed significant differences (GC-content of transcripts is normally distributed, Student's *t*-test, two-sided, $p \leq 0.05$) in percent GC-content between native sequences and HGT candidates (**Table 1**). Sequences belonging to the

Galdieria lineage have an exceptionally low GC-content (39% – 41%) in comparison to the majority of thermophilic organisms that exhibit higher values (~55%). On average, HGT candidates in *Galdieria* display 1% higher GC-content in comparison to their native counterparts. No significant differences were found for *C. merolae* 10D and *C. merolae* Soos in this respect. Because native *Cyanidioschyzon* genes have an elevated GC-content (54% - 56%), this makes it difficult to distinguish between them and HGT-derived genes (**Supplementary Material, Table 2S and Figures 2SA-2SM**).

Spliceosomal Introns and Exon/Gene: Bacterial genes lack spliceosomal introns and therefore the spliceosomal machinery. Consequently, genes acquired through HGT are initially single-exons and may acquire introns over time due to the invasion of existing intervening sequences. We detected significant discrepancies in the ratio of single-exon to multi-exon genes between HGT candidates and native genes in the *Galdieria* lineage. On average, 42% of the *Galdieria* HGT candidates are single-exon genes, whereas only 19.2% of the native gene set are comprised of single-exons. This difference is significant (categorical data, “native” vs “HGT” and “single exon” vs. “multiple exon”, Fisher’s exact test, $p \leq 0.05$) in all *Galdieria* species except *G. sulphuraria* SAG21.92 (**Table 1**). The *Cyanidioschyzon* lineage contains a highly reduced spliceosomal machinery [75], therefore only ~10% of native genes are multi-exonic in *C. merolae* Soos and only 1/34 HGT candidates has gained an intron. *C. merolae* 10D has only 26 multi-exonic genes (~0.5% of all transcripts) and none of its HGT candidates has gained an intron. Enrichment testing is not possible with these small sample sizes (**Supplementary Material, Table 3SA**).

We analyzed the number of exons that are present in multi-exonic genes and obtained similar results for the *Galdieria* lineage (**Table 1**). All *Galdieria* species show significant differences regarding the exon/gene ratio between native and HGT genes (non-normal distribution regarding the number of exons per gene, Wilcoxon-Mann-Whitney-Test, 1000 bootstraps, $p <= 0.05$). HGT candidates in *Galdieria* have 0.97 - 1.36 fewer exons per gene in comparison to their native counterparts. Because the multi-exonic HGT subset in both *Cyanidioschyzon* species combined includes only one multi-exonic HGT candidate, no further analysis was performed (**Supplementary Material, Table 3SB and Figures 3SA-3SM**).

Differential transcription: Several RNA-seq datasets are publicly available for *G. sulphuraria* 074W (*A. W. Rossoni & G. Schoenknecht, under review*) and *C. merolae* 10D

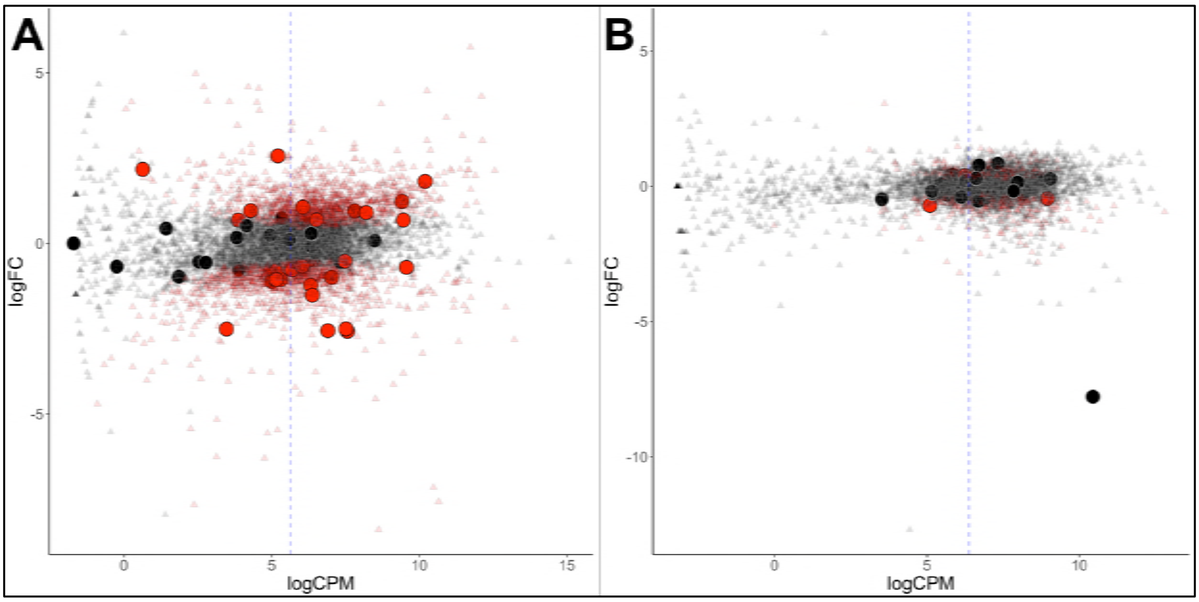

Figure 3 – Differential gene expression of *G. sulphuraria* 074W (**A**) and *C. merolae* 10D (**B**), here measured as log fold change (logFC) vs transcription rate (logCPM). Differentially expressed genes are colored red (quasi-likelihood (QL) F-test, Benjamini-Hochberg, $p <= 0.01$). HGT candidates are shown as large circles. The blue dashes indicate the average logCPM of the dataset. Although HGT candidates are not significantly more or less expressed than native genes, they react significantly stronger to temperature changes in *G. sulphuraria* 074W ("more red than black dots"). This is not the case in high CO_2 treated *C. merolae* 10D.

[48]. We aligned [76] the transcriptome reads to the respective genomes, using an identical data processing pipeline [77] for both datasets to exclude potential algorithmic errors (**Figure 3**). The average read count per gene (measured as counts per million, CPM), of native genes was 154 CPM in *G. sulphuraria* 074W and 196 CPM *C. merolae* 10D. The average read counts for HGT candidates in *G. sulphuraria* 074W and *C. merolae* 10D were 130 CPM and 184 CPM, respectively. No significant differences in RNA abundance between native genes and HGT candidates were observed for these taxa (non-normal distribution of CPM, Wilcoxon-Mann-Whitney-Test, $p < 0.05$). We also tested whether HGT candidates responded differentially to stress in comparison to native genes. This is the case for temperature-stressed *G. sulphuraria* 074W (categorical data, "native" vs. "HGT" and "differentially expressed" vs. "no differential expression", Fisher's exact test, $p = 0$). Consequently, HGT candidates are not only well integrated into the transcriptional machinery of *G. sulphuraria* 074W, but they show significant differential expression under fluctuating temperature, which may reflect an adaptation to thermal stress (**Figure 3A**) [22, 75]. However, no significant enrichment of HGT-derived genes within the differentially transcribed gene set was detected in the transcriptional response of *C. merolae* 10D towards high and low CO_2 conditions (**Figure 3B**), which are not stressful for a wild type *C. merolae* 10D (categorical data, "native" vs. "HGT" and "differential expression" vs. "no differential expression", Fisher's exact test, $p = 0.75$).

Gene function – not passage of time – explains percent protein identity (PID) between Cyanidiales HGT candidates and their non-eukaryotic donors

Once acquired, any HGT-derived gene may be fixed in the genome and propagated across the lineage. The PID data can be further divided into different subsets depending on species composition of the OG. Of the total 96 OGs putatively derived from HGT events, 60 are exclusive to the *Galdieria* lineage (62.5%), 23 are exclusive to the *Cyanidioschyzon* lineage (24%), and 13 are shared by both lineages (13.5%) (**Figure 4A**). Consequently, either a strong prevalence for lineage specific DL exists, or both lineages underwent individual sets of HGT events because they share their habitat with other non-eukaryotic species (which is what the HGT theory would assume). The 96 OGs in question are affected by gene loss or partial fixation. Once acquired only 8/13 of the “Cyanidiales” (including “Multiple HGT” and

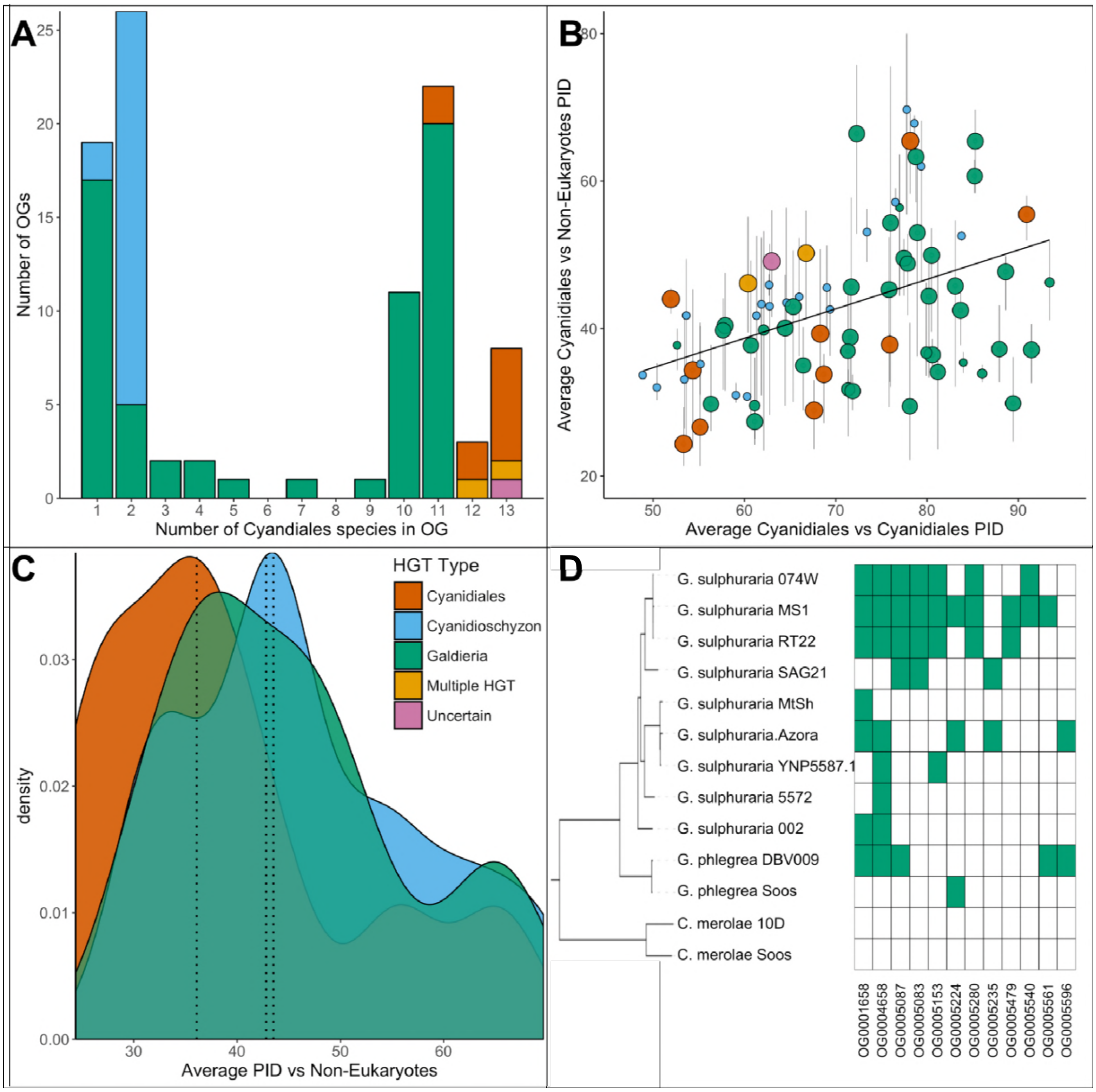

Figure 4 – Comparative analysis of the 96 OGs potentially derived from HGT. **A**| OG count vs. the number of Cyanidiales species contained in an OG (=OG size). Only genes from the sequenced genomes were considered (13 species). A total of 60 OGs are exclusive to the *Galdieria* lineage (11 species), 23 OGs are exclusive to the *Cyanidioschyzon* lineage (2 species), and 13 OGs are shared by both lineages. A total of 46/96 HGT events seem to be affected by later gene erosion/partial fixation. **B**| OG-wise PID between HGT candidates vs. their potential non-eukaryotic donors. Point size represents the number of sequenced species contained in each OG. Because only two genomes of *Cyanidioschyzon* were sequenced, the maximum point size for this lineage is 2. The whiskers span minimum and maximum shared PID of each OG. The PID within Cyanidiales HGTs vs. PID between Cyanidiales HGTs and their potential non-eukaryotic donors is positively correlated (Kendall's tau coefficient, $p = 0.000747$), showing evolutionary constraints that are gene function dependent, rather than time-dependent. **C**| Density curve of average PID towards potential non-eukaryotic donors. The area under each curve is equal to 1. The average PID of HGT candidates found in both lineages ("ancient HGT", left dotted line) is ~5% lower than the average PID of HGT candidates exclusive to *Galdieria* or *Cyandioschyzon* ("recent HGT", right dotted lines). This difference is not significant (pairwise Wilcoxon rank-sum test, Benjamini-Hochberg, $p > 0.05$). **D**| Presence/Absence pattern (green/white) of Cyanidiales species in HGT OGs. Some patterns strictly follow the branching structure of the species tree. They represent either recent HGTs that affect a monophyletic subset of the *Galdieria* lineage, or are the last eukaryotic remnants of an ancient gene that was eroded through differential loss. In other cases, the presence/absence pattern of *Galdieria* species is random and conflicts with the *Galdieria* lineage phylogeny. HGT would assume either multiple independent acquisitions of the same HGT candidate, or a partial fixation of the HGT candidate in the lineage, while still allowing for gene erosion. According to DL, these are the last existing paralogs of an ancient gene, whose erosion within the eukaryotic kingdom is nearly complete.

"Uncertain") OGs and 20/60 of the *Galdieria* specific OGs are encoded by all species. Once acquired by the *Cyanidioschyzon* ancestor, the HGT candidates were retained by both *C. merolae* Soos and *C. merolae* 10D in 22/23 *Cyanidioschyzon* specific OGs. It is not possible to verify whether the only *Cyanidioschyzon* OG containing one HGT candidate is the result of gene loss, individual acquisition, or due to erroneously missing this gene model during gene prediction. The average percent PID between HGT gene candidates of the 13 OGs shared by all Cyanidiales and their non-eukaryotic donors is 41.2% (min = 24.4%; max = 65.4%) (**Figure 4B**). From the HGT perspective, these OGs are derived from ancient HGT events that occurred at the root of the Cyanidiales, well before the split of the *Galdieria* and *Cyanidioschyzon* lineages. The OGs were retained over time in all Cyanidiales, although evidence of subsequent gene loss is observed. Under the DL hypothesis, this group of OGs contains genes that have been lost in all other eukaryotic lineages except the Cyanidiales. Similarly, the average PID between HGT candidates their non-eukaryotic donors in OGs exclusive to the *Cyanidioschyzon* lineage is 46.4% (min = 30.8%; max = 69.7%) and 45.1% (min = 27.4%; max = 69.5%) for those OGs exclusive to the *Galdieria* lineage. According to the HGT view, these subsets of candidates were horizontally acquired either in the *Cyanidioschyzon* lineage, or in the *Galdieria* lineage after the split between *Galdieria* and *Cyanidioschyzon*. DL would impose gene loss on all other eukaryotic lineages except *Galdieria* or *Cyanidioschyzon.* Over time, sequence similarity between the HGT candidate and the non-eukaryotic donor is expected to decrease at a rate that reflects the level of functional constraint. The average PID of "ancient" HGT candidates shared by both lineages (before the split into *Galdieria* and *Cyanidioschyzon* approx. 800 Ma years ago [74]) is ~5% lower than the average PID of HGT candidates exclusive to one lineage which, according to HGT would represent more recent HGT events because their acquisition occurred only after the split (thus lower divergence) (**Figure 4C**). However, no significant difference between *Galdieria*-exclusive HGTs, *Cyandioschyzon*-exclusive HGTs, and HGTs shared by both lineages was found (non-normal distribution of percent protein identity, Shapiro-Wilk normality test, W = 0.95, $p = 0.002$; Pairwise Wilcoxon rank-sum test, Benjamini-Hochberg, all comparisons $p > 0.05$). Therefore, neither *Cyanidioschyzon* nor *Galdieria* specific HGTs, or HGTs shared by all Cyanidiales, are significantly more, or less, similar to their potential prokaryotic donors. We also addressed the differences in PID within the three groups. The average PID within HGT gene candidates of the 13 OGs shared by all Cyanidiales is 75.0% (min = 51.9%; max = 90.9%) (**Figure 4B**). Similarly, the average PID within HGT candidates in OGs exclusive to the *Cyanidioschyzon* lineage is 65.1% (min = 48.9%; max = 83.8%) and 75.0% (min = 52.6%; max = 93.4%) for those OGs exclusive to the *Galdieria* lineage. Because we sampled only two *Cyanidioschyzon* species in comparison to 11 *Galdieria* lineages that are also much more closely related (**Figure 2A**), a comparison between these two groups was not done. However, a significant positive correlation (non-normal distribution of PID across all OGs, Kendall's tau coefficient, $p = 0.000747$) exists between the PID within Cyanidiales HGTs versus PID between Cyanidiales HGTs and their non-eukaryotic donors (**Figure 4B**). Hence, the more similar Cyanidiales sequences are to each other, the more similar they are to their non-eukaryotic donors, showing gene function dependent evolutionary constraints.

Complex origins of HGT-impacted orthogroups

While comparing the phylogenies of HGT candidates, we also noticed that not all Cyanidiales genes within one OG are necessarily originate via HGT. Among the 13 OGs that contain HGT candidates present in both *Galdieria* and *Cyanidioschyzon*, we found two cases (**Figure 4A**, “Multiple HGT”), OG0002305 and OG0003085, in which *Galdieria* and *Cyanidioschyzon* HGT candidates cluster in the same orthogroup. However, these have different non-eukaryotic donors and are located on distinct phylogenetic branches that do not share a monophyletic descent (**Figure 5A**). This is potentially the case for OG0002483 as well, but we were uncertain due to low bootstrap values (**Figure 4A**, “Uncertain”). These OGs either represent two independent acquisitions of the same function or, according to DL, the LECA encoded three paralogs of the same gene which were propagated through evolutionary time.

One of these was retained by the *Galdieria* lineage (and shares sequence similarity with one group of prokaryotes), the second was retained by *Cyanidioschyzon* (and shares sequence similarity with a different group of prokaryotes), and a third paralog was retained by all other eukaryotes. It should be noted that the "other eukaryotes" do not always cluster in one uniformly eukaryotic clade which increases the number of required paralogs in LECA to explain the current pattern. Furthermore, some paralogs could also have already been completely eroded and do not exist in extant eukaryotes. Similarly, 6/60 *Galdieria* specific OGs also contain *Cyanidioschyzon* genes (OG0001929, OG0001938, OG0002191, OG0002574, OG0002785 and OG0003367). Here, they are nested within other eukaryote lineages and would not be derived from HGT (**Figure 5B**). Also, eight of the 23 *Cyanidioschyzon* specific HGT OGs contain genes from *Galdieria* species (OG0001807, OG0001810, OG0001994, OG0002727, OG0002871, OG0003539, OG0003929 and OG0004405) which cluster within the eukaryotic branch and are not monophyletic with *Cyanidioschyzon* HGT candidates (**Figure 5C**). According to the HGT view, this subset of candidates was horizontally acquired in either the *Cyanidioschyzon* lineage, or the *Galdieria* lineage only after the split between *Galdieria* and *Cyanidioschyzon*, possibly replacing the ancestral gene or functionally complementing a function that was lost due to genome reduction. According to DL, the LECA would have encoded two paralogs of the same gene. One was retained by all eukaryotes, red algae, and *Galdieria* or *Cyanidioschyzon*, the other exclusively by *Cyanidioschyzon* or *Galdieria* together with non-eukaryotes.

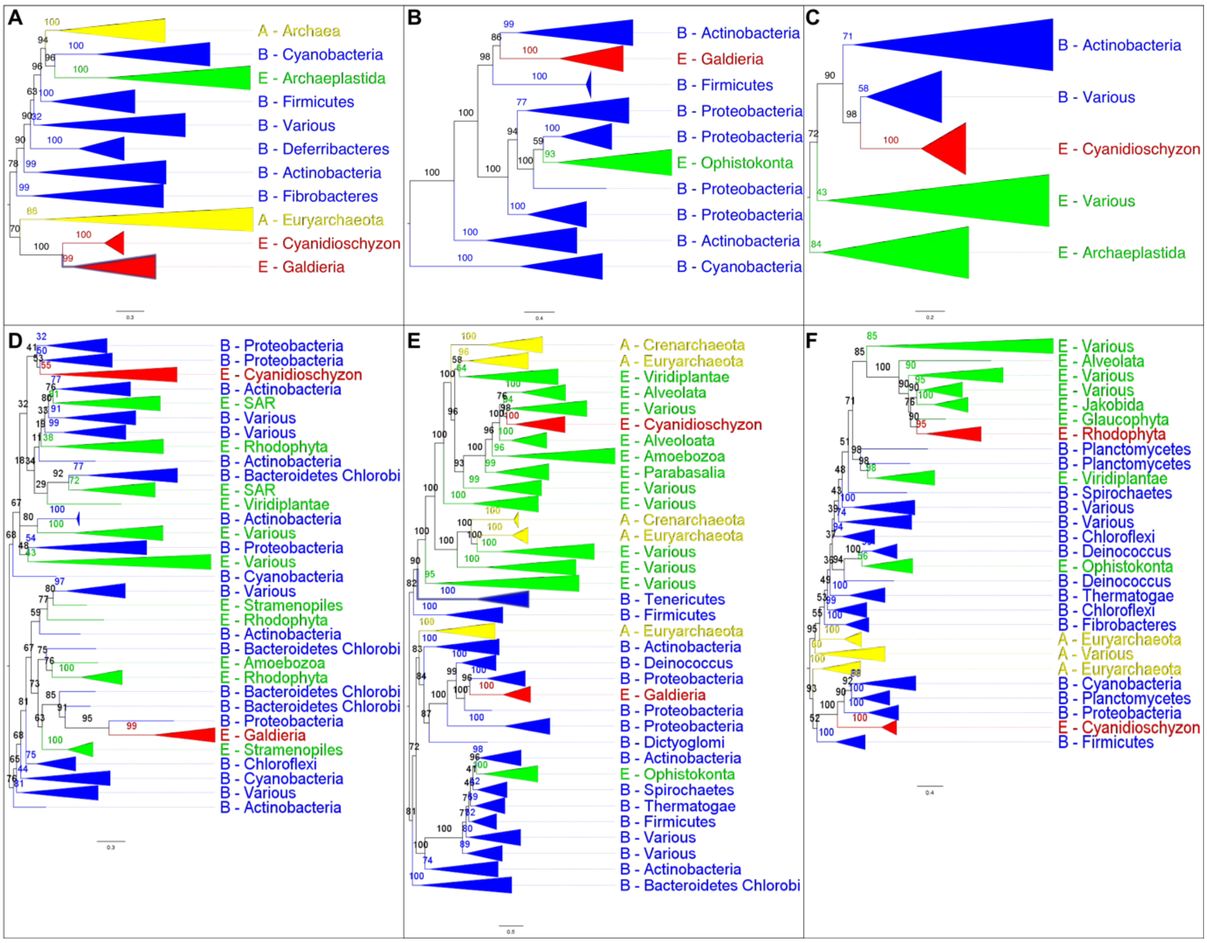

Figure 5 - The analysis of OGs containing HGT candidates revealed different patterns of HGT acquisition. Some OGs contain genes that are shared by all Cyanidiales, whereas others are unique to the *Galdieria* or *Cyanidioschyzon* lineage. In some cases, HGT appears to have replaced the eukaryotic genes in one lineage, whereas the other lineage maintained the eukaryotic ortholog. Here, some examples of OG phylogenies are shown, which were simplified for ease of presentation. The first letter of the tip labels indicates the kingdom. A = Archaea (yellow), B = Bacteria (blue), E = Eukaryota (green). Branches containing Cyanidiales sequences are highlited in red. **A|** Example of an ancient HGT that occurred before *Galdieria* and *Cyanidioschyzon* split into separate lineages. As such, both lineages are monophyletic (e.g., OG0001476). **B|** HGT candidates are unique to the *Galdieria* lineage (e.g. OG0001760). **C|** HGT candidates are unique to the *Cyanidioschyzon* lineage (e.g. OG0005738). **D|** *Galdieria* and *Cyanidioschyzon* HGT candidates are derived from different HGT events and share monophyly with different non-eukaryotic organisms (e.g., OG0003085). **E|** *Galdieria* HGT candidates cluster with non-eukaryotes, whereas the *Cyanidioschyzon* lineage clusters with eukaryotes (e.g., OG0001542). **F|** *Cyanidioschyzon* HGT candidates cluster with non-eukaryotes, whereas the *Galdieria* lineage clusters with eukaryotes (e.g., OG0006136).

Stronger erosion of HGT genes impedes assignment to HGT or DL

As already noted above, only 50/96 of the sampled HGT-impacted OGs do not appear to be affected by erosion. Dense sampling of 11 taxa within the *Galdieria* lineage allowed a more in-depth analysis of this issue. Here, a bimodal distribution is observed regarding the number of species per OG in the native and HGT dataset (**Figure 6C**). Only 52.5% of the native gene set is present in all *Galdieria* strains (defined as 10 and 11 strains in order to account for potential misassemblies and missed gene models during prediction). Approximately 1/3 of the native OGs (36.1%) has been affected by gene erosion to such a degree that it is present in only one, or two *Galdieria* strains. In comparison, 26.7% of the candidate HGT-impacted OGs are encoded in >10 *Galdieria* strains, whereas 53.0% are present in less than three. The latter number might be an underestimation due to the strict threshold for HGT discovery which led to the removal of HGT candidates that were singletons. The HGT distribution is therefore skewed towards OGs containing only a few or one *Galdieria* species as the result of recent HGT events that occurred; e.g., after the split of *G. sulphuraria* and *G. phlegrea*. In spite of the strong erosion which would also lead to partial fixation of presumably recent HGT events, we analyzed whether the distribution patterns of HGT candidates across the sequenced genomes reflect the branching pattern of the species trees (**Figure 4C**). This is true for all HGT candidates that are exclusive to the *Cyanidioschyzon* or *Galdieria* lineage. Either the HGT candidates were acquired after the split of the two lineages (according to HGT), or differentially lost in one of the two lineages (according to DL). In the 60 *Galdieria* specific OGs we found 12 OGs containing less than 10 and more than one *Galdieria* species (**Figure 4C**). In 5/12 of the cases, the presence absence pattern reflects the species tree (OG0005087, OG0005083, GO0005479, OG0005540). Here, the potential HGT candidates are not found in any other eukaryotic species. According to HGT, they were acquired by a monophyletic sub-clade of the *Galdieria* lineage. According to DL, they were lost in all eukaryotes with the exception of this subset of the *Galdieria* lineage (e.g., OG0005280 and OG0005083 were potentially acquired or maintained exclusively by the last common ancestor of *G. sulphuraria* 074W, *G. sulphuraria* MS1, *G. sulphuraria* RT22, and *G. sulphuraria* SAG21). In the remaining OGs, the HGT gene candidate is distributed across the *Galdieria* lineage and conflicts with the branching pattern of the species tree. HGT would assume either multiple independent acquisitions of the same HGT candidate, or partial fixation of the HGT candidate in the lineage, while still allowing for gene erosion. According to DL, these are the last existing paralogs of an ancient gene, whose erosion within the eukaryotic kingdom is nearly complete. However, it must be considered that in some cases, DL must have occurred independently across multiple species in a brief of time after the gene was maintained for hundreds of millions of years across the lineage (e.g., OG0005224 contains *G. phlegrea* Soos, *G. sulphuraria* Azora and *G. sulphuraria* MS1). This implies that the gene was present in the ancestor of the *Galdieria* lineage and also in the last common ancestor of closely related *G. sulphuraria* MS1, *G. sulphuraria* 074W and *G. sulphuraria* RT22 (as well as *G. sulphuraria* SAG21) and the last common ancestor of closely related *G. sulphuraria* MtSh, *G. sulphuraria*

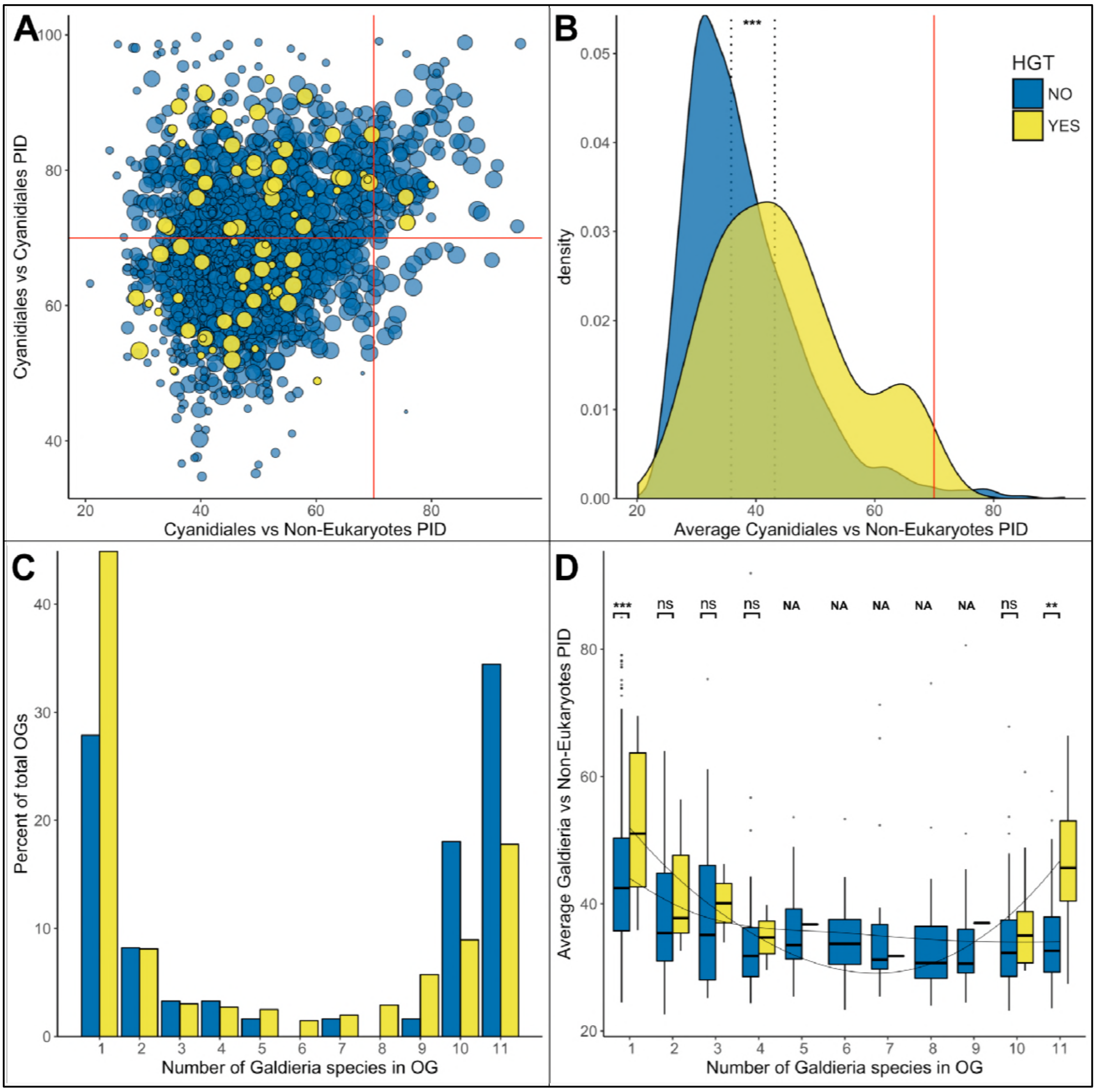

Figure 6 – HGT vs. non-HGT orthogroup comparisons. **A|** Maximum PID of Cyanidiales genes in native (blue) and HGT (yellow) orthogroups when compared to non-eukaryotic sequences in each OG. The red lines denote the 70% PID threshold for assembly artifacts according to "the 70% rule". Dots located in the top-right corner depict the 73 OGs that appear to contradict this rule, plus the 5 HGT candidates that score higher than 70%. 18/73 of those OGs are not derived from EGT or contamination within eukaryotic assemblies. **B|** Density curve of average PID towards non-eukaryotic species in the same orthogroup (potential non-eukaryotic donors in case of HGT candidates). The area under each curve is equal to 1. The average PID of HGT candidates (left dotted line) is 6.1% higher than the average PID of native OGs also containing non-eukaryotic species (right dotted line). This difference is significant (Wilcoxon rank-sum test, $p > 0.01$). **C|** Distribution of OG-sizes (=number of *Galdieria* species present in each OG) between the native and HGT dataset. A total of 80% of the HGT OGs and 89% of the native OGs are present in either ≤ 10 species, or ≤ 2 species. Whereas 52.5% of the native gene set is conserved in ≤ 10 *Galdieria* strains, only 36.1% of the HGT candidates are conserved. In contrast, about 50% of the HGT candidates are present in only one *Galdieria* strain. **D|** Pairwise OG-size comparison between HGT OGs and native OGs. A significantly higher PID when compared to non-eukaryotic sequences was measured in the HGT OGs at OG-sizes of 1 and 11 (Wilcoxon rank-sum test, BH, $p < 0.01$). No evidence of cumulative effects was detected in the HGT dataset. However, the fewer *Galdieria* species that are contained in one OG, the higher the average PID when compared to non-eukaryotic species in the same tree (Jonckheere-Terpstra, $p < 0.01$) in the native dataset.

Azora and *G. sulphuraria* YNP5578.1 (as well as *G. sulphuraria* 5572). A gene that was encoded and maintained since LECA, was lost independently in 6/8 species within the past few million years.

The seventy percent rule

In their analysis regarding eukaryotic HGT [13], Ku and co-authors reach the conclusion that prokaryotic homologs of genes in eukaryotic genomes that share >70% PID are not found outside individual genome assemblies (unless derived from endosymbiotic gene transfer, EGT). Hence, they are assembly artifacts. We analyzed whether our dataset supports this rule, or alternatively, it is arbitrary and a byproduct of the analysis approach used, combined with low eukaryotic sampling [14, 15]. In addition to the 96 OGs potentially acquired through HGT, 2,134 of the 9,075 total OGs contained non-eukaryotic sequences, in which the Cyanidiales sequences cluster within the eukaryotic kingdom, but are similar enough to non-eukaryotic species to produce blast hits. Based on the average PID, no OG contains HGT candidates that share over 70% PID to their non-eukaryotic donors with OG0006191 having the highest average PID (69.68%). However, 5/96 HGT-impacted OGs contain one or more individual HGT candidates that exceed this threshold (5.2% of the HGT OGs) (**Figure 6A**). These sequences are found in OG0001929 (75.56% PID, 11 *Galdieria* species), OG0002676 (75.76% PID, 11 *Galdieria* species), OG0006191 (80.00% PID, both *Cyanidioschyzon* species), OG0008680 (72.37% PID, 1 *Galdieria* species), and OG0008822 (71.17% PID, 1 *Galdieria* species). Moreover, we find 73 OGs with eukaryotes as sisters sharing over 70% PID to non-eukaryotic sequences (0.8% of the native OGs) (**Figure 6A**). On closer inspection, the majority are derived from endosymbiotic gene transfer (EGT): 16/73 of the OGs are of proteobacterial descent and 33/73 OGs are phylogenies with gene origin in Cyanobacteria and/or Chlamydia. These annotations generally encompass mitochondrial/plastid components and reactions, as well as components of the phycobilisome, which is exclusive to Cyanobacteria, red algae, and red algal derived plastids. Of the remaining 24 OGs, 18 cannot be explained through EGT or artifacts alone unless multiple eukaryotic genomes would share the same artifact (and also assuming all gene transfers from Cyanobacteria, Chlamydia, and Proteobacteria are derived from EGT). A total of 6 /24 OGs are clearly cases of contamination within the eukaryotic assemblies. Although “the 70% rule” captures a large proportion of the dataset, increasing the sampling resolution within eukaryotes increased the number of exceptions to the rule. This number is likely to increase as more high-quality eukaryote nuclear genomes are determined. Considering the paucity of these data across the eukaryotic tree of life and the rarity of eukaryotic HGT, the systematic dismissal of eukaryotic singletons located within non-eukaryotic branches as assembly/annotation artifacts (or contamination) may come at the cost of removing true positives.

Cumulative Effects

We assessed our dataset for evidence of cumulative effects within the candidate HGT-derived OGs. If cumulative effects were present, then recent HGT candidates would share higher similarity to their non-eukaryotic ancestors than genes resulting from more ancient HGT. Hence, the fewer species that are present in an OG, the higher likelihood of a recent HGT (unless the tree branching pattern contradicts this hypothesis, such as in OG 0005224, which is limited to 3 *Galdieria* species, but is ancient due to its presence in *G. sulphuraria* and *G. phlegrea*). In the case of DL, no cumulative effects as well as no differences between the HGT and native dataset are expected because the PID between eukaryotes and non-eukaryotes is irrelevant to this issue because all genes are native and occurred in the LECA. According to DL, the monophyletic position of Cyanidiales HGT candidates with non-eukaryotes is determined by the absence of other eukaryotic orthologs (given the limited current data) and may be the product of deep branching effects.

First, we tested for general differences in PID with regard to non-eukaryotic sequences between the native and HGT datasets (**Figure 6B**). Neither the PID with non-eukaryotic species in the same OG for the native dataset, nor the PID with potential non-eukaryotic donors in the same OG for the HGT dataset was normally distributed (Shapiro-Wilk normality test, p = 2.2e-16/0.00765). Consequently, exploratory analysis was performed using non-parametric testing. On average, the PID with non-eukaryotic species in OGs containing HGT candidates is higher by 6.1% in comparison to OGs with eukaryotic descent. This difference is significant (Wilcoxon rank-sum test, p = 0.000008).

Second, we assessed if OGs containing fewer *Galdieria* species would have a higher PID with their potential non-eukaryotic donors in the HGT dataset. We expected a lack of correlation with OG size in the native dataset because the presence/absence pattern of HGT candidates within the *Galdieria* lineage is dictated by gene erosion and thus independent of which non-eukaryotic sequences also cluster in the same phylogeny. Jonckheere's test for trends revealed a significant trend within the native subset: the fewer *Galdieria* species that are contained in one OG, the higher the average PID with non-eukaryotic species in the same tree (Jonckheere-Terpstra, p = 0.002). This was not the case in the "HGT" subset. Here, no general trend was observed (Jonckheere-Terpstra, p = 0.424).

Third, we compared the PID between HGT-impacted OGs and native OGs of the same size (OGs containing the same number of *Galdieria* species). This analysis revealed a significantly higher PID with non-eukaryotic sequences in favor of the HGT subset in OGs containing either one *Galdieria* sequence, or all eleven *Galdieria* sequences (Wilcoxon rank-sum test, Benjamini-Hochberg, p = 2.52e-08| 3.39e-03) (**Figure 6D**). Hence, the "most recent" and "most complete ancient" HGT candidates share the highest idenitity with their non-eukaryotic donors, which is also significantly higher when compared to native genes in OGs of the same size.

Potential HGT donors share the same habitats with Cyanidiales

To identify the potential sources of HGT, we counted the frequency at which any non-eukaryotic species shared monophyly with Cyanidiales (**Table 2**). A total of 568 non-eukaryotic species (19 Archaea, 549 Bacteria), from 365 different genera representing 24 divisions share monophyly with the 96 OGs containing HGT candidates. The most prominent source of HGT are Proteobacteria that are sister phyla to 53/96 OGs. This group is followed by Firmicutes (28), Actinobacteria (19), Chloroflexi (12), and Bacteroidetes/Chlorobi (10). The only frequently occurring Archaeal donors were the Euryarchaeota, which may be the potential source of HGT in 6 OGs. Because the Cyanidiales are extremophiles, we hypothesized that potential non-eukaryotic HGT donors might share similar habitats because proximity is thought to favor HGT. We evaluated the habitats of the most frequently identified HGT donors. The most prominent was *Sulfobacillus thermosulfidooxidans* (Firmicutes), a mixotrophic, acidophilic (pH 2.0) and moderately thermophilic (45°C)

Table 2 (below) – List of the most recurring potential non-eukaryotic HGT donors. Numbers in brackets represent how many times HGT candidates from Cyanidiales shared monophyly with non-eukaryotic organisms. E.g: Proteobacteria were found in 53/96 of the OG monophylies. **Kingdom**: Taxon at kingdom level. **Species**: Scientific species name. **Habitat**: habitat description of the original sampling site. **pH**: pH of the original sampling site. **Temp**: Temperature in Celsius of the sampling site. **Salt**: Ion concentration of the original sampling site. **na**: no information available.

Kingdom	Phylogeny		Natural habitat of potential HGT donor			
	Division	Species	Habitat description	pH	Max. Temp	Salt
Bacteria	Proteobacteria (53)	*Acidithiobacillus thiooxidans (4)*	Mine drainage/Mineral ores	2.0 - 2.5	30°C	"hypersaline"
		Carnimonas nigrificans (4)	Raw cured meat	3	35°C	8% NaCl
		Methylosarcina fibrata (4)	Landfill	5 - 9	37°C	1% NaCl
		Sphingomonas phyllosphaerae (3)	Phyllosphere of Acacia caven	na	28°C	na
		Gluconacetobacter diazotrophicus (3)	Symbiont of various plant species	2 - 6	na	"high salt"
		Gluconobacter frateurii (3)	na	na	na	na
		Luteibacter yeojuensis (3)	River	na	na	na
		Thioalkalivibrio sulfidiphilus (3)	Soda lake	8 - 10.5	40°C	15% total salts
		Thiomonas arsenitoxydans (3)	Disused mine site	3 - 8	30°C	"halophilic"
	Firmicutes (28)	*Sulfobacillus thermosulfidooxidans (6)*	Copper mining	2 - 2.5	45°C	"salt tolerant"
		Alicyclobacillus acidoterrestris (4)	Soil sample	2 - 6	53°C	5% NaCl
		Gracilibacillus lacisalsi (3)	Salt lake	7.2–7.6	50°C	25% total salts
	Actinobacteria (19)	*Amycolatopsis halophila (3)*	Salt lake	6 - 8	45°C	15% NaCl
		Rubrobacter xylanophilus (3)	Thermal industrial runoff	6 - 8	60°C	6.0% NaCl
	Chloroflexi (12)	*Caldilinea aerophila (4)*	Thermophilic granular sludge	6 - 8	65°C	3% NaCl
		Ardenticatena maritima (3)	Coastal hydrothermal field	5.5 - 8.0	70°C	6% NaCl
		Ktedonobacter racemifer (3)	Soil sample	4.8 - 6.8	33°C	> 3% NaCl
	Bacteroidetes Chlorobi (10)	*Salinibacter ruber (4)*	Saltern crystallizer ponds	6.5 - 8	52°C	30% total salts
		Salisaeta longa (3)	Experimental mesocosm (Salt)	6.5-8.5.	46°C	20% NaCl
	Nitrospirae (7)	*Leptospirillum ferriphilum (4)*	Arsenopyrite biooxidation tank	0 - 3	40°C	2% NaCl
	Fibrobacteres (6)	*Acidobacteriaceae bacterium TAA166 (3)*	na	na	na	na
	Deinococcus (5)	*Truepera radiovictrix (3)*	Hot spring runoffs	7.5 - 9.5	na	6% NaCl
Archaea	Euryarchaeota (6)	*Ferroplasma acidarmanus (3)*	Acid mine drainage	0 - 2.5	40°C	"halophilic"

bacterium that was isolated from acid mining environments in northern Chile (where *Galdieria* is also present). *Sulfobacillus thermosulfidooxidans* shares monophyly in 6/96 HGT-derived OGs and is followed in frequency by several species that are either thermophiles, acidophiles, or halophiles and share habitats common with Cyanidiales (**Table 2**).

Functions of horizontally acquired genes in Cyanidiales

We analyzed the putative molecular functions and processes acquired through HGT. Annotations were curated using information gathered from blast, GO-terms, PFAM, KEGG, and EC. A total of 72 GO annotations occurred more than once within the 96 HGT-impacted OGs. Furthermore, 37/72 GO annotations are significantly enriched (categorical data, "native" vs "HGT", Fisher's exact test, Benjamini-Hochberg, $p \leq 0.05$). The most frequent terms were: "decanoate-CoA ligase activity" (5/72 GOs, $p = 0$), "oxidation-reduction process" (16/72 GOs, $p = 0.001$), "transferase activity" (14/72 GOs, $p = 0.009$), "carbohydrate metabolic process" (5/72 GOs, $p = 0.01$), "oxidoreductase activity" (9/72 GOs, $p = 0.012$), "methylation" (6/72 GOs, $p = 0.013$), "methyltransferase activity" (5/72 GOs, $p = 0.023$), "transmembrane transporter activity" (4/72 GOs, $p = 0.043$), and "hydrolase activity" (9/72 GOs, $p = 0.048$). In comparison to previous studies, our analysis did not report a significant enrichment of membrane proteins in the HGT dataset ("membrane", 11/72 OGs, $p = 0.699$; "integral component of membrane", 22/72 GOs, $p = 0.416$. The GO annotation "extracellular region" was absent in the HGT dataset) [22]. As such, we report a strong bias for metabolic functions among HGT candidates (**Figure 7**).

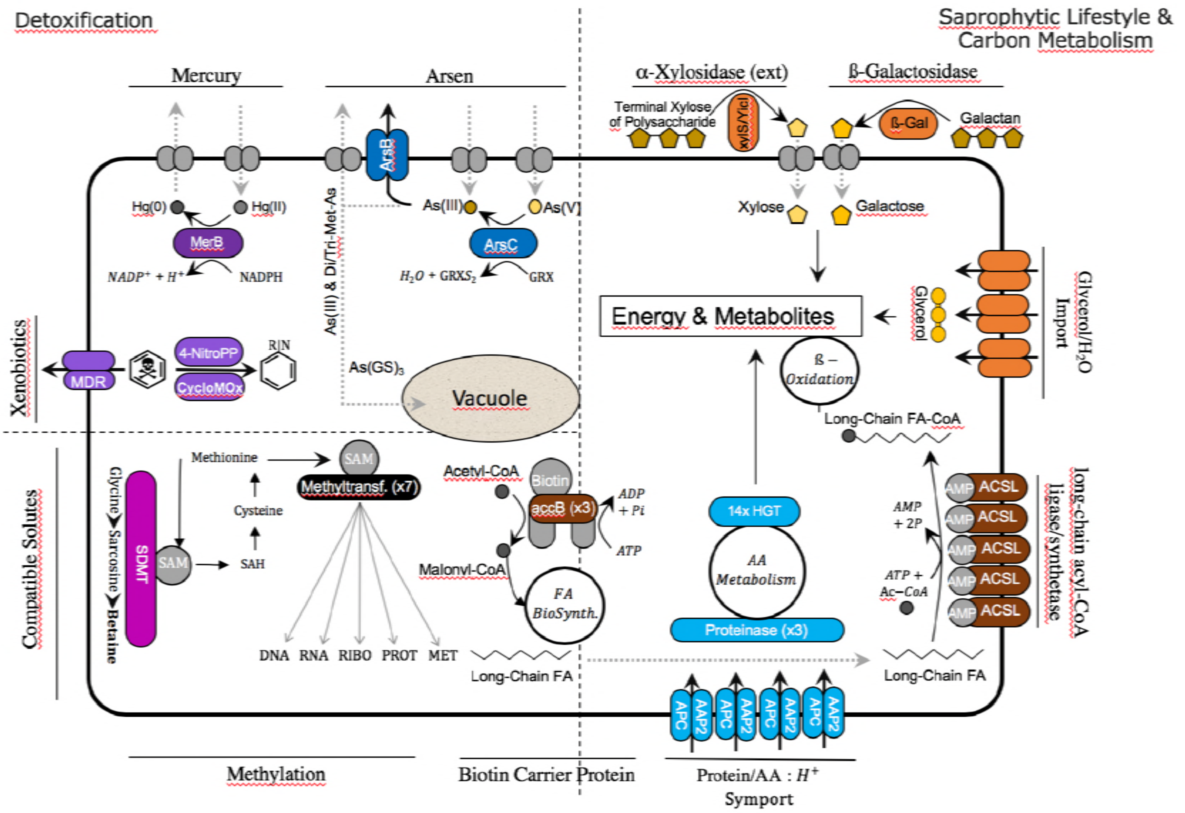

Figure 7 – Cyanidiales live in hostile habitats, necessitating a broad range of adaptations to polyextremophily. The majority of the 96 HGT-impacted OGs were annotated and putative functions identified (in the image, colored fields are from HGT, whereas gray fields are native functions). The largest number of HGT candidates is involved in carbon and amino acid metabolism, especially in the *Galdieira* lineage. The excretion of lytic enzymes and the high number of importers (protein/AA symporter, glycerol/H_2O symporter) within the HGT dataset suggest a preference for import and catabolic function.

Metal and xenobiotic resistance/detoxification

Geothermal environments often contain high arsenic (Ar) concentrations, up to a several g/L as well as high levels of mercury (Hg), such as > 200 g/g in soils of the Norris Geyser Basin (Yellowstone National Park) and volcanic waters in southern Italy [78, 79], both known Cyanidiales habitats [16, 29, 80, 81]. Studies with *G. sulphuraria* have shown an increased efficiency and speed regarding the biotransformation of $HgCl_2$ compared to eukaryotic algae [82]. Orthologs of OG0002305, which are present in all 13 Cyanidiales genomes, encode mercuric reductase that catalyzes the critical step in Hg^{2+} detoxification, converting cytotoxic Hg^{2+} into the less toxic metallic mercury, Hg^{0}. Arsenate (As(V)) is imported into the cell by high-affinity P$_i$ transport systems [83, 84], whereas aquaporins regulate arsenite (As(III)) uptake [85]. *Galdieria* and *Cyanidioschyzon* possess a eukaryotic gene-set for the chemical detoxification and extrusion of As through biotransformation and direct efflux [22]. Arsenic tolerance was expanded in the *Galdieria* lineage through the acquisition (OG0001513) of a bacterial ***arsC*** gene, thus enabling the reduction of As(V) to As(III) using thioredoxin as the electron acceptor. It is known that As(III) can be converted into volatile dimethylarsine and trimethylarsine through a series of reactions, exported, or transported to the vacuole in conjugation with glutathione. Two separate acquisitions of a transporter annotated as ArsB are present in *G. sulphuraria* RT22 and *G. sulphuraria* 5572 (OG0006498, OG0006670), as well as a putative cytoplasmic heavy metal binding protein (OG0006191) in the *Cyanidioschyzon* lineage.

In the context of xenobiotic detoxification, we found an aliphatic nitrilase (OG0001760) involved in styrene degradation and three (OG0003250, OG0005087, OG0005479) *Galdieria* specific 4-nitrophenylphosphatases likely involved in the bioremediation of highly toxic hexachlorocyclohexane (HCH) [86], or more generally other cyclohexyl compounds, such as cyclohexylamine. In this case, bioremediation can be achieved through the hydrolysis of 4-nitrophenol to 4-nitrophenyl phosphate coupled with phosophoesterase/metallophosphatase activity. The resulting cyclohexyl compounds serve as multifunctional intermediates in the biosynthesis of various heterocyclic and aromatic metabolites. A similar function in the *Cyanidioschyzon* lineage could be taken up by OG0006252, a cyclohexanone monooxygenase [87] oxidizing phenylacetone to benzyl acetate that can also oxidize various aromatic ketones, aliphatic ketones (e.g., dodecan- 2-one) and sulfides (e.g., 1-methyl-4-(methylsulfanyl)benzene). In this context, a probable multidrug-resistance/quaternary ammonium compound exporter (OG0002896), which is present in all Cyanidiales, may control relevant efflux functions whereas a phosphatidylethanolamine (penicillin?) binding protein (OG0004486) could increase the stability of altered peptidoglycan cell walls. If these annotations are correct, then *Galdieria* is an even more promising target for industrial bioremediation applications than previously thought [88, 89].

Cellular oxidant reduction

Increased temperature leads to a higher metabolic rate and an increase in the production of endogenous free radicals (FR), such as reactive oxygen species (ROS) and reactive nitrogen species (RNS), for example during cellular respiration [90]. Furthermore, heavy metals such as lead and mercury, as well as halogens (fluorine, chlorine, bromine, iodine) stimulate formation of FR [91]. FR are highly biohazard and cause damage to lipids [92], proteins [93] and DNA [94]. In the case of the superoxide radical ($^{\bullet}O^{2-}$), enzymes such as superoxide dismutase enhance the conversion of 2 x $^{\bullet}O^{2-}$, into hydrogen peroxide (H_2O_2) which is in turn reduced to H_2O through the glutathione-ascorbate cycle. Other toxic hydroperoxides (R-OOH) can be decomposed various peroxidases to H_2O and alcohols (R-OH) at the cost of oxidizing the enzyme, which is later recycled (re-reduced) through oxidation of thioredoxin [95]. The glutathione and thioredoxin pools and their related enzymes are thus factors contributing to a successful adaptation to geothermal environments. Here, we found a cytosolic and/or extracellular peroxiredoxin-6 (OG0005984) specific to the *Cyanidioschyzon* lineage and two peroxidase-related enzymes (probable alkyl hydroperoxide reductases acting on carboxymuconolactone) in the *Galdieria* lineage (OG0004203, OG0004392) [96]. In addition, a thioredoxin oxidoreductase related to alkyl hydroperoxide reductases (OG0001486) as well as a putative glutathione-specific gamma-glutamylcyclotransferase 2 (OG0003929) are present in all Cyanidiales. The latter has been experimentally linked to the process of heavy metal detoxification in *Arabidopsis thaliana* [97].

Carbon Metabolism

Galdieria sulphuraria is able to grow heterotrophically using a large variety of different carbon sources and compounds released from dying cells [98, 99]. In contrast, *C. merolae* is strictly photoautotrophic [100]. *G. sulphuraria* can be maintained on glycerol as the sole carbon source [98] making use of a family of glycerol uptake transporters likely acquired via HGT [22]. We confirm the lateral acquisition of glycerol transporters in *G. sulphuraria* RT22 (OG0006482), *G. sulphuraria* Azora and *G. sulphuraria* SAG21 (OG0005235). The putative HGT glycerol transporters found in *G. sulphuraria* 074W did not meet the required threshold of two Cyanidiales sequences (from different strains) in one OG. In addition, another MIP family aquaporin, permeable to H_2O, glycerol and other small uncharged molecules [101] is encoded by *G. sulphuraria* Azora (OG0007123). This could be an indication of a very diverse horizontal acquisition pattern regarding transporters. OG0003954 is the only exception to this rule, because it is present in all *Galdieria* lineages and is orthologous to AcpA|SatP acetate permeases involved with the uptake of acetate and succinate [102, 103].

We found evidence of saprophytic adaptations in *Galdieria* through the potential horizontal acquisition of an extracellular beta-galactosidase enzyme [104, 105]. This enzyme contains all five bacterial beta-galactosidase domains (OG0003441) involved in the catabolism of glycosaminoglycans, a polysaccharide deacetylase/peptidoglycan-N-acetylglucosamine deacetylase (OG0004030) acting on glucosidic (but note peptide bonds) that may degrade chitooligosaccharides, chitin, and/or xylan [106, 107] as well as an α-amylase (OG0004658) converting starch/glycogen to dextrin/maltose [108] which is missing only in *G. sulphuraria* SAG21. All other HGT OGs involved in sugar metabolism are involved in the intercellular breakdown and interconversions of sugar carbohydrates.

OG0006623 contains a non-phosphorylating glyceraldehyde-3-phosphate dehydrogenase found in hyperthermophile archaea [109] (*G. sulphuraria* 002). The OG0005153 encodes a glycosyl transferase family 1 protein involved in carbon metabolism (*G. sulphuraria* 074W, *G. sulphuraria* MS1, *G. sulphuraria* RT22, *G. sulphuraria* YNP5587.1). All *Galdieria* have an alpha-xylosidase resembling an extremely thermo-active and thermostable α-galactosidase (OG0001542) [110, 111]. The only horizontal acquisition in this category present in all Cyanidiales is a cytoplasmic ribokinase involved in the D-ribose catabolic process (OG0001613).

The irreversible synthesis of malonyl-CoA from acetyl-CoA through acetyl-CoA carboxylase (ACCase) is the rate limiting and step in fatty acid biosynthesis. The bacterial ACCase complex consists of three separate subunits, whereas the eukaryotic ACCase is composed of a single multifunctional protein. Plants contain both ACCase isozymes. The eukaryotic enzyme is located in the cytosol and a bacterial-type enzyme consisting of four subunits is plastid localized. Three of the HGT orthogroups (OG0002051, OG0007550 and OG0007551) were annotated as bacterial biotin carboxyl carrier proteins (AbbB/BCCP), which carry biotin and carboxybiotin during the critical and highly regulated carboxylation of acetyl-CoA to form malonyl-CoA [ATP + Acetyl-CoA + HCO^{3-} ⇌ ADP + Orthophosphate + Malonyl-CoA]. Whereas OG0002051 is present in all Cyanidiales and located in the cytoplasm, OG0007550 and OG0007551 are unique to *C. merolae* Soos and annotated as "chloroplastic". Prior to fatty acid (FA) beta-oxidation, FAs need to be transformed to a FA-CoA before entering cellular metabolism as an exogenous or endogenous carbon source (eicosanoid metabolism is the exception). This process is initiated by long-chain-fatty-acid-CoA ligases/acyl-CoA synthetases (ACSL) [112][ATP + long-chain carboxylate + CoA ⇌ AMP + diphosphate + Acyl-CoA]. Five general non-eukaryotic ACSL candidates were found (OG0001476, OG0002999, OG0005540, OG0008579, OG0008822). Only OG0001476 is present in all species, whereas OG0002999 is present in all *Galdieria,* OG0005540 in *G. sulphuraria* 074W and *G. sulphuraria* MS1, and OG0008579 and OG0008822 are unique to *G. phlegrea* DBV009. The GO annotation suggests moderate specificity to decanoate-CoA. However, OG0002999 also indicates involvement in the metabolism of linoleic acid, a $C_{18}H_{32}O_2$ polyunsaturated acid found in plant glycosides. ACSL enzymes share significant sequence identity but show partially overlapping substrate preferences in terms of length and saturation as well as unique transcription patterns. Furthermore, ACSL proteins play a role in channeling FA degradation to various pathways, as well as enhancing FA uptake and FA cellular retention. Although an annotation of the different ACSL to their specific functions was not possible, their involvement in the saprophytic adaptation of *Cyanidioschyzon* and especially *Galdieria* appears to be plausible.

Amino Acid Metabolism

Oxidation of amino acids (AA) can be used as an energy source. Once AAs are deaminated, the resulting α-ketoacids ("carbon backbone") can be used in the tricarboxylic acid cycle for energy generation, whereas the remaining NH_4^+ can be used for the biosynthesis of novel AAs, nucleotides, and ammonium containing compounds, or dissipated through the urea cycle. In this context, we confirm previous observations regarding a horizontal origin of the urease accessory protein UreE (OG0003777) present in the *Galdieria* lineage [23] (the other urease genes reported in *G. phlegrea* DBV009 appear to be unique to this species and were thus removed from this analysis as singletons; e.g., *ureG*, OG0008984). AAs are continuously synthesized, interconverted, and degraded using a complex network of balanced enzymatic reactions (e.g., peptidases, lyases, transferases, isomerases). Plants maintain a functioning AA catabolism that is primarily used for the interconversion of metabolites because photosynthesis is the primary source of energy. The Cyanidiales, and particularly the *Galdieria* lineage is known for its heterotrophic lifestyle. We assigned 19/96 HGT-impacted OGs to this category. In this context, horizontal acquisition of protein|AA:proton symporter AA permeases (OG0001658, OG0005224, OG0005596, OG0007051) may be the first indication of adaptation to a heterotrophic lifestyle in *Galdieria*. Once a protein is imported, peptidases cleave single AAs by hydrolyzing the peptide bonds. Although no AA permeases were found in the *Cyanidioschyzon* lineage, a cytoplasmic threonine-type endopeptidase (OG0001994) and a cytosolic proline iminopeptidase involved in arginine and proline metabolism (OG0006143) were potentially acquired through HGT. At the same time, the *Galdieria* lineage acquired a Clp protease (OG0007596). The remaining HGT candidates are involved in various amino acid metabolic pathways. The first subset is shared by all Cyanidiales, such as a cytoplasmic imidazoleglycerol-phosphate synthase involved in the biosynthetic process of histidine (OG0002036), a phosphoribosyltransferase involved in phenylalanine/tryptophan/tyrosine biosynthesis (OG0001509) and a peptydilproline peptidyl-prolyl cis-trans isomerase acting on proline (OG0001938) [113]. The second subset is specific to the *Cyanidium* lineage. It contains a glutamine/leucine/phenylalanine/valine dehydrogenase (OG0006136) [114], a glutamine cyclotransferase (OG0006251) [115], a cytidine deaminase (OG0003539) as well as an adenine deaminase (OG0005683) and a protein binding hydrolase containing a NUDIX domain (OG0005694). The third subset is specific to the *Galdieria* lineage and contains an ornithine deaminase, a glutaryl-CoA dehydrogenase (OG0007383) involved in the oxidation of lysine, tryptophan, and hydroxylysine [116], as well as an ornithine cyclodeaminase (OG0004258) involved in arginine and/or proline metabolism. Finally, a lysine decarboxylase (OG0007346), a bifunctional ornithine acetyltransferase/N-acetylglutamate synthase [117] involved in the arginine biosynthesis (OG0008898) and an aminoacetone oxidase family FAD-binding enzyme (OG0007383), probably catalytic activity against several different L-amino acids were found as unique acquisitions in *G. sulphuraria* SAG21, *G. phlegrea* DBV009 and *G. sulphuraria* YNP5578.1 respectively.

One Carbon Metabolism and Methylation

One-carbon (1C) metabolism based on folate describes a broad set of reactions involved in the activation and transfer C1 units in various processes including the synthesis of purine, thymidine, methionine, and homocysteine re-methylation. C1 units can be mobilized using tetrahydrofolate (THF) as a cofactor in enzymatic reactions, vitamin B12 (cobalamin) as a co-enzyme in methylation/rearrangement reactions and S-adenosylmethionine (SAM) [118]. In terms of purine biosynthesis, OG0005280 encodes an ortholog of a bacterial FAD-dependent thymidylate (dTMP) synthase converting dUMP to dTMP by oxidizing THF present in *G. sulphuraria* 074W*, G. sulphuraria* MS1, and *G. sulphuraria* RT22. In terms of vitamin B12 biosynthesis, an ortholog of the cobalamin biosynthesis protein CobW was found in the *Cyanidioschyzon* lineage (OG0002609). Much of the methionine generated through C1 metabolism is converted to SAM, the second most abundant cofactor after ATP, which is a universal donor of methyl (-CH_3) groups in the synthesis and modification of DNA, RNA, hormones, neurotransmitters, membrane lipids, proteins and also play a central role in epigenetics and posttranslational modifications. Within the 96 HGT-impacted dataset we found a total of 9 methyltransferases (OG0003901, OG0003905, OG0002191, OG0002431, OG0002727, OG0003907, OG0005083 and OG0005561) with diverse functions, 8 of which are SAM-dependent methyltransferases. OG0002431 (Cyanidiales), OG0005561 (*G. sulphuraria* MS1 and *G. phlegrea* DBV009) and OG0005083 (*G. sulphuraria* SAG21) encompass rather unspecific SAM-dependent methyltransferases with a broad range of possible methylation targets. OG0002727, which is exclusive to *Cyanidioschyzon*, and OG0002191, which is exclusive to *Galdieria,* both methylate rRNA. OG0002727 belongs to the Erm rRNA methyltransferase family that methylate adenine on 23S ribosomal RNA [119]. Whether it confers macrolide-lincosamide-streptogramin (MLS) resistance, or shares only adenine methylating properties remains unclear. The OG0002191 is a 16S rRNA (cytidine1402-2'-O)-methyltransferase involved the modulation of translational fidelity [120].

Osmotic resistance and salt tolerance

Cyanidiales withstand salt concentrations up to 10% NaCl [121]. The two main strategies to prevent the accumulation of cytotoxic salt concentrations and to withstand low water potential are the active removal of salt from the cytosol and the production of compatible solutes. Compatible solutes are small metabolites that can accumulate to very high concentrations in the cytosol without negatively affecting vital cell functions while keeping the water potential more negative in relation to the saline environment, thereby avoiding loss of water. The *G. sulphuraria* lineage produces glycine/betaine as compatible solutes under salt stress in the same manner as halophilic bacteria [122] through the successive methylation of glycine via sarcosine and dimethylglycine to yield betaine using S-adenosyl methionine (SAM) as a cofactor [123-125]. This reaction is catalyzed by the enzyme sarcosine dimethylglycine methyltransferase (SDMT), which has already been characterized in *Galdieria* [126]. Our results corroborate the HGT origin of this gene, supporting two separate acquisitions of this function (OG0003901, OG0003905). In this context, a inositol 2-dehydrogenase possibly involved in osmoprotective functions [127] in *G. phlegrea* DBV009 was also found in the HGT dataset (OG0008335).

Non-Metabolic functions

Outside the context of HGT involving enzymes that perform metabolism related functions, we found 6/96 OGs that are annotated as transcription factors, ribosomal components, rRNA, or fulfilling functions not directly involved in metabolic fluxes. Specifically, two OGs associated with the bacterial 30S ribosomal subunit were found, whereas OG0002627 (*Galdieria*) is orthologous to the tRNA binding translation initiation factor eIF1a which binds the fMet-tRNA(fMet) start site to the ribosomal 30S subunit and defines the reading frame for mRNA translation [128], and OG0004339 (*Galdieria*) encodes the S4 structural component of the S30 subunit. Three genes functioning as regulators were found in *Cyanidioschyzon*, a low molecular weight phosphotyrosine protein phosphatase with an unknown regulator function (OG0002785), a SfsA nuclease [129], similar to the sugar fermentation stimulation protein A and (OG0002871) a MRP family multidrug resistance transporter connected to parA plasmid partition protein, or generally involved in chromosome partitioning (mrp). Additionally, we found a *Cyanidioschyzon*-specific RuvX ortholog (OG0002578) involved in chromosomal crossovers with endonucleolytic activity [130] as well as a likely Hsp20 heat shock protein ortholog (OG0004102) unique to the *Galdieria* lineage.

Various functions and uncertain annotations

The remaining OGs were annotated with a broad variety of functions. For example, OG0001929, OG0001810, OG0004405, and OG0001087 are possibly connected to the metabolism of cell wall precursors and components and OG0001929 (*Galdieria*) is an isomerizing glutamine-fructose-6-phosphate transaminase most likely involved in regulating the availability of precursors for N- and O-linked glycosylation of proteins, such as for peptidoglycan. In contrast, OG0004405 (*Cyanidioschyzon*) synthesizes exopolysaccharides on the plasma membrane and OG0001087 (*Cyanidiales*) and OG0001810 (*Cyanidioschyzon*) are putative undecaprenyl transferases (UPP) which function as lipid carrier for glycosyl transfer in the biosynthesis of cell wall polysaccharide components in bacteria [131]. The OGs OG0002483 and OG0001955 are involved in purine nucleobase metabolic processes, probably in cAMP biosynthesis [132] and IMP biosynthesis [133]. A *Cyanidioschyzon* specific 9,15,9'-tri-cis-zeta-carotene isomerase (OG0002574) may be involved in the biosynthesis of carotene [134]. Two of the 96 HGT OGs obtained the tag “hypothetical protein” and could not be further annotated. Others had non-specific annotations, such as “selenium binding protein” (OG0003856) or contained conflicting annotations.

Discussion

Making an argument for the importance of HGT in eukaryote (specifically, Cyanidiales) evolution, as we do here, requires that three major issues are addressed: a mechanism for foreign gene uptake and integration, the apparent absence of eukaryotic pan-genomes, and the lack of evidence for cumulative effects [12]. The latter two arguments are dealt with below but the first concern no longer exists. For example, recent work has shown that red algae harbor naturally occurring plasmids, regions of which are integrated into the plastid DNA of a taxonomically wide array of species [135]. Genetic transformation of the unicellular red alga *Porphyridium purpureum* has demonstrated that introduced plasmids accumulate episomally in the nucleus and are recognized and replicated by the eukaryotic DNA synthesis machinery [136]. These results suggest that a connection can be made between the observation of bacterium-derived HGTs in *P. purpureum* [34] and a putative mechanism of bacterial gene origin *via* long-term plasmid maintenance. Other proposed mechanisms for the uptake and integration of foreign DNA in eukaryotes are well-studied, observed in nature, and can be successfully recreated in the lab [15, 136].

HGT- the eukaryotic pan-genome

Eukaryotic HGT is rare and affected by gene erosion. Within the 13 analyzed genomes of the polyextremophilic Cyanidiales [35, 36], we identified and annotated 96 OGs containing 641 single HGT candidates. Given an approximate age of 1,400 Ma years and ignoring gene erosion, on average, one HGT event occurs every 14.6 Ma years in Cyanidiales. This figure ranges from one HGT every 33.3 Ma years in *Cyanidioschyzon* and one HGT every 13.3 Ma in *Galdieria*. Still, one may ask, given that eukaryotic HGT exists, what comprises the eukaryotic pan-genome and why does it not increase in size as a function of time due to HGT accumulation? In response, it should be noted that evolution is "blind" to the sources of genes and selection does not act upon native genes in a manner different from those derived from HGT. In our study, we report examples of genes derived from HGT that are affected by gene erosion and/or partial fixation (**Figure 4A**). As such, only 8/96 of the HGT-impacted OGs (8.3%) are encoded by all 13 Cyanidiales species. Looking at the *Galdieria* lineage alone (**Figure 6C**), 28 of the 60 lineage-specific OGs (47.5%) show clear signs of erosion (HGT orthologs are present in ≤ 10 *Galdieria* species), to the point where a single ortholog of an ancient HGT event may remain.

When considering HGT in the Cyanidiales it is important to keep in mind the ecological boundaries of this group, the distance between habitats, the species composition of habitats, and the mobility of Cyanidiales within those borders that control HGT. Hence, we would not expect the same HGT candidates derived from the same non-eukaryotic donors to be shared between Cyanidiales and marine/freshwater red algae (unless they predate the split between Cyanidiales and other red algae), but rather between Cyanidiales and other polyextremophilic organisms. In this context, inspection of the habitats and physiology of potential HGT donors revealed that the vast majority is extremophilic and, in some cases, shares the same habitat as Cyanidiales (**Table 2**). A total of 84/96 of the inherited gene functions could be connected to ecologically important traits such as heavy metal detoxification, xenobiotic detoxification, ROS scavenging, and metabolic functions related to carbon, fatty acid, and amino acid turnover. In contrast, only 6/96 OGs are related to methylation and ribosomal functions. We did not find HGTs contributing other traits such as ultrastructure, development, or behavior (**Figure 7**). If cultures were exposed to abiotic stress, the HGT candidates were significantly enriched within the set of differentially expressed genes (**Figure 3**). These results not only provide evidence of successful integration into the transcriptional circuit of the host, but also support an adaptive role of HGT as a mechanism to acquire beneficial traits. Because eukaryotic HGT is the exception rather than the rule, its number in eukaryotic genomes does not need to increase as a function of time and may have reached equilibrium in the distant past between acquisition and erosion.

HGT vs. DL

Ignoring the cumulative evidence from this and many other studies, one may still dismiss the phylogenetic inference as mere assembly artefact and overlook all the significant differences and trends between native genes and HGT candidates. This could be done by superimposing vertical inheritance (and thus eukaryotic origin) on all HGT events outside the context of pathogenicity and endosymbiosis. Under this extreme view, all extant genes would have their roots in LECA. Consequently, patchy phylogenetic distributions are the result of multiple putative ancient paralogs existing in the LECA followed by mutation, gene duplication, and gene loss. Following this line of reasoning, all HGT candidates in the Cyanidiales would be the product of DL acting on all other eukaryotic species, with the exception of the Cyanidiales, *Galdieria* and/or *Cyanidioschyzon* (**Figure 5A-C**). However, we found cases where either *Galdieria* HGT candidates (6 orthogroups), or *Cyanidioschyzon* HGT candidates (8 orthogroups) show non-eukaryotic origin, whereas the others cluster within the eukaryotic branch (**Figure 5E-F**). In addition, we find two cases in which *Galdieria* and *Cyanidioschyzon* HGT candidates are located in different non-eukaryotic branches (**Figure 5D**). DL would require LECA to have encoded three paralogs of the same gene, one of which was retained by *Cyanidioschyzon*, another by *Galdieria*, whereas the third by all other eukaryotes. The number of required paralogs in the LECA would be further increased when taking into consideration that some ancient paralogs of LECA may have been eroded in all eukaryotes and that eukaryote phylogenies are not always monophyletic which would additionally increase the number of required paralogs in the LECA in order to explain the current pattern. The strict superimposition of vertical inheritance would thus require a complex LECA, an issue known as “the genome of Eden”.

Cumulative effects are observed when genes derived from HGT increasingly diverge as a function of time. Hence, a gradual increase in protein identity towards their non-eukaryotic donor species is expected the more recent an individual HGT event is. The absence of cumulative effects in eukaryotic HGT studies has this been used as argument in favor of strict vertical inheritance followed by DL. Here, we also did not find evidence for cumulative effects in the HGT dataset. "Recent" HGT events that are exclusive to either the *Cyanidioschyzon* or *Galdieria* lineage shared 5% higher PID with their potential non-eukaryotic donors in comparison to ancient HGT candidates that predate the split, but this difference was not significant (**Figure 4C**). We also tested for cumulative effects between the number of species contained in orthogroups compared to the percent protein identity shared with potential non-eukaryotic donors under the assumption that recent HGT events would be present in fewer species in comparison to ancient HGT events that occurred at the root of *Galdieria* (**Figure 6D**). Neither a gradual increase in protein identity for potentially recent HGT events, nor a general trend could be determined. Only orthogroups containing one *Galdieria* species reported a statistically significant higher protein identity to their potential non-eukaryotic donors which could be an indication of "most recent" HGT.

What has not been considered thus far, is that the absence of cumulative effects may speak against HGT, but does not automatically argue in favor of strict vertical inheritance followed by DL. Here, the null hypothesis would be that no differences exist between HGT genes and native genes because all genes are descendants of LECA. This null hypothesis is rejected on multiple levels. At the molecular level, the HGT subset differs significantly from native genes with respect to various genomic and molecular features (e.g., GC-content, frequency of multiexonic genes, number of exons per gene, responsiveness to temperature stress) (**Table 1, Figure 3**). Furthermore, HGT candidates in *Galdieria* are significantly more similar (6.1% average PID) to their potential non-eukaryotic donors when compared to native genes and non-eukaryotic sequences in the same orthogroup (**Figure 6B**). This difference cannot be explained by the absence of eukaryotic orthologs. We also find significant differences in PID with regard to non-eukaryotic sequences between HGT and native genes in orthogroups containing either one *Galdieria* sequence, or all eleven *Galdieria* sequences regarding (**Figure 6D**). Hence, the "most recent" and "most ancient" HGT candidates share the highest resemblance to their non-eukaroytic donors, which is also significantly higher when compared to native genes in OGs of the same size. Intriguingly, a general trend towards "cumulative effects" could be observed for native genes, highlighting the differences between these two gene sources in Cyanidiales.

Given these results and interpretations, we advocate the following view of eukaryotic HGT. Specifically, two forces may act simultaneously on HGT candidates in eukaryotes. The first is strong evolutionary pressure for adaptation of eukaryotic genetic features and compatibility with native replication and transcriptional mechanisms to ensure integration into existing metabolic circuits (e.g., codon usage, splice sites, methylation, pH differences in the cytosol). The second however is that key structural aspects of HGT-derived sequence cannot be significantly altered by the first process because they ensure function of the transferred gene (e.g., protein domain conservation, three-dimensional structure, ligand interaction). Consequently, HGT candidates may suffer more markedly from gene erosion than native genes due to these countervailing forces, in spite of potentially providing beneficial adaptive traits. This view suggests that we need to think about eukaryotic HGT in fundamentally different ways than is the case for prokaryotes, necessitating a taxonomically broad genome-based approach that is slowly taking hold.

In summary, we do not discount the importance of DL in eukaryotic evolution because it can impact ca. 99% of the gene inventory in Cyanidiales. What we strongly espouse is that strict vertical inheritance in combination with DL cannot explain all the data. HGTs in Cyanidiales are significant because the 1% (values will vary across different eukaryotic lineages) helps explain the remarkable evolutionary history of these extremophiles. Lastly, we question the validity of the premise regarding the applicability of cumulative effects in the prokaryotic sense to eukaryotic HGT. The absence of cumulative effects and a eukaryotic pan-genome are neither arguments in favor of HGT, nor DL.

Data Deposit

The genomic, chloroplast and mitochondrial sequences of the 10 novel genomes, as well as gene models, ESTs, protein sequences, and gene annotations are available at http://porphyra.rutgers.edu. Raw PacBio RSII reads, and also the genomic, chloroplast and mitochondrial sequences, have been submitted to the NCBI and are retrievable via BioProject ID PRJNA512382.

Disclosures

The authors have no conflict of interests to declare.

Acknowledgements

This work was supported by the Deutsche Forschungsgemeinschaft (EXC 1028 and WE 2231/21-1 to A.P.M.W) and by the Heine Research Academy (A.W.R). We thank Dr. Luke Tallon and Dr. Bruno Hüttel for the excellent technical assistance for PacBio sequencing. Dr. Marion Eisenhut for her fantastic Power Point templates. D.C.P and D.B. are grateful to the New Jersey Agricultural Experiment Station and the Rutgers University School of Environmental and Biological Sciences Genome Cooperative for supporting this research.

References

1. Doolittle, W.F., *Lateral genomics.* Trends Cell Biol, 1999. **9**(12): p. M5-8.
2. Ochman, H., J.G. Lawrence, and E.A. Groisman, *Lateral gene transfer and the nature of bacterial innovation.* Nature, 2000. **405**(6784): p. 299-304.
3. Boucher, Y., et al., *Lateral gene transfer and the origins of prokaryotic groups.* Annu Rev Genet, 2003. **37**: p. 283-328.
4. Nelson-Sathi, S., et al., *Acquisition of 1,000 eubacterial genes physiologically transformed a methanogen at the origin of Haloarchaea.* Proc Natl Acad Sci U S A, 2012. **109**(50): p. 20537-42.
5. Tettelin, H., et al., *Genome analysis of multiple pathogenic isolates of Streptococcus agalactiae: implications for the microbial "pan-genome".* Proc Natl Acad Sci U S A, 2005. **102**(39): p. 13950-5.
6. Vernikos, G., et al., *Ten years of pan-genome analyses.* Curr Opin Microbiol, 2015. **23**: p. 148-54.
7. Philippe, H. and C.J. Douady, *Horizontal gene transfer and phylogenetics.* Curr Opin Microbiol, 2003. **6**(5): p. 498-505.
8. Doolittle, W.F. and T.D. Brunet, *What Is the Tree of Life?* PLoS Genet, 2016. **12**(4): p. e1005912.
9. Danchin, E.G., *Lateral gene transfer in eukaryotes: tip of the iceberg or of the ice cube?* BMC Biol, 2016. **14**(1): p. 101.
10. Husnik, F. and J.P. McCutcheon, *Functional horizontal gene transfer from bacteria to eukaryotes.* Nat Rev Microbiol, 2018. **16**(2): p. 67-79.
11. Martin, W.F., *Eukaryote lateral gene transfer is Lamarckian.* Nat Ecol Evol, 2018. **2**(5): p. 754.
12. Martin, W.F., *Too Much Eukaryote LGT.* Bioessays, 2017. **39**(12).
13. Ku, C. and W.F. Martin, *A natural barrier to lateral gene transfer from prokaryotes to eukaryotes revealed from genomes: the 70 % rule.* BMC Biol, 2016. **14**(1): p. 89.
14. Richards, T.A. and A. Monier, *A tale of two tardigrades.* Proc Natl Acad Sci U S A, 2016. **113**(18): p. 4892-4.
15. Leger, M.M., et al., *Demystifying Eukaryote Lateral Gene Transfer (Response to Martin 2017 DOI: 10.1002/bies.201700115).* Bioessays, 2018. **40**(5): p. e1700242.
16. Castenholz, R.W. and T.R. McDermott, *The Cyanidiales: ecology, biodiversity, and biogeography*, in *Red Algae in the Genomic Age*. 2010, Springer. p. 357-371.
17. Yoon, H.S., et al., *A molecular timeline for the origin of photosynthetic eukaryotes.* Mol Biol Evol, 2004. **21**(5): p. 809-18.
18. Reyes-Prieto, A., A.P. Weber, and D. Bhattacharya, *The origin and establishment of the plastid in algae and plants.* Annu Rev Genet, 2007. **41**: p. 147-68.
19. Price, D.C., et al., *Cyanophora paradoxa genome elucidates origin of photosynthesis in algae and plants.* Science, 2012. **335**(6070): p. 843-7.
20. Matsuzaki, M., et al., *Genome sequence of the ultrasmall unicellular red alga Cyanidioschyzon merolae 10D.* Nature, 2004. **428**(6983): p. 653-7.
21. Nozaki, H., et al., *A 100%-complete sequence reveals unusually simple genomic features in the hot-spring red alga Cyanidioschyzon merolae.* BMC Biol, 2007. **5**: p. 28.
22. Schonknecht, G., et al., *Gene transfer from bacteria and archaea facilitated evolution of an extremophilic eukaryote.* Science, 2013. **339**(6124): p. 1207-10.
23. Qiu, H., et al., *Adaptation through horizontal gene transfer in the cryptoendolithic red alga Galdieria phlegrea.* Curr Biol, 2013. **23**(19): p. R865-6.
24. Doemel, W.N. and T.J.M. Brock, *The physiological ecology of Cyanidium caldarium.* 1971. **67**(1): p. 17-32.

25. Reeb, V. and D. Bhattacharya, *The thermo-acidophilic cyanidiophyceae (Cyanidiales)*, in *Red algae in the genomic age*. 2010, Springer. p. 409-426.
26. Hsieh, C.J., et al., *The effects of contemporary selection and dispersal limitation on the community assembly of acidophilic microalgae.* 2018. **54**(5): p. 720-733.
27. Seckbach, J.J.M., *On the fine structure of the acidophilic hot-spring alga Cyanidium caldarium: a taxonomic approach.* 1972. **5**(18): p. 133-142.
28. Gross, W., et al., *Characterization of a non-thermophilic strain of the red algal genus Galdieria isolated from Soos (Czech Republic).* 2002. **37**(3): p. 477-483.
29. Ciniglia, C., et al., *Hidden biodiversity of the extremophilic Cyanidiales red algae.* Mol Ecol, 2004. **13**(7): p. 1827-38.
30. Barcytė, D., J. Elster, and L. Nedbalová, *Plastid-encoded rbcL phylogeny suggests widespread distribution of Galdieria phlegrea (Cyanidiophyceae, Rhodophyta).* 2018. **36**(7): p. e01794.
31. Iovinella, M., et al., *Cryptic dispersal of Cyanidiophytina (Rhodophyta) in non-acidic environments from Turkey.* 2018: p. 1-11.
32. Qiu, H., et al., *Evidence of ancient genome reduction in red algae (Rhodophyta).* J Phycol, 2015. **51**(4): p. 624-36.
33. Raymond, J.A. and H.J.J.P.o. Kim, *Possible role of horizontal gene transfer in the colonization of sea ice by algae.* 2012. **7**(5): p. e35968.
34. Bhattacharya, D., et al., *Genome of the red alga Porphyridium purpureum.* Nat Commun, 2013. **4**: p. 1941.
35. Foflonker, F., et al., *Genomic Analysis of Picochlorum Species Reveals How Microalgae May Adapt to Variable Environments.* Molecular Biology and Evolution, 2018: p. msy167-msy167.
36. Schönknecht, G., A.P. Weber, and M.J.J.B. Lercher, *Horizontal gene acquisitions by eukaryotes as drivers of adaptive evolution.* 2014. **36**(1): p. 9-20.
37. Boothby, T.C., et al., *Evidence for extensive horizontal gene transfer from the draft genome of a tardigrade.* Proc Natl Acad Sci U S A, 2015. **112**(52): p. 15976-81.
38. Crisp, A., et al., *Expression of multiple horizontally acquired genes is a hallmark of both vertebrate and invertebrate genomes.* Genome Biol, 2015. **16**: p. 50.
39. Koutsovoulos, G., et al., *No evidence for extensive horizontal gene transfer in the genome of the tardigrade Hypsibius dujardini.* Proc Natl Acad Sci U S A, 2016. **113**(18): p. 5053-8.
40. Salzberg, S.L., *Horizontal gene transfer is not a hallmark of the human genome.* Genome Biol, 2017. **18**(1): p. 85.
41. Rhoads, A. and K.F. Au, *PacBio Sequencing and Its Applications.* Genomics Proteomics Bioinformatics, 2015. **13**(5): p. 278-89.
42. Allen, M.B.J.A.f.M., *Studies with Cyanidium caldarium, an anomalously pigmented chlorophyte.* 1959. **32**(3): p. 270-277.
43. Koren, S., et al., *Canu: scalable and accurate long-read assembly via adaptive k-mer weighting and repeat separation.* Genome Res, 2017. **27**(5): p. 722-736.
44. Chin, C.S., et al., *Nonhybrid, finished microbial genome assemblies from long-read SMRT sequencing data.* Nat Methods, 2013. **10**(6): p. 563-9.
45. Simao, F.A., et al., *BUSCO: assessing genome assembly and annotation completeness with single-copy orthologs.* Bioinformatics, 2015. **31**(19): p. 3210-2.
46. Geer, L.Y., et al., *The NCBI BioSystems database.* Nucleic Acids Res, 2010. **38**(Database issue): p. D492-6.
47. Cantarel, B.L., et al., *MAKER: an easy-to-use annotation pipeline designed for emerging model organism genomes.* Genome Res, 2008. **18**(1): p. 188-96.

48. Rademacher, N., et al., *Photorespiratory glycolate oxidase is essential for the survival of the red alga Cyanidioschyzon merolae under ambient CO2 conditions.* J Exp Bot, 2016. **67**(10): p. 3165-75.
49. UniProt Consortium, T., *UniProt: the universal protein knowledgebase.* Nucleic Acids Res, 2018. **46**(5): p. 2699.
50. Stanke, M. and B. Morgenstern, *AUGUSTUS: a web server for gene prediction in eukaryotes that allows user-defined constraints.* Nucleic Acids Res, 2005. **33**(Web Server issue): p. W465-7.
51. Borodovsky, M. and A. Lomsadze, *Eukaryotic gene prediction using GeneMark.hmm-E and GeneMark-ES.* Curr Protoc Bioinformatics, 2011. **Chapter 4**: p. Unit 4 6 1-10.
52. Haas, B.J., et al., *Automated eukaryotic gene structure annotation using EVidenceModeler and the Program to Assemble Spliced Alignments.* Genome Biol, 2008. **9**(1): p. R7.
53. Finn, R.D., et al., *The Pfam protein families database: towards a more sustainable future.* Nucleic Acids Res, 2016. **44**(D1): p. D279-85.
54. Gotz, S., et al., *High-throughput functional annotation and data mining with the Blast2GO suite.* Nucleic Acids Res, 2008. **36**(10): p. 3420-35.
55. Jones, P., et al., *InterProScan 5: genome-scale protein function classification.* Bioinformatics, 2014. **30**(9): p. 1236-40.
56. Ashburner, M., et al., *Gene ontology: tool for the unification of biology. The Gene Ontology Consortium.* Nat Genet, 2000. **25**(1): p. 25-9.
57. Bairoch, A., *The ENZYME database in 2000.* Nucleic Acids Res, 2000. **28**(1): p. 304-5.
58. Ogata, H., et al., *KEGG: Kyoto Encyclopedia of Genes and Genomes.* Nucleic Acids Res, 1999. **27**(1): p. 29-34.
59. Moriya, Y., et al., *KAAS: an automatic genome annotation and pathway reconstruction server.* Nucleic Acids Res, 2007. **35**(Web Server issue): p. W182-5.
60. Emms, D.M. and S. Kelly, *OrthoFinder: solving fundamental biases in whole genome comparisons dramatically improves orthogroup inference accuracy.* Genome Biol, 2015. **16**: p. 157.
61. Buchfink, B., C. Xie, and D.H. Huson, *Fast and sensitive protein alignment using DIAMOND.* Nat Methods, 2015. **12**(1): p. 59-60.
62. Nordberg, H., et al., *The genome portal of the Department of Energy Joint Genome Institute: 2014 updates.* Nucleic Acids Res, 2014. **42**(Database issue): p. D26-31.
63. O'Brien, E.A., et al., *TBestDB: a taxonomically broad database of expressed sequence tags (ESTs).* Nucleic Acids Res, 2007. **35**(Database issue): p. D445-51.
64. Boguski, M.S., T.M. Lowe, and C.M. Tolstoshev, *dbEST--database for "expressed sequence tags".* Nat Genet, 1993. **4**(4): p. 332-3.
65. Keeling, P.J., et al., *The Marine Microbial Eukaryote Transcriptome Sequencing Project (MMETSP): illuminating the functional diversity of eukaryotic life in the oceans through transcriptome sequencing.* PLoS Biol, 2014. **12**(6): p. e1001889.
66. Katoh, K. and D.M. Standley, *MAFFT multiple sequence alignment software version 7: improvements in performance and usability.* Mol Biol Evol, 2013. **30**(4): p. 772-80.
67. Nguyen, L.-T., et al., *IQ-TREE: a fast and effective stochastic algorithm for estimating maximum-likelihood phylogenies.* 2014. **32**(1): p. 268-274.
68. Brawley, S.H., et al., *Insights into the red algae and eukaryotic evolution from the genome of Porphyra umbilicalis (Bangiophyceae, Rhodophyta).* Proc Natl Acad Sci U S A, 2017. **114**(31): p. E6361-E6370.
69. Blanc-Mathieu, R., et al., *An improved genome of the model marine alga Ostreococcus tauri unfolds by assessing Illumina de novo assemblies.* BMC Genomics, 2014. **15**: p. 1103.

70. Merchant, S.S., et al., *The Chlamydomonas genome reveals the evolution of key animal and plant functions.* Science, 2007. **318**(5848): p. 245-50.

71. Qiu, H., H.S. Yoon, and D. Bhattacharya, *Red Algal Phylogenomics Provides a Robust Framework for Inferring Evolution of Key Metabolic Pathways.* PLoS Curr, 2016. **8**.

72. Moreira, D., et al., *Characterization of two new thermoacidophilic microalgae: genome organization and comparison with Galdieria sulphuraria.* 1994. **122**(1-2): p. 109-114.

73. Weber, A.P., et al., *A genomics approach to understanding the biology of thermo-acidophilic red algae*, in *Algae and Cyanobacteria in Extreme Environments*. 2007, Springer. p. 503-518.

74. Yang, E.C., et al., *Divergence time estimates and the evolution of major lineages in the florideophyte red algae.* 2016. **6**: p. 21361.

75. Qiu, H., et al., *Unexpected conservation of the RNA splicing apparatus in the highly streamlined genome of Galdieria sulphuraria.* BMC Evol Biol, 2018. **18**(1): p. 41.

76. Kim, D., B. Langmead, and S.L. Salzberg, *HISAT: a fast spliced aligner with low memory requirements.* Nat Methods, 2015. **12**(4): p. 357-60.

77. Robinson, M.D., D.J. McCarthy, and G.K. Smyth, *edgeR: a Bioconductor package for differential expression analysis of digital gene expression data.* Bioinformatics, 2010. **26**(1): p. 139-40.

78. Stauffer, R.E. and J.M.J.G.e.C.A. Thompson, *Arsenic and antimony in geothermal waters of Yellowstone National Park, Wyoming, USA.* 1984. **48**(12): p. 2547-2561.

79. Aiuppa, A., et al., *The aquatic geochemistry of arsenic in volcanic groundwaters from southern Italy.* 2003. **18**(9): p. 1283-1296.

80. Toplin, J., et al., *Biogeographic and phylogenetic diversity of thermoacidophilic cyanidiales in Yellowstone National Park, Japan, and New Zealand.* 2008. **74**(9): p. 2822-2833.

81. Pinto, G.T., Roberto, *Nuove stazioni italiane di "Cyanidium caldarium".* Delpinoa 1975. **14-15**: p. 125-139.

82. Kelly, D.J., K. Budd, and D.D.J.A.o.m. Lefebvre, *Biotransformation of mercury in pH-stat cultures of eukaryotic freshwater algae.* 2007. **187**(1): p. 45-53.

83. Meharg, A. and M.J.J.o.E.B. Macnair, *Suppression of the high affinity phosphate uptake system: a mechanism of arsenate tolerance in Holcus lanatus L.* 1992. **43**(4): p. 519-524.

84. Catarecha, P., et al., *A mutant of the Arabidopsis phosphate transporter PHT1; 1 displays enhanced arsenic accumulation.* 2007. **19**(3): p. 1123-1133.

85. Zhao, F.-J., S.P. McGrath, and A.A.J.A.r.o.p.b. Meharg, *Arsenic as a food chain contaminant: mechanisms of plant uptake and metabolism and mitigation strategies.* 2010. **61**: p. 535-559.

86. van Doesburg, W., et al., *Reductive dechlorination of β-hexachlorocyclohexane (β-HCH) by a Dehalobacter species in coculture with a Sedimentibacter sp.* 2005. **54**(1): p. 87-95.

87. Chen, Y., O. Peoples, and C.J.J.o.b. Walsh, *Acinetobacter cyclohexanone monooxygenase: gene cloning and sequence determination.* 1988. **170**(2): p. 781-789.

88. Henkanatte-Gedera, S., et al., *Removal of dissolved organic carbon and nutrients from urban wastewaters by Galdieria sulphuraria: Laboratory to field scale demonstration.* 2017. **24**: p. 450-456.

89. Fukuda, S.-y., et al., *Cellular accumulation of cesium in the unicellular red alga Galdieria sulphuraria under mixotrophic conditions.* 2018: p. 1-5.

90. Phaniendra, A., D.B. Jestadi, and L.J.I.J.o.C.B. Periyasamy, *Free radicals: properties, sources, targets, and their implication in various diseases.* 2015. **30**(1): p. 11-26.

91. Dietz, K.-J., M. Baier, and U. Krämer, *Free radicals and reactive oxygen species as mediators of heavy metal toxicity in plants*, in *Heavy metal stress in plants*. 1999, Springer. p. 73-97.

92. YLÄ-HERTTUALA, S.J.A.o.t.N.Y.A.o.S., *Oxidized LDL and Atherogenesisa.* 1999. **874**(1): p. 134-137.

93. Standman, E. and R.J.A.N.A.S. Levine, *Protein oxidation.* 2000. **899**: p. 191-208.

94. Marnett, L.J.J.c., *Oxyradicals and DNA damage.* 2000. **21**(3): p. 361-370.

95. Rouhier, N., S.D. Lemaire, and J.-P.J.A.R.P.B. Jacquot, *The role of glutathione in photosynthetic organisms: emerging functions for glutaredoxins and glutathionylation.* 2008. **59**: p. 143-166.

96. Chae, H.Z., et al., *Cloning and sequencing of thiol-specific antioxidant from mammalian brain: alkyl hydroperoxide reductase and thiol-specific antioxidant define a large family of antioxidant enzymes.* 1994. **91**(15): p. 7017-7021.

97. Paulose, B., et al., *A γ-glutamyl cyclotransferase protects Arabidopsis plants from heavy metal toxicity by recycling glutamate to maintain glutathione homeostasis.* 2013: p. tpc. 113.111815.

98. Gross, W., C.J.P. Schnarrenberger, and C. Physiology, *Heterotrophic growth of two strains of the acido-thermophilic red alga Galdieria sulphuraria.* 1995. **36**(4): p. 633-638.

99. Gross, W., et al., *Cryptoendolithic growth of the red alga Galdieria sulphuraria in volcanic areas.* 1998. **33**(1): p. 25-31.

100. De Luca, P., R. Taddei, and L.J.W. Varano, *«Cyanidioschyzon merolae»: a new alga of thermal acidic environments.* 1978. **33**(1): p. 37-44.

101. Liu, Y., et al., *Aquaporin 9 is the major pathway for glycerol uptake by mouse erythrocytes, with implications for malarial virulence.* 2007. **104**(30): p. 12560-12564.

102. Robellet, X., et al., *AcpA, a member of the GPR1/FUN34/YaaH membrane protein family, is essential for acetate permease activity in the hyphal fungus Aspergillus nidulans.* 2008. **412**(3): p. 485-493.

103. Sá-Pessoa, J., et al., *SATP (YaaH), a succinate–acetate transporter protein in Escherichia coli.* 2013. **454**(3): p. 585-595.

104. Rojas, A., et al., *Crystal structures of β-galactosidase from Penicillium sp. and its complex with galactose.* 2004. **343**(5): p. 1281-1292.

105. Rico-Díaz, A., et al., *Crystallization and preliminary X-ray diffraction data of β-galactosidase from Aspergillus niger.* 2014. **70**(11): p. 1529-1531.

106. Psylinakis, E., et al., *Peptidoglycan N-acetylglucosamine deacetylases from Bacillus cereus, highly conserved proteins in Bacillus anthracis.* 2005. **280**(35): p. 30856-30863.

107. Lee, H.-S., et al., *Cyclomaltodextrinase, neopullulanase, and maltogenic amylase are nearly indistinguishable from each other.* 2002. **277**(24): p. 21891-21897.

108. Diderichsen, B.r. and L.J.F.m.l. Christiansen, *Cloning of a maltogenic alpha-amylase from Bacillus stearothermophilus.* 1988. **56**(1): p. 53-60.

109. Ettema, T.J., et al., *The non-phosphorylating glyceraldehyde-3-phosphate dehydrogenase (GAPN) of Sulfolobus solfataricus: a key-enzyme of the semi-phosphorylative branch of the Entner–Doudoroff pathway.* 2008. **12**(1): p. 75-88.

110. van Lieshout, J.F., et al., *Identification and molecular characterization of a novel type of α-galactosidase from Pyrococcus furiosus.* 2003. **21**(4-5): p. 243-252.

111. Okuyama, M., et al., *Overexpression and characterization of two unknown proteins, YicI and YihQ, originated from Escherichia coli.* 2004. **37**(1): p. 170-179.

112. Mashek, D.G., L.O. Li, and R.A.J.F.l. Coleman, *Long-chain acyl-CoA synthetases and fatty acid channeling.* 2007. **2**(4): p. 465-476.

113. Dilworth, D., et al., *The roles of peptidyl-proline isomerases in gene regulation.* 2011. **90**(1): p. 55-69.

114. Kloosterman, T.G., et al., *Regulation of glutamine and glutamate metabolism by GlnR and GlnA in Streptococcus pneumoniae.* 2006. **281**(35): p. 25097-25109.

115. Dahl, S.W., et al., *Carica papaya glutamine cyclotransferase belongs to a novel plant enzyme subfamily: cloning and characterization of the recombinant enzyme.* 2000. **20**(1): p. 27-36.

116. Rao, K.S., et al., *Kinetic mechanism of glutaryl-CoA dehydrogenase.* 2006. **45**(51): p. 15853-15861.

117. Martin, P.R. and M.H.J.J.o.b. Mulks, *Sequence analysis and complementation studies of the argJ gene encoding ornithine acetyltransferase from Neisseria gonorrhoeae.* 1992. **174**(8): p. 2694-2701.

118. Ducker, G.S. and J.D.J.C.m. Rabinowitz, *One-carbon metabolism in health and disease.* 2017. **25**(1): p. 27-42.

119. Yu, L., et al., *Solution structure of an rRNA methyltransferase (ErmAM) that confers macrolide-lincosamide-streptogramin antibiotic resistance.* 1997. **4**(6): p. 483.

120. Kimura, S. and T.J.N.a.r. Suzuki, *Fine-tuning of the ribosomal decoding center by conserved methyl-modifications in the Escherichia coli 16S rRNA.* 2009. **38**(4): p. 1341-1352.

121. Albertano, P., et al., *The taxonomic position of Cyanidium, Cyanidioschyzon and Galdieria: an update.* 2000. **433**(1-3): p. 137-143.

122. Imhoff, J.F. and F.J.J.o.b. Rodriguez-Valera, *Betaine is the main compatible solute of halophilic eubacteria.* 1984. **160**(1): p. 478-479.

123. Lu, W.-D., Z.-M. Chi, and C.-D.J.A.o.m. Su, *Identification of glycine betaine as compatible solute in Synechococcus sp. WH8102 and characterization of its N-methyltransferase genes involved in betaine synthesis.* 2006. **186**(6): p. 495-506.

124. Waditee, R., et al., *Isolation and Functional Characterization ofN-Methyltransferases That Catalyze Betaine Synthesis from Glycine in a Halotolerant Photosynthetic Organism Aphanothece halophytica.* 2003. **278**(7): p. 4932-4942.

125. Nyyssölä, A., et al., *Extreme halophiles synthesize betaine from glycine by methylation.* 2000. **275**(29): p. 22196-22201.

126. McCoy, J.G., et al., *Discovery of sarcosine dimethylglycine methyltransferase from Galdieria sulphuraria.* Proteins, 2009. **74**(2): p. 368-77.

127. Kingston, R.L., R.K. Scopes, and E.N.J.S. Baker, *The structure of glucose-fructose oxidoreductase from Zymomonas mobilis: an osmoprotective periplasmic enzyme containing non-dissociable NADP.* 1996. **4**(12): p. 1413-1428.

128. Simonetti, A., et al., *A structural view of translation initiation in bacteria.* 2009. **66**(3): p. 423.

129. Takeda, K., et al., *Effects of the Escherichia coli sfsA gene on mal genes expression and a DNA binding activity of SfsA.* 2001. **65**(1): p. 213-217.

130. Nautiyal, A., et al., *Mycobacterium tuberculosis RuvX is a Holliday junction resolvase formed by dimerisation of the monomeric YqgF nuclease domain.* 2016. **100**(4): p. 656-674.

131. Apfel, C.M., et al., *Use of genomics to identify bacterial undecaprenyl pyrophosphate synthetase: cloning, expression, and characterization of the essential uppS gene.* 1999. **181**(2): p. 483-492.

132. Galperin, M.Y.J.B.m., *A census of membrane-bound and intracellular signal transduction proteins in bacteria: bacterial IQ, extroverts and introverts.* 2005. **5**(1): p. 35.

133. Schrimsher, J., et al., *Purification and characterization of aminoimidazole ribonucleotide synthetase from Escherichia coli.* 1986. **25**(15): p. 4366-4371.

134. Chen, Y., F. Li, and E.T.J.P.P. Wurtzel, *Isolation and characterization of the Z-ISO gene encoding a missing component of carotenoid biosynthesis in plants.* 2010. **153**(1): p. 66-79.

135. Lee, J., et al., *Reconstructing the complex evolutionary history of mobile plasmids in red algal genomes.* Sci Rep, 2016. **6**: p. 23744.

136. Li, Z. and R. Bock, *Replication of bacterial plasmids in the nucleus of the red alga Porphyridium purpureum.* Nat Commun, 2018. **9**(1): p. 3451.

SUPPLEMENTARY MATERIAL

The genomes of polyextremophilic Cyanidiales contain 1% horizontally transferred genes with diverse adaptive functions

Alessandro W. Rossoni[1#], Dana C. Price[2], Mark Seger[3], Dagmar Lyska[1], Peter Lammers[3], Debashish Bhattacharya[4] & Andreas P.M. Weber[1*]

[1]Institute of Plant Biochemistry, Cluster of Excellence on Plant Sciences (CEPLAS), Heinrich Heine University, Universitätsstraße 1, 40225 Düsseldorf, Germany
[2]Department of Plant Biology, Rutgers University, New Brunswick, NJ 08901, USA
[3]Arizona Center for Algae Technology and Innovation, Arizona State University, Mesa, AZ 85212, USA
[4]Department of Biochemistry and Microbiology, Rutgers University, New Brunswick, NJ 08901, USA

*Corresponding author: Prof. Dr. Andreas P.M. Weber,
e-mail: andreas.weber@uni-duesseldorf.de

SUMMPLEMENTARY FIGURE 1S – RAW READ LENGTH DISTRIBUTION

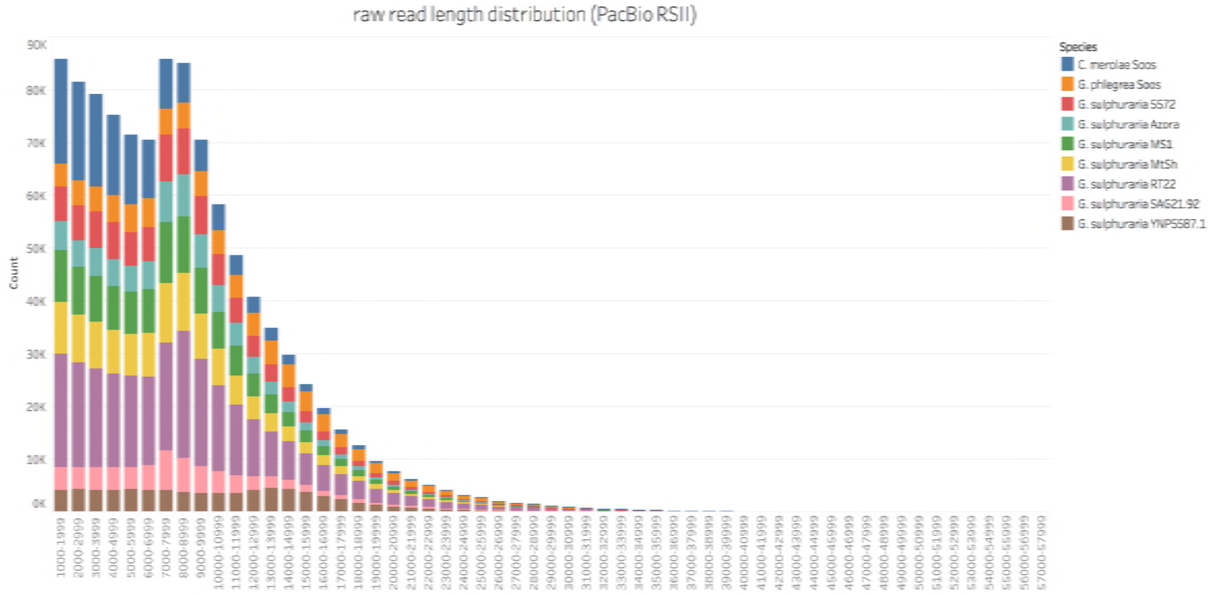

Sum of Count for each Window. Color shows details about Species.

Figure 1S – Raw read length distribution of the sequenced Cyanidiales strains. The strains were sequenced in 2016/2017 using PacBio's RS2 sequencing technology and P6-C4 chemistry (the only exception being *C. merolae Soos*, which was sequenced as pilot study using P4-C2 chemistry in 2014). Seven strains, namely *G. sulphuraria* 5572, *G. sulphuraria* 002, *G. sulphuraria* SAG21.92, *G. sulphuraria* Azora, *G. sulphuraria* MtSh, *G. sulphuraria* RT22 and *G. sulphuraria* MS1 were sequenced at the University of Maryland Institute for Genome Sciences (Baltimore, USA). The remaining three strains, *G. sulphuraria YNP5578.1*, *G. phlegrea* Soos and *C. merolae* Soos, were sequenced at the Max-Planck-Institut für Pflanzenzüchtungsforschung (Cologne, Germany).

SUMMPLEMENTARY TABLE 1S – SEQUENCING AND ASSEMBLY STATS

Table 1S – Sequencing and Assembly stats. The strains were sequenced using PacBio's RS2 sequencing technology and P6-C4 chemistry (the only exception being *C. merolae Soos*, which was sequenced using

P4-C2 chemistry). For genome assembly, canu version 1.5 was used, followed by polishing three times using the Quiver algorithm. Genes were predicted with MAKER v3 beta[1][1]. The performance of genome assemblies (not shown here) and gene prediction was assessed using BUSCO v.3. **Raw Reads**: Number of raw PacBio RSII reads. **Raw Reads N50**: 50% of the raw sequence is contained in reads with sizes greater than the N50 value. **Raw Reads GC**: GC content of the raw reads in percent. **Raw Reads (bp)**: Total number of sequenced basepairs (nucleotides) per species. **Raw Coverage (bp)**: Genomic coverage by raw reads. This figure was computed once the assembly was finished. **Unitigging (bp):** Total number of basepairs that survived read correction and trimming. This amount of sequence is what the assembler considered when constructing the genome. **Unitigging Coverage**: Genomic coverage by corrected and trimmed reads. **Genome Size (bp)**: Size of the polished genome. **Genome GC**: GC content of the polished genome. **Contigs**: Number of contigs. **Contig N50**: 50% of the final genomic sequence is contained in contigs sizes greater than the N50 value. **Genes**: Number of genes predicted by Maker v3 beta. **BUSCO (C)**: Percentage of complete gene models. **BUSCO (C + F)**: Percentage of complete and fragmented gene models. Fragmented gene models are also somewhat present. **BUSCO (D)**: Percentage of duplicated gene models. **BUSCO (M)**: Percentage of missing gene models.

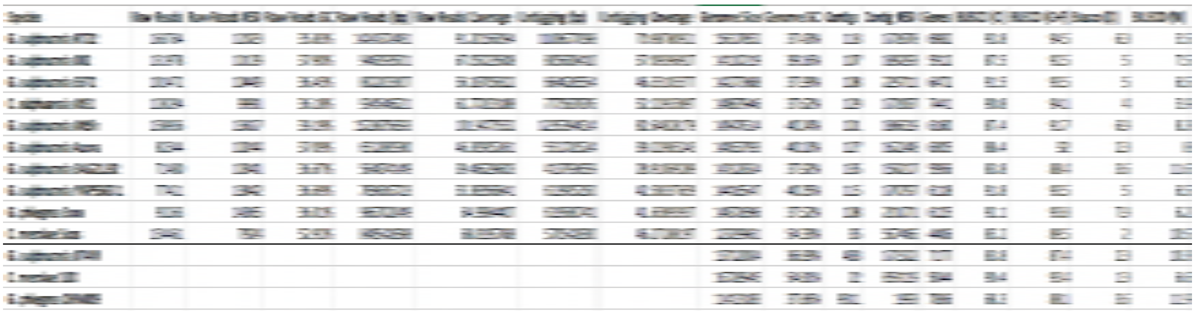

SUMMPLEMENTARY CHAPTER 1S – ARCHAEAL ATPases & "OLD" HGT

We compared the HGT results of this study to previous published claims of HGT in *G. sulphuraria* 074W (75 separate acquisitions followed by gene family expansion, 335 transcripts in total) [2] and *G. phlegrea* DBV009 (13 genes from 11 acquisitions unique to this strain, excluding those shared with *G. sulphuraria* 074W and other red algae) [3]. Each HGT candidate was queried against our database, mapped to the existing OGs and phylogenetic trees were built for each sequence (where possible). The HGT candidates of *G. sulphuraria* 074W mapped into 100 different OGs, thus increasing the number of separate origins from 75 to 100 (more separate origins = less gene family expansion). 211 out of the 335 HGT candidates in *G. sulphuraria* 074W are "archaeal STAND ATPases". They clustered into OG0000000, OG0000003 and OG0000001 which are not classified as HGT. Thus, HGT origin for those gene families can be excluded. The remaining 124 *G. sulphuraria* 074W HGT candidates are spread across 98 OGs. Of those, 20 OGs overlap with our HGT findings, whereas 78 are OGs that do not have HGT origins (one was classified as EGT). All 13 HGT candidates in *G. phlegrea* DBV009 were found and their HGT origin could be confirmed. Some do not make the cut due to individual acquisitions by *G. phlegrea* DBV009 alone. However, considering the operon structures of the acquisition it seems plausible in this case.

In order to exclude the possibility that our database was "missing" crucial non-eukaryotic species we queried all protein sequences against our own database and NCBI's uncurated nr database, including predicted models and environmental samples and implementing various search strategies. 219 out of the 335 HGT candidates in *G. sulphuraria* 074W did not report any hits outside the species itself (including the 211 "archaeal ATPases") and no functional evidence could be found besides the one obtained through manual curation of sequence alignments as reported by the author [2].

As seen in the case of the human and the Tardigrade genome, the overestimation of HGT in eukaryotic genomes, followed by later re-correction, is not a new phenomenon [4-7]. There are several reasons that may have led to the drastic overestimation of HGT candidates in the case of *G. sulphuraria* 074W (100 OGs derived from HGT, instead of 58 OGs). Although published in 2013, the HGT analysis was performed in early 2007. By then, the RefSeq database contained 4.7 million accessions compared to 163.9 million accessions in May 2018. The low resolution regarding eukaryotic species may have led to many singletons, here defined as *Galdieria* being the only eukaryotic species in otherwise bacterial clusters, leading to the mislabelling of HGT. Further, the many small contigs derived from short read sequencing technologies of the last decade, combined with older assembly software [8] are known potential pitfalls [9] for missassembly that may lead to the inclusion of bacterial contigs into the reference genome as a consequence of prior culture contamination. Lastly, this analysis occurred a decade prior to the tardigrade and human case that led to raised awareness and standards regarding HGT annotation as many claims of HGT were later refuted by further analyses. From a biological view the HGT origin of the Archaeal ATPases is disputable as a re-sequencing of the Genome using MinION technology (A. W. Rossoni, data unpublished, October 2017) shows they always occur immediately adjacent to every single telomere, therefore adding another layer of complexity. The "archaeal ATPase" was not only integrated into the genome, but also put under influence a non-random duplication mechanism responsible for spreading copies in a targeted manner to the subtelomeric region of each single contig (no exception!). Examples of similar cases may be found in the Variant Surface Glycoproteins (VSGs) of the Trypanosoma [10] and the Candidates for Secreted Effector Proteins (CSEPs) in the powdery mildew fungus Blumeria graminis [11]. As those genes are vital for the infection of the host, they are subjects of very strong natural selection and profit from high evolutionary rates achieved at the subtelomeric regions. But the high evolutionary rates also made it impossible to correctly embed the aforementioned gene families in a phylogenetic tree. As such, it is not to be excluded that a similar case occurred regarding *Galdieria sulphuraria*'s "archaeal ATPases", although a permissive search might indicate an archaeal origin of single protein domains. Also, as only a patchy subset of the ATPases reacts to temperature fluctuations, it cannot be determined that temperature is the driving factor.

SUMMPLEMENTARY TABLE 2S, GC CONTENT COMPARISON

Table 2S – %GC analysis of the Cyanidiales transcriptomes. %GC content of HGT genes was compared to the %GC content of native genes using students test. Legend: **HGT Genes**: number of HGT gene candidates found in species. **Avg. %GC Native**: average %GC of native transcripts. **Avg. %GC HGT**: average %GC of HGT candidates. **P-Val (T-test)**: significance value (p-value) of student's test. **Delta:** difference in %GC between average %GC of native genes and the average %GC of HGT candidates.

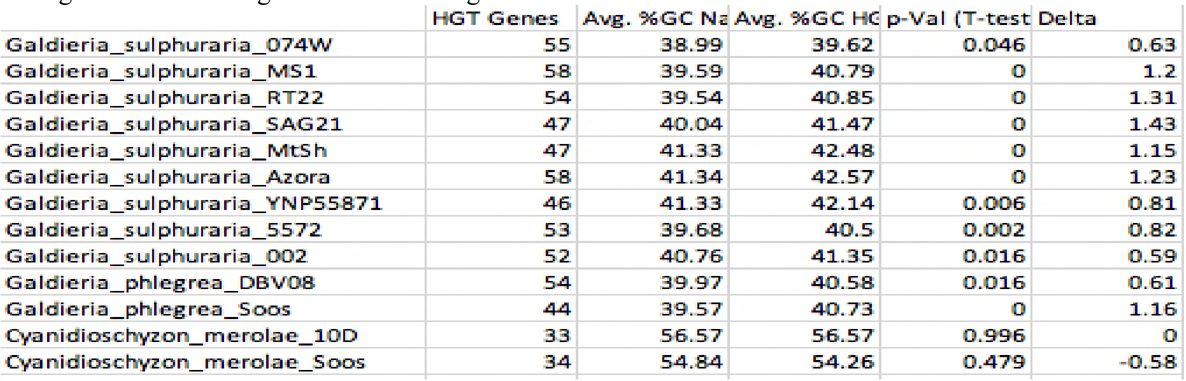

	HGT Genes	Avg. %GC Na	Avg. %GC HG	p-Val (T-test	Delta
Galdieria_sulphuraria_074W	55	38.99	39.62	0.046	0.63
Galdieria_sulphuraria_MS1	58	39.59	40.79	0	1.2
Galdieria_sulphuraria_RT22	54	39.54	40.85	0	1.31
Galdieria_sulphuraria_SAG21	47	40.04	41.47	0	1.43
Galdieria_sulphuraria_MtSh	47	41.33	42.48	0	1.15
Galdieria_sulphuraria_Azora	58	41.34	42.57	0	1.23
Galdieria_sulphuraria_YNP55871	46	41.33	42.14	0.006	0.81
Galdieria_sulphuraria_5572	53	39.68	40.5	0.002	0.82
Galdieria_sulphuraria_002	52	40.76	41.35	0.016	0.59
Galdieria_phlegrea_DBV08	54	39.97	40.58	0.016	0.61
Galdieria_phlegrea_Soos	44	39.57	40.73	0	1.16
Cyanidioschyzon_merolae_10D	33	56.57	56.57	0.996	0
Cyanidioschyzon_merolae_Soos	34	54.84	54.26	0.479	-0.58

SUMMPLEMENTARY FIGURES 2S, A – S , GC CONTENT COMPARISON

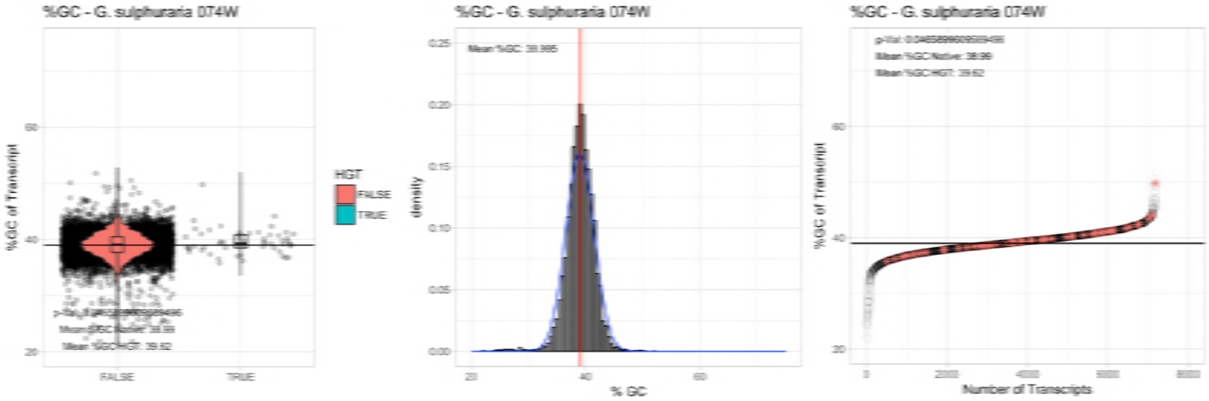

Figure 2SA – %GC – *Galdieria sulphuraria 074W:* (Left) Violin plot showing the %GC distribution across native transcripts and HGT candidates. (Mid) Cumulative %GC distribution of transcripts. Red line shows the average, blue line a normal distribution based on the average value. (Right) Ranking all transcripts based upon their %GC content. Red "*" demarks HGT candidates. As the %GC content was normally distributed, students test was applied for the determination of significant differences between the native gene and the HGT candidate subset.

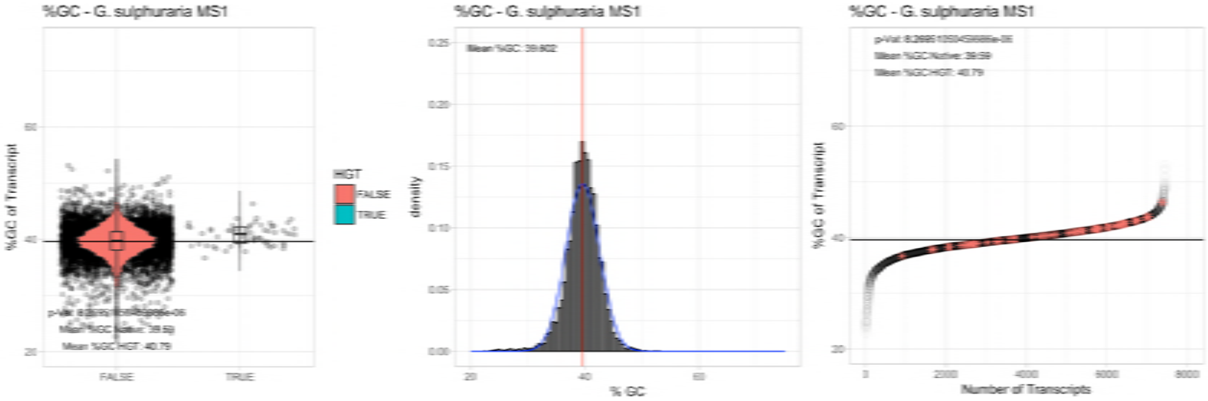

Figure 2SB – %GC – *Galdieria sulphuraria MS1:* (Left) Violin plot showing the %GC distribution across native transcripts and HGT candidates. (Mid) Cumulative %GC distribution of transcripts. Red line shows the average, blue line a normal distribution based on the average value. (Right) Ranking all transcripts based upon their %GC content. Red "*" demarks HGT candidates. As the %GC content was normally distributed, students test was applied for the determination of significant differences between the native gene and the HGT candidate subset.

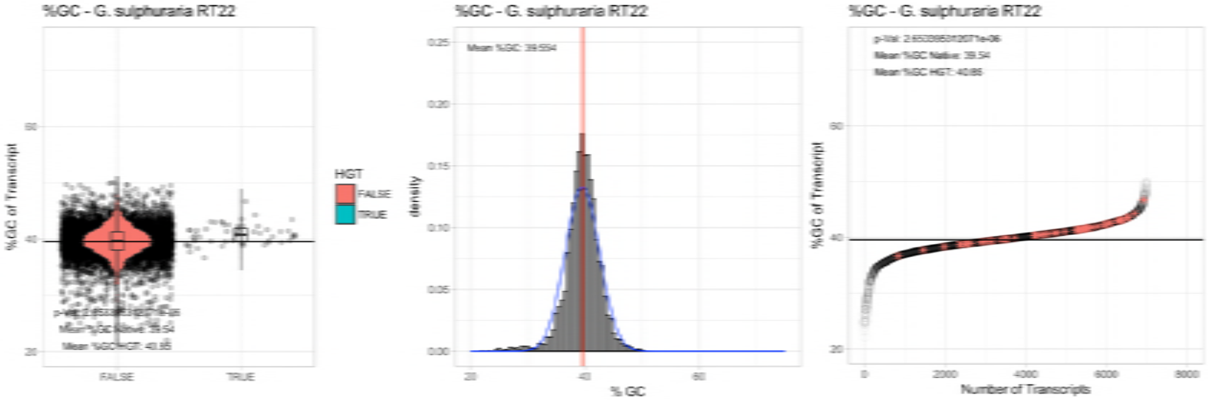

Figure 2SC – %GC – *Galdieria sulphuraria RT22:* (Left) Violin plot showing the %GC distribution across native transcripts and HGT candidates. (Mid) Cumulative %GC distribution of transcripts. Red line shows the average, blue line a normal distribution based on the average value. (Right) Ranking all transcripts based upon their %GC content. Red "*" demarks HGT candidates. As the %GC content was normally distributed, students test was applied for the determination of significant differences between the native gene and the HGT candidate subset.

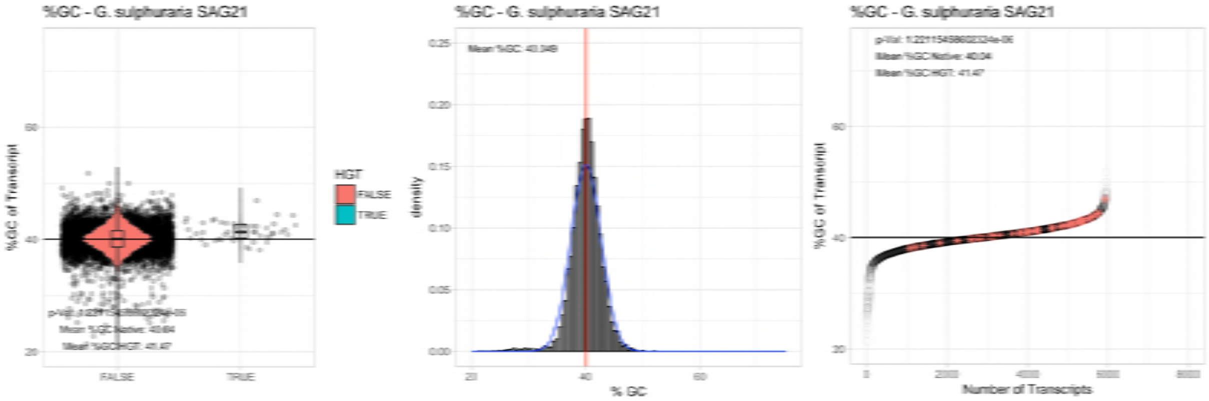

Figure 2SD – %GC – *Galdieria sulphuraria SAG21:* (Left) Violin plot showing the %GC distribution across native transcripts and HGT candidates. (Mid) Cumulative %GC distribution of transcripts. Red line shows the average, blue line a normal distribution based on the average value. (Right) Ranking all transcripts based upon their %GC content. Red "*" demarks HGT candidates. As the %GC content was normally distributed, students test was applied for the determination of significant differences between the native gene and the HGT candidate subset.

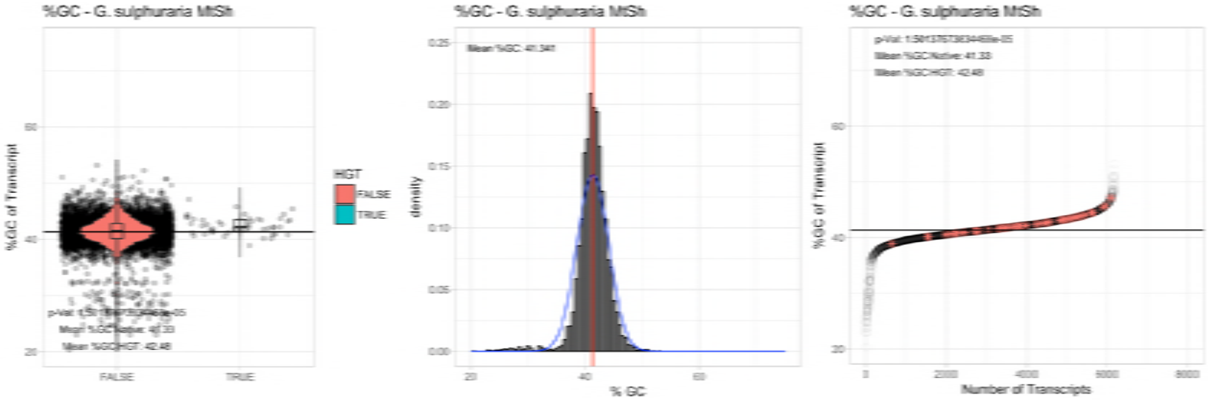

Figure 2SE – %GC – *Galdieria sulphuraria Mount Shasta (MtSh):* (Left) Violin plot showing the %GC distribution across native transcripts and HGT candidates. (Mid) Cumulative %GC distribution of transcripts. Red line shows the average, blue line a normal distribution based on the average value. (Right) Ranking all transcripts based upon their %GC content. Red "*" demarks HGT candidates. As the %GC content was normally distributed, students test was applied for the determination of significant differences between the native gene and the HGT candidate subset.

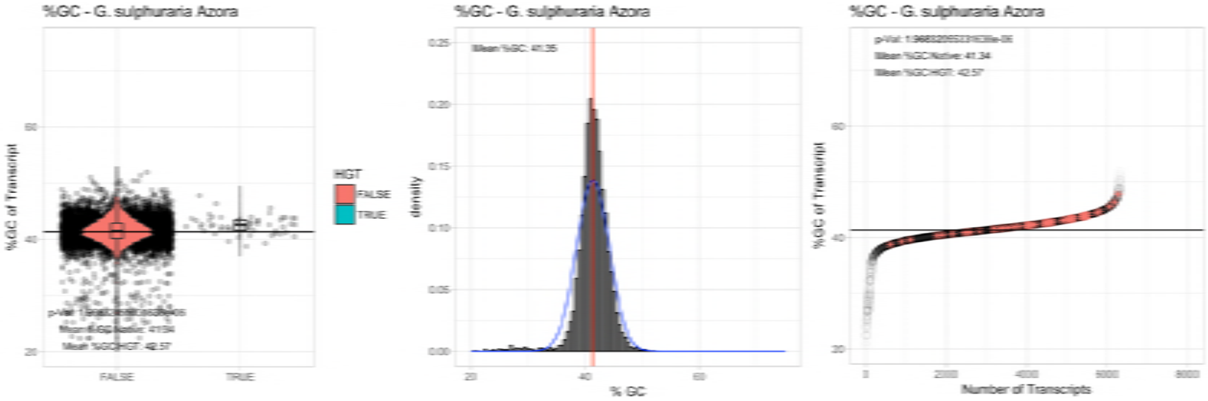

Figure 2SF – %GC – *Galdieria sulphuraria Azora:* (Left) Violin plot showing the %GC distribution across native transcripts and HGT candidates. (Mid) Cumulative %GC distribution of transcripts. Red line shows the average, blue line a normal distribution based on the average value. (Right) Ranking all transcripts based upon their %GC content. Red "*" demarks HGT candidates. As the %GC content was normally distributed, students test was applied for the determination of significant differences between the native gene and the HGT candidate subset.

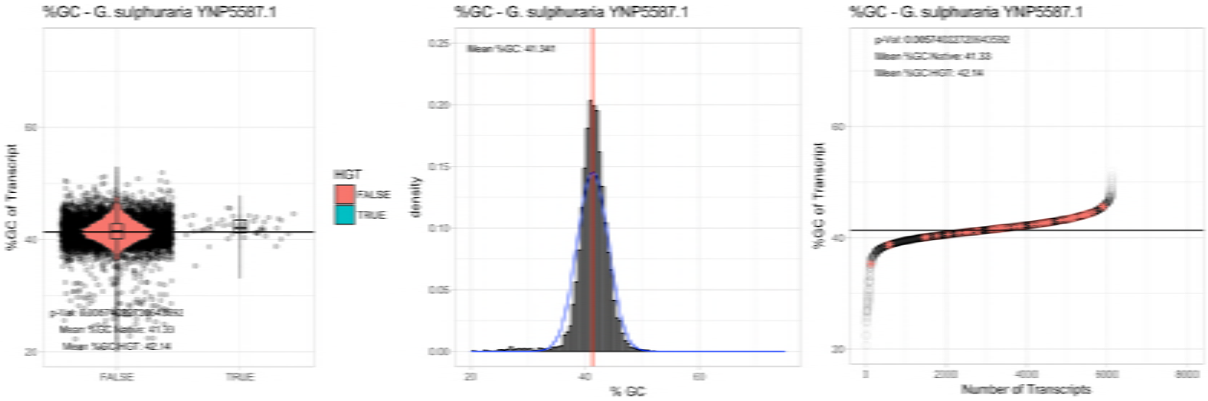

Figure 2SG – %GC – *Galdieria sulphuraria Mount Shasta YNP5578.1:* (Left) Violin plot showing the %GC distribution across native transcripts and HGT candidates. (Mid) Cumulative %GC distribution of transcripts. Red line shows the average, blue line a normal distribution based on the average value. (Right) Ranking all transcripts based upon their %GC content. Red "*" demarks HGT candidates. As the %GC content was normally distributed, students test was applied for the determination of significant differences between the native gene and the HGT candidate subset.

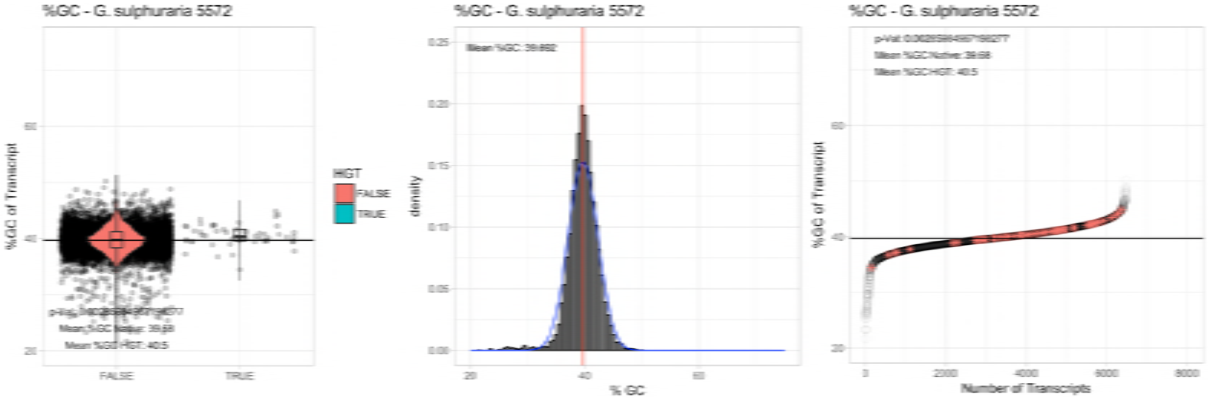

Figure 2SH – %GC – *Galdieria sulphuraria 5572:* (Left) Violin plot showing the %GC distribution across native transcripts and HGT candidates. (Mid) Cumulative %GC distribution of transcripts. Red line shows the average, blue line a normal distribution based on the average value. (Right) Ranking all transcripts based upon their %GC content. Red "*" demarks HGT candidates. As the %GC content was normally distributed, students test was applied for the determination of significant differences between the native gene and the HGT candidate subset.

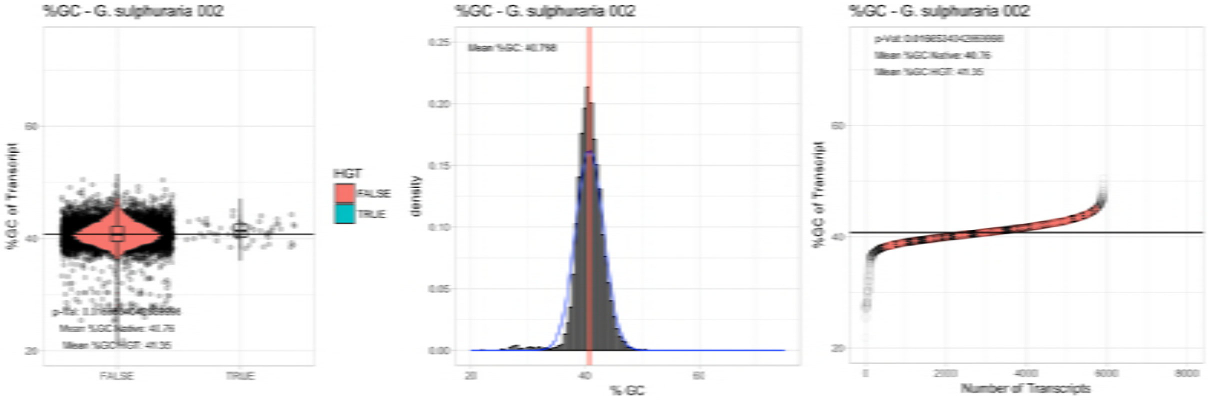

Figure 2SI – %GC – *Galdieria sulphuraria 002:* (Left) Violin plot showing the %GC distribution across native transcripts and HGT candidates. (Mid) Cumulative %GC distribution of transcripts. Red line shows the average, blue line a normal distribution based on the average value. (Right) Ranking all transcripts based upon their %GC content. Red "*" demarks HGT candidates. As the %GC content was normally distributed, students test was applied for the determination of significant differences between the native gene and the HGT candidate subset.

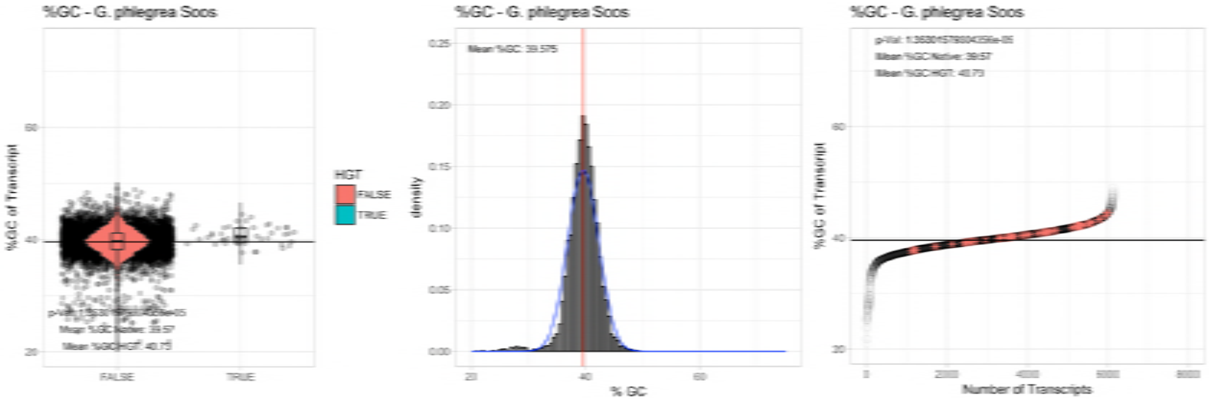

Figure 2SJ – %GC – *Galdieria phlegrea Soos:* (Left) Violin plot showing the %GC distribution across native transcripts and HGT candidates. (Mid) Cumulative %GC distribution of transcripts. Red line shows the average, blue line a normal distribution based on the average value. (Right) Ranking all transcripts based upon their %GC content. Red "*" demarks HGT candidates. As the %GC content was normally distributed, students test was applied for the determination of significant differences between the native gene and the HGT candidate subset.

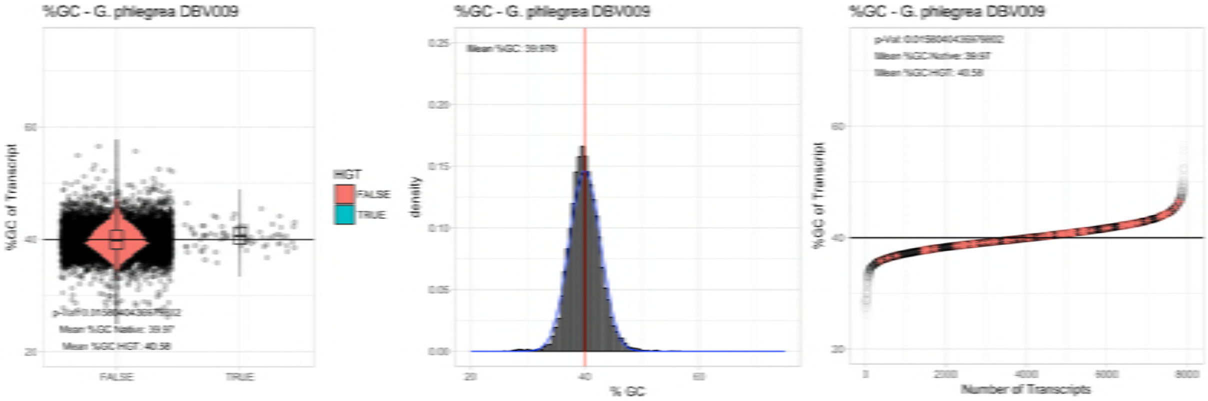

Figure 2SK – %GC – *Galdieria phlegrea DBV009:* (Left) Violin plot showing the %GC distribution across native transcripts and HGT candidates. (Mid) Cumulative %GC distribution of transcripts. Red line shows the average, blue line a normal distribution based on the average value. (Right) Ranking all transcripts based upon their %GC content. Red "*" demarks HGT candidates. As the %GC content was normally distributed, students test was applied for the determination of significant differences between the native gene and the HGT candidate subset.

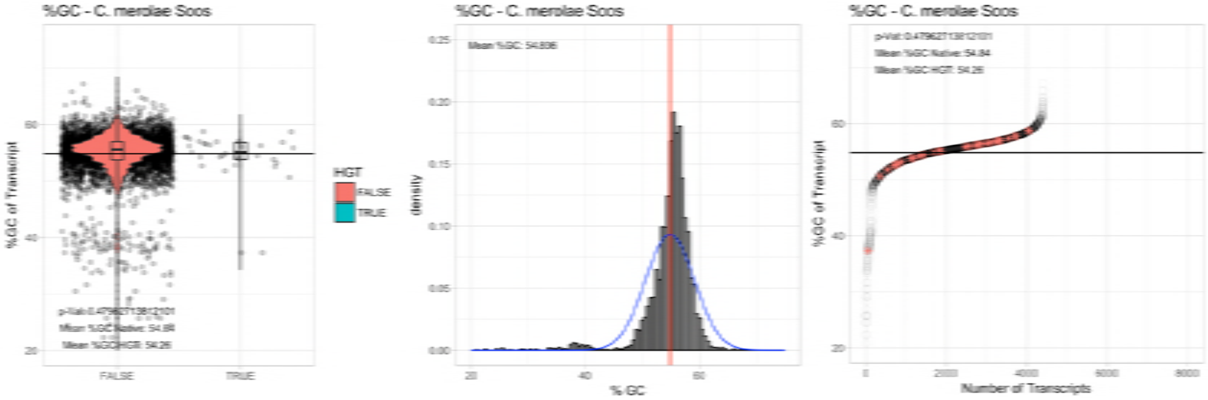

Figure 2SL – %GC – *Cyanidioschyzon merolae Soos:* (Left) Violin plot showing the %GC distribution across native transcripts and HGT candidates. (Mid) Cumulative %GC distribution of transcripts. Red line shows the average, blue line a normal distribution based on the average value. (Right) Ranking all transcripts based upon their %GC content. Red "*" demarks HGT candidates. As the %GC content was normally distributed, students test was applied for the determination of significant differences between the native gene and the HGT candidate subset.

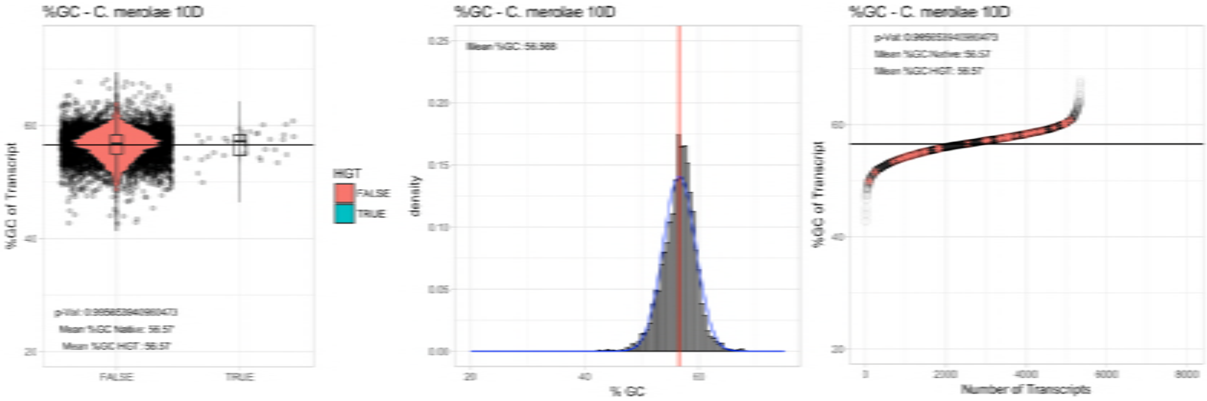

Figure 2SM – %GC – *Cyanidioschyzon merolae 10D:* (Left) Violin plot showing the %GC distribution across native transcripts and HGT candidates. (Mid) Cumulative %GC distribution of transcripts. Red line shows the average, blue line a normal distribution based on the average value. (Right) Ranking all transcripts based upon their %GC content. Red "*" demarks HGT candidates. As the %GC content was normally distributed, students test was applied for the determination of significant differences between the native gene and the HGT candidate subset.

SUMMPLEMENTARY TABLE 4S

Table 3SA – Single exon genes vs multiexonic. The ratio of single exon genes vs multiexonic genes was compared between HGT candidates and native Cyanidiales genes (Fisher enrichment test). Legend: **HGT Genes**: number of HGT gene candidates found in species. **Single Exon HGT**: number of single exon genes in HGT candidates. **Multi Exon HGT**: number of multiexonic genes in HGT candidates. **Single Exon Native**: number of single exon genes in native Cyanidiales genes. **Multi Exon Native**: number of multiexonic genes in native Cyanidiales genes. **HGT SM Ratio** percentage of single exon genes within the HGT candidate genes. **Native SM Ratio** percentage of single exon genes within the native genes. **Delta:** difference in percent between the percentage of single exon genes between the native genes and HGT candidates. **Fisher p-val**: p-value of fisher enrichment test.

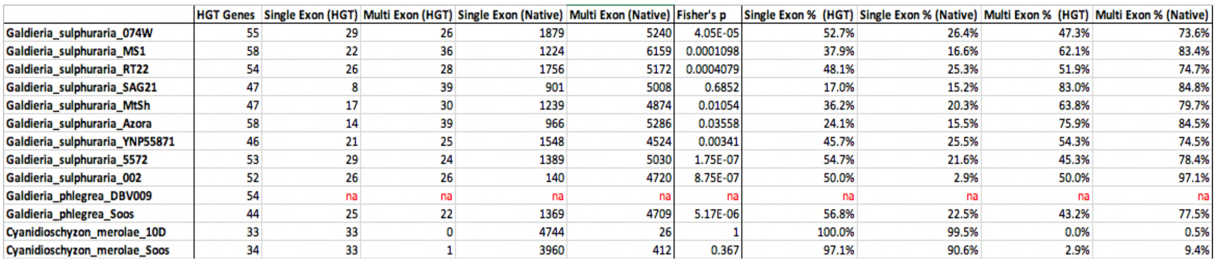

	HGT Genes	Single Exon (HGT)	Multi Exon (HGT)	Single Exon (Native)	Multi Exon (Native)	Fisher's p	Single Exon % (HGT)	Single Exon % (Native)	Multi Exon % (HGT)	Multi Exon % (Native)
Galdieria_sulphuraria_074W	55	29	26	1879	5240	4.05E-05	52.7%	26.4%	47.3%	73.6%
Galdieria_sulphuraria_MS1	58	22	36	1224	6159	0.0001098	37.9%	16.6%	62.1%	83.4%
Galdieria_sulphuraria_RT22	54	26	28	1756	5172	0.0004079	48.1%	25.3%	51.9%	74.7%
Galdieria_sulphuraria_SAG21	47	8	39	901	5008	0.6852	17.0%	15.2%	83.0%	84.8%
Galdieria_sulphuraria_MtSh	47	17	30	1239	4874	0.01054	36.2%	20.3%	63.8%	79.7%
Galdieria_sulphuraria_Azora	58	14	39	966	5286	0.03558	24.1%	15.5%	75.9%	84.5%
Galdieria_sulphuraria_YNP55871	46	21	25	1548	4524	0.00341	45.7%	25.5%	54.3%	74.5%
Galdieria_sulphuraria_5572	53	29	24	1389	5030	1.75E-07	54.7%	21.6%	45.3%	78.4%
Galdieria_sulphuraria_002	52	26	26	140	4720	8.75E-07	50.0%	2.9%	50.0%	97.1%
Galdieria_phlegrea_DBV009	54	na	na	na	na	na	na	na	na	na
Galdieria_phlegrea_Soos	44	25	22	1369	4709	5.17E-06	56.8%	22.5%	43.2%	77.5%
Cyanidioschyzon_merolae_10D	33	33	0	4744	26	1	100.0%	99.5%	0.0%	0.5%
Cyanidioschyzon_merolae_Soos	34	33	1	3960	412	0.367	97.1%	90.6%	2.9%	9.4%

Table 3SB – Exon/Gene ratio. The ratio of exons per gene was compared between HGT candidates and native Cyanidiales genes (Wilcox ranked test). Legend: **HGT Genes**: number of HGT gene candidates found in species. **E/G All:** average number of exons per gene across the whole transcriptome. **E/G Native:** average number of exons per gene across in native genes. **E/G HGT**: average number of exons per gene in HGT gene candidates. **p-Val (Wilcox) SM Ratio** p-value of non-parametric Wilcox test for significant differences. **Delta:** difference in average number of exons per gene the native genes and HGT candidates.

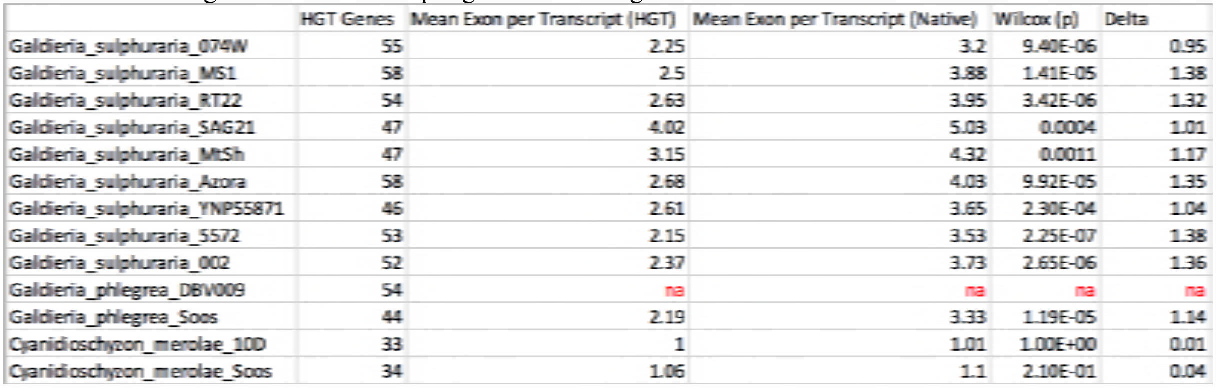

	HGT Genes	Mean Exon per Transcript (HGT)	Mean Exon per Transcript (Native)	Wilcox (p)	Delta
Galdieria_sulphuraria_074W	55	2.25	3.2	9.40E-06	0.95
Galdieria_sulphuraria_MS1	58	2.5	3.88	1.41E-05	1.38
Galdieria_sulphuraria_RT22	54	2.63	3.95	3.42E-06	1.32
Galdieria_sulphuraria_SAG21	47	4.02	5.03	0.0004	1.01
Galdieria_sulphuraria_MtSh	47	3.15	4.32	0.0011	1.17
Galdieria_sulphuraria_Azora	58	2.68	4.03	9.92E-05	1.35
Galdieria_sulphuraria_YNP55871	46	2.61	3.65	2.30E-04	1.04
Galdieria_sulphuraria_5572	53	2.15	3.53	2.25E-07	1.38
Galdieria_sulphuraria_002	52	2.37	3.73	2.65E-06	1.36
Galdieria_phlegrea_DBV009	54	na	na	na	na
Galdieria_phlegrea_Soos	44	2.19	3.33	1.19E-05	1.14
Cyanidioschyzon_merolae_10D	33	1	1.01	1.00E+00	0.01
Cyanidioschyzon_merolae_Soos	34	1.06	1.1	2.10E-01	0.04

SUMMPLEMENTARY FIGURES 3S, A – M, EXON/INTRON STATS

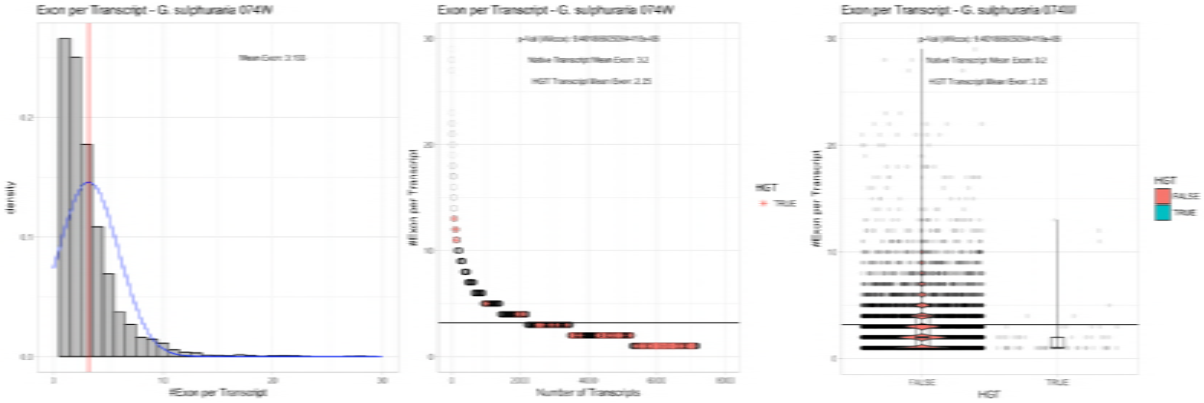

Figure 3SA – Exon/Intron – *Galdieria sulphuraria 074W:* (Left) Mid) Cumulative %GC distribution of transcripts. Red line shows the average, blue line a normal distribution based on the average value. The data is categorical (genes have either one, two, three etc. exons) and does not follow a normal distribution. (Mid) Ranking all transcripts based upon their number of exons. Red "*" demarks HGT candidates. As the number of exons was not normally distributed, transcripts were ranked by number of exons. In order to resolve the high number of tied ranks (e.g. many transcripts have 2 exons) a bootstrap was implied by which the rank of transcripts sharing the same number of exons was randomly assigned 1000 times. Wilcoxon-Mann-Whitney-Test applied for the determination of significant rank differences between the native gene and the HGT candidate subset. (Right) Violin plot showing the number of exons per transcript distribution across native transcripts and HGT candidates.

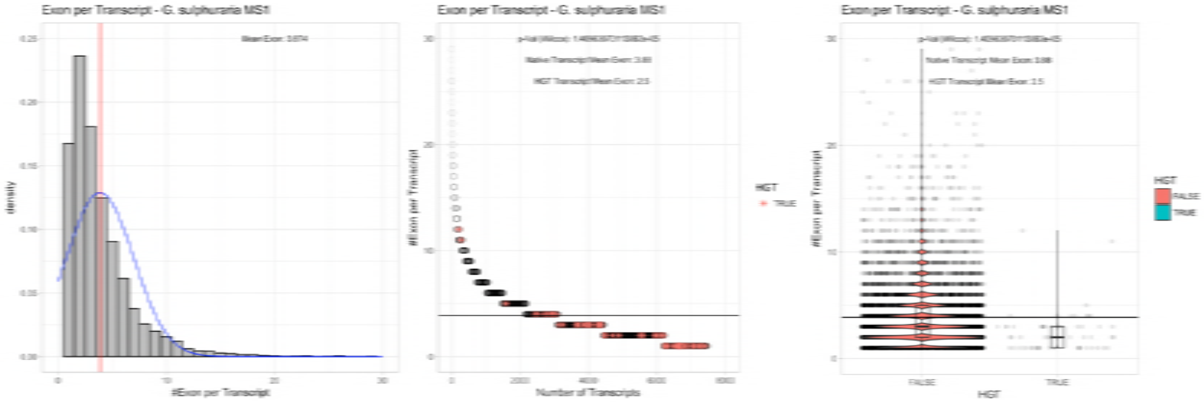

Figure 3SB – Exon/Intron – *Galdieria sulphuraria MS1:* (Left) Mid) Cumulative %GC distribution of transcripts. Red line shows the average, blue line a normal distribution based on the average value. The data is categorical (genes have either one, two, three etc. exons) and does not follow a normal distribution. (Mid) Ranking all transcripts based upon their number of exons. Red "*" demarks HGT candidates. As the number of exons was not normally distributed, transcripts were ranked by number of exons. In order to resolve the high number of tied ranks (e.g. many transcripts have 2 exons) a bootstrap was implied by which the rank of transcripts sharing the same number of exons was randomly assigned 1000 times. Wilcoxon-Mann-Whitney-Test applied for the determination of significant rank differences between the native gene and the HGT candidate subset. (Right) Violin plot showing the number of exons per transcript distribution across native transcripts and HGT candidates.

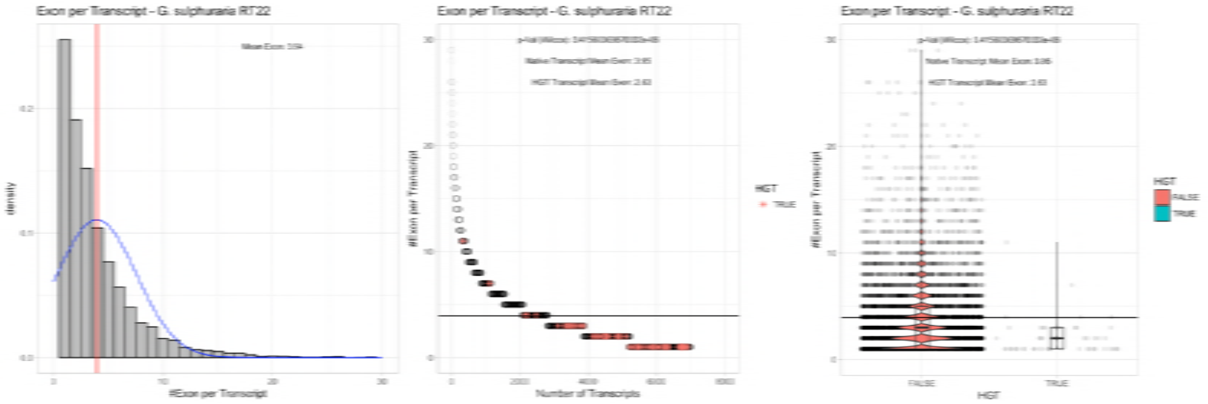

Figure 3SC – Exon/Intron – *Galdieria sulphuraria RT22:* (Left) Mid) Cumulative %GC distribution of transcripts. Red line shows the average, blue line a normal distribution based on the average value. The data is categorical (genes have either one, two, three etc. exons) and does not follow a normal distribution. (Mid) Ranking all transcripts based upon their number of exons. Red "*" demarks HGT candidates. As the number of exons was not normally distributed, transcripts were ranked by number of exons. In order to resolve the high number of tied ranks (e.g. many transcripts have 2 exons) a bootstrap was implied by which the rank of transcripts sharing the same number of exons was randomly assigned 1000 times. Wilcoxon-Mann-Whitney-Test applied for the determination of significant rank differences between the native gene and the HGT candidate subset. (Right) Violin plot showing the number of exons per transcript distribution across native transcripts and HGT candidates.

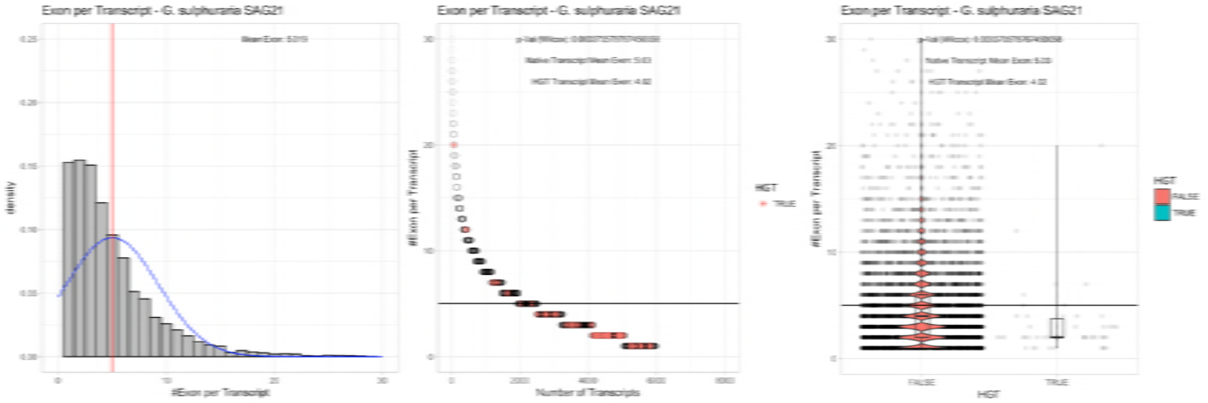

Figure 3SD – Exon/Intron – *Galdieria sulphuraria SAG21:* (Left) Mid) Cumulative %GC distribution of transcripts. Red line shows the average, blue line a normal distribution based on the average value. The data is categorical (genes have either one, two, three etc. exons) and does not follow a normal distribution. (Mid) Ranking all transcripts based upon their number of exons. Red "*" demarks HGT candidates. As the number of exons was not normally distributed, transcripts were ranked by number of exons. In order to resolve the high number of tied ranks (e.g. many transcripts have 2 exons) a bootstrap was implied by which the rank of transcripts sharing the same number of exons was randomly assigned 1000 times. Wilcoxon-Mann-Whitney-Test applied for the determination of significant rank differences between the native gene and the HGT candidate subset. (Right) Violin plot showing the number of exons per transcript distribution across native transcripts and HGT candidates.

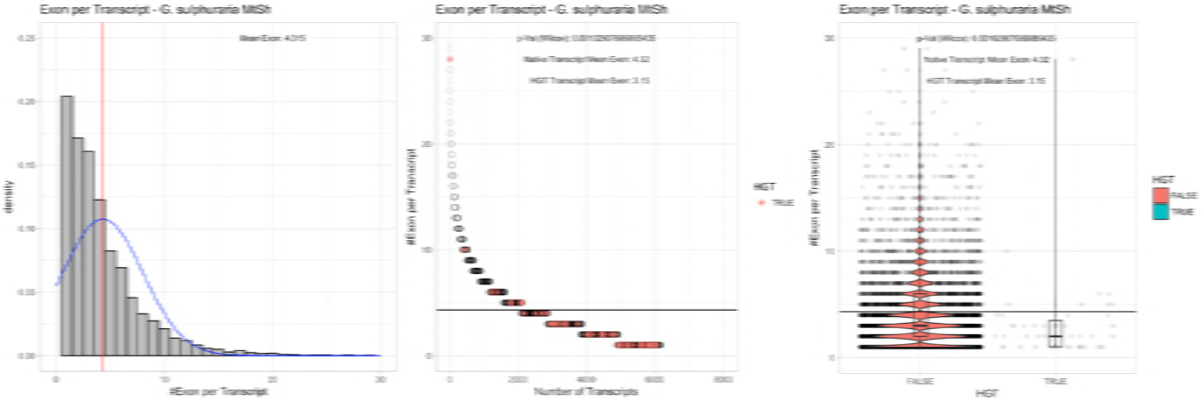

Figure 3SE – Exon/Intron – *Galdieria sulphuraria MtSh:* (Left) Mid) Cumulative %GC distribution of transcripts. Red line shows the average, blue line a normal distribution based on the average value. The data is categorical (genes have either one, two, three etc. exons) and does not follow a normal distribution. (Mid) Ranking all transcripts based upon their number of exons. Red "*" demarks HGT candidates. As the number of exons was not normally distributed, transcripts were ranked by number of exons. In order to resolve the high number of tied ranks (e.g. many transcripts have 2 exons) a bootstrap was implied by which the rank of transcripts sharing the same number of exons was randomly assigned 1000 times. Wilcoxon-Mann-Whitney-Test applied for the determination of significant rank differences between the native gene and the HGT candidate subset. (Right) Violin plot showing the number of exons per transcript distribution across native transcripts and HGT candidates.

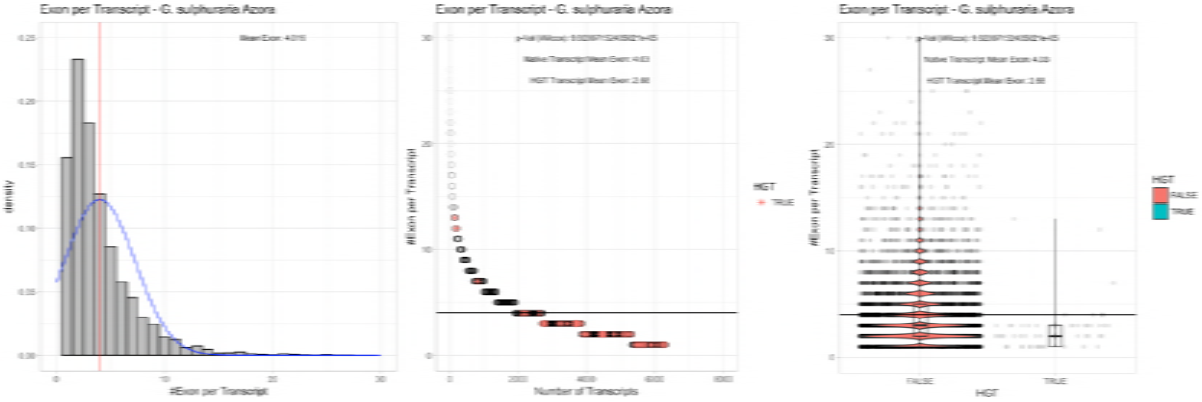

Figure 3SF – Exon/Intron – *Galdieria sulphuraria Azora:* (Left) Mid) Cumulative %GC distribution of transcripts. Red line shows the average, blue line a normal distribution based on the average value. The data is categorical (genes have either one, two, three etc. exons) and does not follow a normal distribution. (Mid) Ranking all transcripts based upon their number of exons. Red "*" demarks HGT candidates. As the number of exons was not normally distributed, transcripts were ranked by number of exons. In order to resolve the high number of tied ranks (e.g. many transcripts have 2 exons) a bootstrap was implied by which the rank of transcripts sharing the same number of exons was randomly assigned 1000 times. Wilcoxon-Mann-Whitney-Test applied for the determination of significant rank differences between the native gene and the HGT candidate subset. (Right) Violin plot showing the number of exons per transcript distribution across native transcripts and HGT candidates.

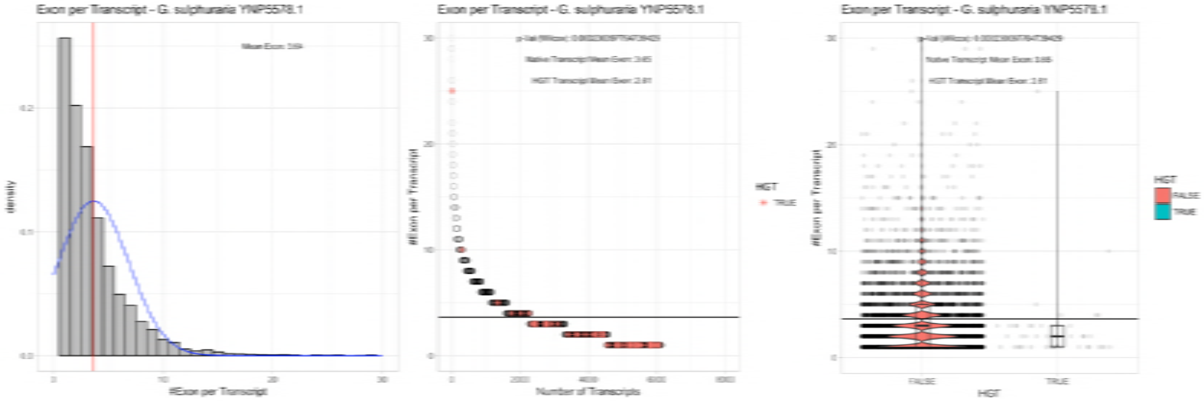

Figure 3SG – Exon/Intron – *Galdieria sulphuraria YNP5578.1:* (Left) Mid) Cumulative %GC distribution of transcripts. Red line shows the average, blue line a normal distribution based on the average value. The data is categorical (genes have either one, two, three etc. exons) and does not follow a normal distribution. (Mid) Ranking all transcripts based upon their number of exons. Red "*" demarks HGT candidates. As the number of exons was not normally distributed, transcripts were ranked by number of exons. In order to resolve the high number of tied ranks (e.g. many transcripts have 2 exons) a bootstrap was implied by which the rank of transcripts sharing the same number of exons was randomly assigned 1000 times. Wilcoxon-Mann-Whitney-Test applied for the determination of significant rank differences between the native gene and the HGT candidate subset. (Right) Violin plot showing the number of exons per transcript distribution across native transcripts and HGT candidates.

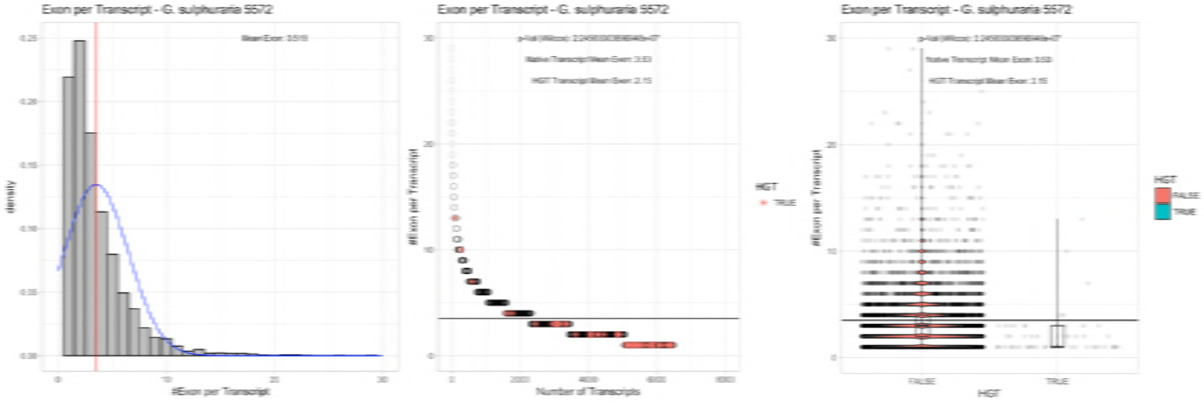

Figure 3SH – Exon/Intron – *Galdieria sulphuraria 5572:* (Left) Mid) Cumulative %GC distribution of transcripts. Red line shows the average, blue line a normal distribution based on the average value. The data is categorical (genes have either one, two, three etc. exons) and does not follow a normal distribution. (Mid) Ranking all transcripts based upon their number of exons. Red "*" demarks HGT candidates. As the number of exons was not normally distributed, transcripts were ranked by number of exons. In order to resolve the high number of tied ranks (e.g. many transcripts have 2 exons) a bootstrap was implied by which the rank of transcripts sharing the same number of exons was randomly assigned 1000 times. Wilcoxon-Mann-Whitney-Test applied for the determination of significant rank differences between the native gene and the HGT candidate subset. (Right) Violin plot showing the number of exons per transcript distribution across native transcripts and HGT candidates.

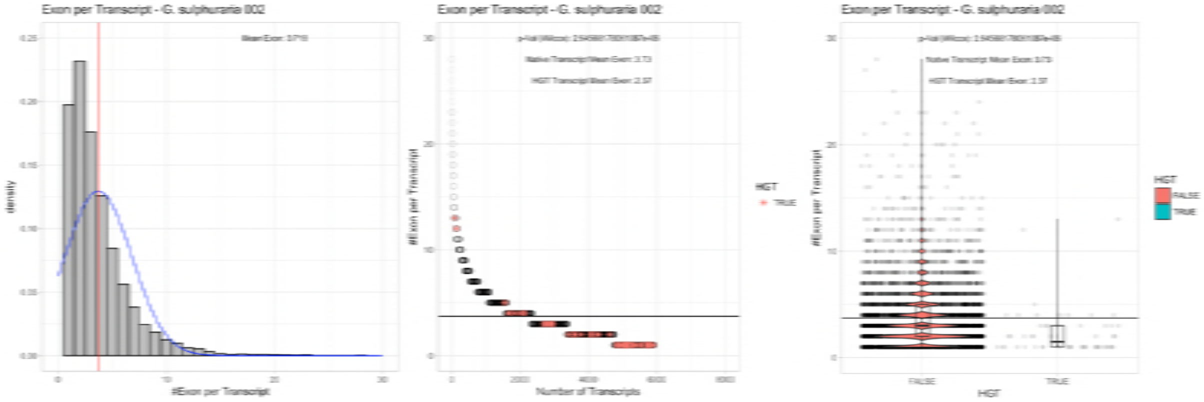

Figure 3SI – Exon/Intron – *Galdieria sulphuraria 002:* (Left) Mid) Cumulative %GC distribution of transcripts. Red line shows the average, blue line a normal distribution based on the average value. The data is categorical (genes have either one, two, three etc. exons) and does not follow a normal distribution. (Mid) Ranking all transcripts based upon their number of exons. Red "*" demarks HGT candidates. As the number of exons was not normally distributed, transcripts were ranked by number of exons. In order to resolve the high number of tied ranks (e.g. many transcripts have 2 exons) a bootstrap was implied by which the rank of transcripts sharing the same number of exons was randomly assigned 1000 times. Wilcoxon-Mann-Whitney-Test applied for the determination of significant rank differences between the native gene and the HGT candidate subset. (Right) Violin plot showing the number of exons per transcript distribution across native transcripts and HGT candidates.

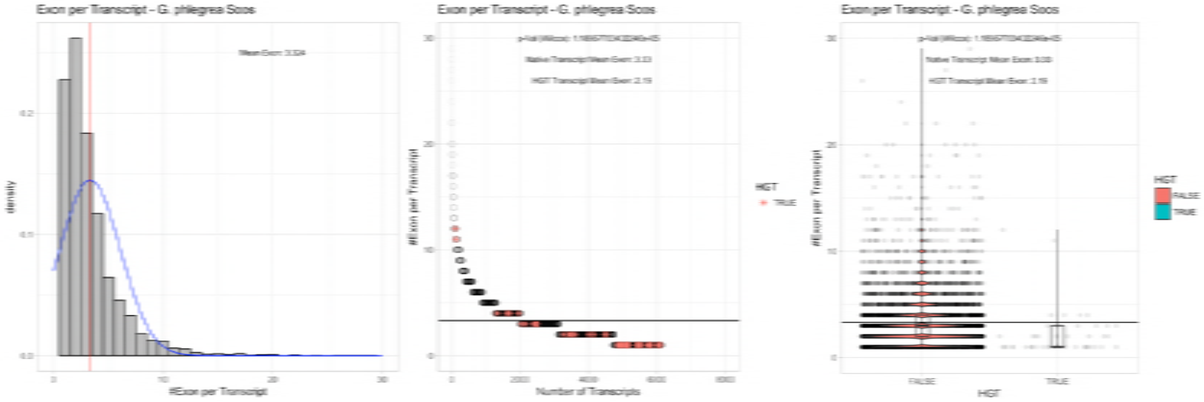

Figure 3SJ – Exon/Intron – *Galdieria phlegrea Soos:* (Left) Mid) Cumulative %GC distribution of transcripts. Red line shows the average, blue line a normal distribution based on the average value. The data is categorical (genes have either one, two, three etc. exons) and does not follow a normal distribution. (Mid) Ranking all transcripts based upon their number of exons. Red "*" demarks HGT candidates. As the number of exons was not normally distributed, transcripts were ranked by number of exons. In order to resolve the high number of tied ranks (e.g. many transcripts have 2 exons) a bootstrap was implied by which the rank of transcripts sharing the same number of exons was randomly assigned 1000 times. Wilcoxon-Mann-Whitney-Test applied for the determination of significant rank differences between the native gene and the HGT candidate subset. (Right) Violin plot showing the number of exons per transcript distribution across native transcripts and HGT candidates.

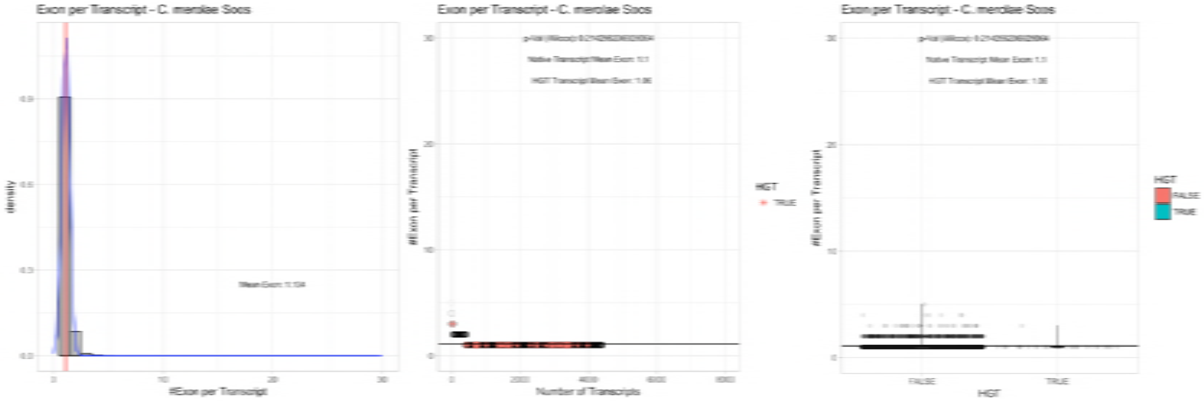

Figure 3SL – Exon/Intron – *Cyanidioschyzon merolae Soos:* (Left) Mid) Cumulative %GC distribution of

transcripts. Red line shows the average, blue line a normal distribution based on the average value. The data is categorical (genes have either one, two, three etc. exons) and does not follow a normal distribution. (Mid) Ranking all transcripts based upon their number of exons. Red "*" demarks HGT candidates. As the number of exons was not normally distributed, transcripts were ranked by number of exons. In order to resolve the high number of tied ranks (e.g. many transcripts have 2 exons) a bootstrap was implied by which the rank of transcripts sharing the same number of exons was randomly assigned 1000 times. Wilcoxon-Mann-Whitney-Test applied for the determination of significant rank differences between the native gene and the HGT candidate subset. (Right) Violin plot showing the number of exons per transcript distribution across native transcripts and HGT candidates.

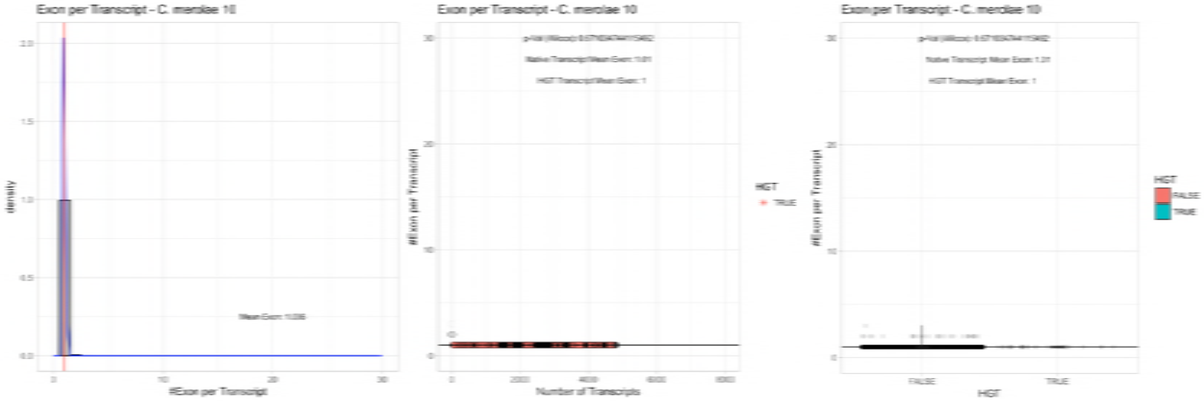

Figure 3SM – Exon/Intron – *Cyanidioschyzon merolae 074W:* (Left) Mid) Cumulative %GC distribution of transcripts. Red line shows the average, blue line a normal distribution based on the average value. The data is categorical (genes have either one, two, three etc. exons) and does not follow a normal distribution. (Mid) Ranking all transcripts based upon their number of exons. Red "*" demarks HGT candidates. As the number of exons was not normally distributed, transcripts were ranked by number of exons. In order to resolve the high number of tied ranks (e.g. many transcripts have 2 exons) a bootstrap was implied by which the rank of transcripts sharing the same number of exons was randomly assigned 1000 times. Wilcoxon-Mann-Whitney-Test applied for the determination of significant rank differences between the native gene and the HGT candidate subset. (Right) Violin plot showing the number of exons per transcript distribution across native transcripts and HGT candidates.

1. Cantarel, B.L., et al., *MAKER: an easy-to-use annotation pipeline designed for emerging model organism genomes.* Genome Res, 2008. **18**(1): p. 188-96.
2. Schonknecht, G., et al., *Gene transfer from bacteria and archaea facilitated evolution of an extremophilic eukaryote.* Science, 2013. **339**(6124): p. 1207-10.
3. Qiu, H., et al., *Adaptation through horizontal gene transfer in the cryptoendolithic red alga Galdieria phlegrea.* Curr Biol, 2013. **23**(19): p. R865-6.
4. Boothby, T.C., et al., *Evidence for extensive horizontal gene transfer from the draft genome of a tardigrade.* Proc Natl Acad Sci U S A, 2015. **112**(52): p. 15976-81.
5. Crisp, A., et al., *Expression of multiple horizontally acquired genes is a hallmark of both vertebrate and invertebrate genomes.* Genome Biol, 2015. **16**: p. 50.
6. Koutsovoulos, G., et al., *No evidence for extensive horizontal gene transfer in the genome of the tardigrade Hypsibius dujardini.* Proc Natl Acad Sci U S A, 2016. **113**(18): p. 5053-8.
7. Salzberg, S.L., *Horizontal gene transfer is not a hallmark of the human genome.* Genome Biol, 2017. **18**(1): p. 85.
8. Boschetti, C., et al., *Biochemical diversification through foreign gene expression in bdelloid rotifers.* PLoS Genet, 2012. **8**(11): p. e1003035.
9. Danchin, E.G., *Lateral gene transfer in eukaryotes: tip of the iceberg or of the ice cube?* BMC Biol, 2016. **14**(1): p. 101.
10. Horn, D., *Antigenic variation in African trypanosomes.* Mol Biochem Parasitol, 2014. **195**(2): p. 123-9.
11. Pedersen, C., et al., *Structure and evolution of barley powdery mildew effector candidates.* BMC Genomics, 2012. **13**: p. 694.